INVESTIGATION OF MACROMOLECULAR SOLUTIONS BY LIGHT SCATTERING AND ELECTRO-OPTIC EFFECTS

by

N. KHALIL

A thesis submitted for the degree of Master of Philosophy at the University of Southampton.

August 1976

ABSTRACT

FACULTY OF SCIENCE

PHYSICS

Master of Philosophy

INVESTIGATION OF MACROMOLECULAR SOLUTIONS BY LIGHT SCATTERING AND ELECTRO-OPTIC EFFECTS

by N. Khalil

In these investigations the light scattering method was used for the determination of the weight average molecular weight M_w, the z-average radius of gyration ρ_z and the coefficient of interaction B of the following macromolecular substances in aqueous solutions. (1) Wyoming bentonite, (2) North African bentonies, (3) hectorite, (4) collagen and (5) DNA. The values of M_w and ρ_z were then used to calculate the dimensions of these macromolecular substances. Assuming the particles of bentonite being disc-shaped, of uniform thickness, the z-average diameter of the particles of samples (a) and (2) were found to be 3020 and 2120 $\mathring{A}$ respectively. The particles of samples 3, 4 and 5 were assumed to be rod shaped. The z-average length, L_z, and the diameter of the particles of hectorite were found to be 7715 $\mathring{A}$ and 58 $\mathring{A}$ respectively.

The molecular weight and the length of collagen particles were found to be 1.65×10^6 and 7300 $\mathring{A}$ respectively. The molecular weight was thus approximately four times and the length twice of the values reported for a monomer. It was concluded from these results that a side to side aggregation of two dimers, joined end to end represented the aggregated particles.

For the DNA, the values of M_w and L_z were found to be 4.5×10^6 and 10,500 $\mathring{A}$ respectively. The value of L_z is much less than expected for fully stretched particles of such molecular weights. This indicates the inadequacy of the rod model to represent DNA of high molecular

weight.

The electrical properties and the relaxation time, τ, for the two bentonite samples were studied using the method of light scattering in the presence of electric fields. Both a.c. and square pulsed fields were employed. The dispersion of the steady component (its frequency dependence) indicated that the disc shaped particles have both a permanent (μ) and an induced dipole moment. These were at right angles to each other with the direction of μ being along the axis of symmetry. The values of α and the excess polarisability were found to be 3.3×10^{-14} e.s.u. and 2.7×10^{-14} cm^3 respectively. Using the values of τ, the diameters of the particles of Wyoming bentonite and N.A. bentonite were found to be 2000 $\mathring{A}$ and 1500 $\mathring{A}$ respectively. It is demonstrated that with square pulsed fields, this method can be very insensitive.

The free decay of the electric birefringence (Kerr effect method) was used to determine the relaxation time(s) and thus the range of the size of the particles of the above mentioned substances. The diameters of the smallest and the largest particles were found to be $1960 \alpha 3120$ $\mathring{A}$ for substance (1) and $1140 \alpha 1960$ $\mathring{A}$ for substance (2) respectively. For hectorite the values of τ were found to be 4.5 and 163. μ sec. For rod like particles of dimensions as determined from the light scattering such small values of τ result only from the rotation of these particles about their major axis. Thus the particles have no dipole moment along their major axis. For collagen only a single relaxation time was detected. Its value of 0.39 μ sec. was significantly smaller than previously reported. Again this was interpreted as due to rotation of the above mentioned aggregated particles about their major axis. The values of τ for the DNA were found to be 3 and 43 μ.sec. These values combined with the light scattering results suggested that the particles were flexible and rotate in segments.

Acknowledgement

The author would like to thank sincerely Dr. H.G. Jerrard, B.Sc., Ph.D., F.Inst.P., for his supervision throughout this work, and also Professors E.W. Lee and G.W. Hutchinson for providing laboratory facilities in the Physics Department.

I am grateful to the staff in the electronics workshop, and in particular to Mr. R.G. Garment and F.P. Lund for their help in building the pulse generator and the frequency doubler. I am also grateful to the staff of the workshop, in particular to Mr. P.J. Fewell and Mr. K. Osman for constructing the electrode assemblies. My thanks to Mr. H. Williams for the continuous technical assistance.

I would also like to thank the University of Damascus, my parents and several of my friends in particular Mr. A. Sewehili and wife for the financial support given.

Finally, the author would like to thank Mrs. Audrey Lampard for typing this thesis.

C O N T E N T S

CHAPTER IV

THEORY OF THE KERR EFFECT

CHAPTER V

PART A

PART B

CHAPTER VI

CHAPTER VII

RESULTS

CHAPTER I

General Introduction

When a beam of light traverses a non-absorptive medium, part of the light will be scattered and the remainder will be transmitted unperturbed along the incident direction. The intensity of the scattered light, its angular distribution and degree of polarisation are dependent on the properties of the scatterer; that is its size, shape and refractive index. For solutions of finite concentration, the scattered intensity is also dependent upon the interaction of the particles both with each other and with the solvent.

Although the basic theory of light scattering is over a hundred years old, its use in investigating macro-molecular solution has been rare (Gans - 1919, and Putzeys and Brosteaux 1935) until the pioneer theoretical and experimental work of Debye (1944, 1947) and Zimm (1948a and b). Since then the method has become widely used and interesting new contributions have been made.

The molecular properties that can be obtained without any prior assumptions about the particles are the weight average molecular weight, M_w, the Z-average of the radius of gyration ρ_z, and the second virial coefficient of interaction B. The radius of gyration is related to the size and shape of the particles and assumes very different values for different configurations. Thus a determination of this parameter can give evidence on the configuration of the particles.

The importance of the light scattering method is that it is the only method that enables the direct determination of the radius of gyration. In addition, it has the advantage that certain biological substances can

be studied in an environment similar to that from which they were extracted.

The method has been extended by Wippler (1953 - 1957) to investigate the electrical properties of macromolecular solutions. This extension is based on the fact that, for particles which are non spherical and of size comparable to that of the wave length of the incident beam, the angular scattered intensity is dependent not only on the size and shape of the particles but also on their orientation relative to a specific direction. Thus when measurements are made in the absence and the presence of electric fields, a change in the scattered intensity takes place. This change is dependent on the intensity of the applied field and the electrical properties of the substance. Wippler's original theory for both rigid rods and Gaussian chains has been further developed and extended by other workers (Stoylov - 1966 & 7, Wallach and Benoit - 1966 and Jennings et al - 1970). These theories indicate that, for all rigid particles the changes arising from the application of sine wave electric fields of low intensity consist of a steady component which is in general frequency dependent and also an alternating component oscillating at twice the frequency of the applied field ω. These theories also indicate that at any frequency, the steady component is in general composed of the sum of two terms. The first represents the contribution of the permanent dipole moment, μ, that can be associated with the particles and the second represents the contribution of the dipole moment induced by the applied field when the

particles are electrically anisotropic. The contribution of the permanent dipole becomes negligible at sufficiently high frequencies as the particles can no longer follow the changing direction of the applied field. It is possible therefore to determine the contribution of each of the dipoles acting on the particles by measuring the dispersion of the steady component (i.e. its frequency dependence). It is also possible from such dispersion measurements to determine the relaxation time, τ, which is an important parameter as it is related to the size and shape of the particles. Similar information may be obtained by analysing the alternating component. In general, this analysis is not easily achieved because there is a phase difference between the two terms representing the contributions of these two dipoles. However, for non polar particles (i.e. $\mu = 0$) τ can be obtained only from the dispersion of the alternating component.

An advantage of this method is that it can easily be used to distinguish between rigid and flexible particles. This is achieved by determining the rigidity parameter, R, which assumes very different values for these two kinds of particles.

A more widely used method for the investigation of the electrical properties of macromolecular solutions is the Kerr effect (electric birefringence). This is based on the phenomenon that an electric field applied to a solution of optically anisotropic particles will cause the solution to become birefringent. The solution acts as an optically isotropic medium in the absence of the

electric field because the particles are then randomly orientated. However, on the application of the electric field a certain degree of order is achieved by the particles, which because of their optical anisotropy cause birefringence. Thus clearly this method can not be applied to solutions of optically isotropic particles, as there would be no birefringence produced by the applied field.

The theory of electric birefringence arising from the application of sine wave electric fields to macromolecular solutions was originally developed by Peterlin and Stuart (1943). It was extended for square pulsed fields by Benoit (1951). Further extensions of the theory and method have been made by many other workers (Tinoco - 1955, O'Konski et al - 1959, Shah - 1963 and Nishinari & Yoshioka - 1969).

The above mentioned methods have been used to investigate the solutions of a large number of macromolecular substances (O'Konski - 1968, Stoylov - 1971 and Jennings - 1972). In the present work these methods were employed to study a) three mineral clays of the montmorillonite type (namely; Wyoming sodium bentonite, North African calcium bentonite, hectorite) and b) two biological samples: colagen and deoxyribonucleic acid (DNA). These investigations were carried out mainly to:
i) determine the electrical parameters for a freshly prepared solution of Wyoming bentonite in which the particles have a narrow size distribution. Under these conditions, the effects on these parameters arising from polydispersity of the particles and the age of the solutions, which can be considerable and very difficult to analyse, are significantly reduced. Thus the values obtained would be more representative

than some of those previously reported on solutions having a higher degree of polydispersity and not as fresh.

ii) obtain information on the macromolecular and the electrical properties of North African calcium bentonite which has not been previously studied.

iii) explain the observed relaxation times for the hectorite and the collagen samples.

iv) resolve the conflicting electrical properties of DNA (for recent studies on DNA see Greve and Heij - 1975).

CHAPTER II

THEORY OF LIGHT SCATTERED BY MACROMOLECULAR SOLUTIONS

2.1 Introduction

The original theory of light scattered by optically isotropic particles which are randomly located and of small size compared to the wave length of the incident light beam has been derived by Lord Rayleigh (1871). Later Smoluchowski (1908) introduced the fluctuation theory to account for the scattering by liquids where the particles can no longer be considered as randomly located. At the same time an exact theory for the scattering from isolated spheres of arbitrary size was postulated by Mie (1908). Einstein (1910) extended the fluctuation theory to include solutions of small particles of finite concentration. The theory for solutions of particles whose dimensions are comparable to the wave length and whose relative refractive index is close to unity was developed mainly by Rayleigh (1881-1918) and Debye (1915). At nearly the same period, Zernicke (1915) developed a theory for the scattering from multi-component systems. The use of these theories in the investigation of macromolecular solutions by the light scattering technique has been very rare until the pioneering work of Debye (1947) and Zimm (1948). Since then a vigorous activity in this field developed which led to the further understanding of the behaviour of macromolecular solutions.

The theory and practice of light scattering has been dealt with extensively and is constantly being updated with many monographs and reviews, e.g. Stacey (1956), Peterlin (1959), Kratohvil (1964,1966a),

Kerker (1969), Timasheff and Townend (1970) and the book "Light Scattering from Polymer Solutions" edited by Huglin (1972).

2.2 Rayleigh Scattering Theory

2.2.1 Scattering by optically isotropic particles, small compared to the wave length of light.

The following discussion applies to particles that satisfy the following conditions:

i) The particles must be small* compared to the wave length of light in the medium.

ii) The particles have refractive index close to that of the medium.

iii) The particles must be optically isotropic.

iv) The particles are far apart so that they can be considered as randomly located.

Consider a single particle in space subjected to an electric field $\bar{E}$, the particle becomes polarized and a dipole moment $\bar{P}$ is set up in the particle which will be parallel to the direction of the electric field vector, if the particle is optically isotropic. The magnitude of $\bar{P}$ is proportional to the electric field strength. The proportionality constant α, in general a tensor, is called the polarisability of the particle, therefore:

$$\bar{P} = \alpha \cdot \bar{E} \qquad (2.1)$$

Consider now a large number of randomly located particles of uniform chemical composition and density (e.g. gases under very low pressure, or solutions of very low concentration) in the path of a parallel and linearly polarised beam of light of wave length λ. The

* According to Debye (1944) the dividing line is 1/20 to 1/10 of the wave length.

equation for the electric field for such a wave may be expressed by:

$$E = E_o e^{i(\omega t - kx)} \qquad (2.2)$$

Here E_o is the maximum amplitude of the electric field,

$i = \sqrt{-1}$

t = time

k = wave number = $2\pi/\lambda$

c = velocity of light

ω = angular frequency = $k.c$

x = location of the particle along the line of propagation

Combining (2.1and 2.2) we see at once that the light wave will induce an oscillating dipole in any particle in its path given by:

$$P = \alpha E_o e^{i(\omega t - kx)} \qquad (2.3)$$

Such a dipole according to the classical electro magnetic theory is itself a source of electro magnetic radiation of the same frequency whose field strength is proportional to d^2P/dt^2. The radiation is emitted in all directions. At large distances from the dipole, where the distance r from the observer to all parts of the dipole are almost equal (Fig. 2.1), the field due to the positive end of the dipole will almost cancel that due to the negative end. The residual field E_s is perpendicular to the line from the observer to the dipole. Its strength at a given r is proportional to $\sin \theta_z$ where θ_z is the angle between the dipole and the line joining the centre of the dipole with the point of observation. The electric field strength must decrease as 1/r because the intensity of the scattered light I_s which

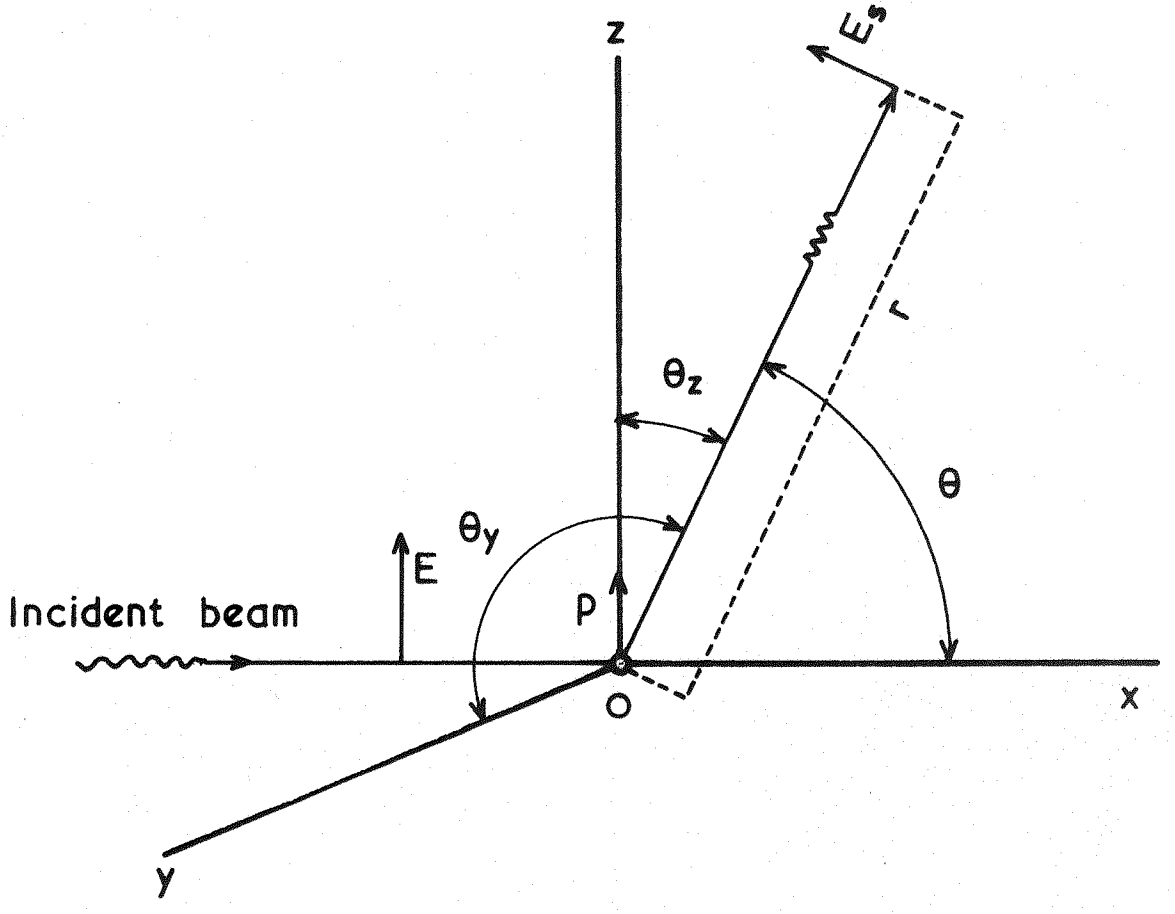

Fig. 2.1 Geometric scheme for basic scattering phenomenon. Scattered light observed in the direction (relative to the incident wave) θ at distance r

E Electric field of the incident light beam

E_s Electric field of scattered light

P Dipole moment induced by the incident light wave.

is proportional to E_s^2 decreases as $1/r^2$ due to the energy conservation principle. by differentiating (2.3) and introducing the factor $\sin\theta_z/r$ we get:

$$E_s = \frac{\omega^2\alpha\, E_o \sin\theta_z}{c^2 r} e^{i[\omega t - k(x+r)]} \qquad (2.4)$$

c the velocity of light is introduced for dimensional corrections.

The intensity of scattered light can now be calculated, but what is more important is the ratio of scattered to incident light I_s/I which is given by:

$$\frac{I_s}{I} = \frac{E_s^2}{E^2} = \frac{16\pi^4\alpha^2 \sin^2\theta_z}{\lambda^4 r^2} \qquad (2.5)$$

For a large number of particles characterised by their number $N\ cm^{-3}$ we sum up the scattering due to individual particles. Therefore for a unit volume:

$$\frac{I_s}{I} = \frac{16\pi^4\alpha^2 N \sin^2\theta_z}{\lambda^4 r^2} \qquad (2.6)$$

If, as is usual, the light is unpolarised the beam may be considered to be equivalent to the superposition of two linearly polarised beams, independent in phase and of equal intensity, with their plane of polarisation perpendicular to one another. The relative intensity of scattered light when the light is unpolarised is therefore the sum of two terms of the form (2.6). Each term represents the scattering from half the incident intensity. The two terms will be identical except that one contains $\sin^2\theta_z$ and the other $\sin^2\theta_y$. Also from Fig. (2.1) we have

$$\sin^2\theta_z + \sin^2\theta_y = 1 + \cos^2\theta \qquad (2.7)$$

Therefore for unpolarised light

$$\frac{I_s}{I} = \frac{8\pi^4\alpha^2 N}{\lambda^4 r^2}(1 + \cos^2\theta) \qquad (2.8)$$

This derivation is due to Lord Rayleigh (1871).

The polarisability α is not a quantity that can be determined experimentally. However, it is related to the optical dielectric constant ε, and therefore to the square of the refractive index n, which is a measurable quantity.

$$4\pi N\alpha = \frac{\varepsilon - \varepsilon_o}{\varepsilon_o} = \frac{n^2 - n_o^2}{n_o^2} \qquad (2.9)$$

Subscript o refers to the medium (solvent or vacuum) and absence of any subscript to the particles. If n is not very different from n_o, then we can write

$$n = n_o + C(dn/dC)$$

$$n^2 = n_o^2 + 2n_o C(dn/dC)$$

Therefore
$$\alpha = \frac{C(dn/dC)}{2\pi N n_o} \qquad (2.10)$$

C here is the weight concentration and it is related to the number concentration N by

$$N = \frac{C}{M} N_A \qquad (2.11)$$

where M is the molecular weight and N_A is Avogadro's constant.

Using eqs. (2.10) and (2.11) and using the relation $\lambda = \lambda_o/n_o$ where λ_o is the wave lengthin vacuo then eq. (2.8) can be written as

$$\frac{I_s}{I} = \frac{2\pi^2 n_o^2 \, MC(dn/dC)^2}{\lambda_o^4 \, r^2 N_A} (1 + \cos^2\theta) \qquad (2.12)$$

Eq. (2.12) shows clearly that the molecular weight can be determined by measuring I_s/I and (dn/dC).

A more compact form of (2.12) can be obtained by combining all the constants in one and using the so called Rayleigh ratio R_θ, or the reduced intensity defined by

$$R_\theta = \frac{I_s r}{I} = K' \, . \, C \, . \, M(1 + \cos^2\theta) \qquad (2.13)$$

Therefore when $\theta = 90^o$ (i.e. $R_\theta = R_{90}$)

$$\frac{K'.C}{R_{90}} = \frac{1}{M} \qquad (2.14)$$

where $$K' = \frac{2\pi^2 n_o^2 \, (dn/dC)^2}{\lambda_o^4 \, N_A} \qquad (2.15)$$

Equation (2.6) indicates, that if polarised light is used the intensity is zero along the direction of polarisation. Therefore if unpolarised light is used there will be completely polarised light in the direction perpendicular to the incident beam (i.e. $\theta = 90^o$). The experimental arrangement is most convenient when the incident and scattered beam to be measured are in the horizontal plane. In such a configuration the scattered light observed at $\theta=90^o$ is vertically polarised and represents the whole intensity at that angle.

2.2.2 Transparent crystals and pure liquids

In the previous section the scattering particles were considered to be randomly located with respect to one another. However, in a crystal, the particles are rigidly fixed and have a regular structure. Therefore destructive interference between light scattered from individual particles occurs. In fact if the wave length is much larger than the distance between the particles, the interference is complete because it is always possible to pair off the particles in such a way so that the light paths from each pair to an observer in any direction differs exactly by $\lambda/2$.

Pure liquids, due to thermal agitation and because the particles have greater degree of freedom than in solids, have much less degree of order and therefore they give rise to some scattering.

The problem has been solved by the method of fluctuation by Smoluchowski (1908). In this method the liquid is considered to be composed of small equal volume elements Δv, the elements are small enough compared with the wave length λ and separated by just the right distance so that the light paths to an observer differ by $\lambda/2$. If the elements were those of a crystal, then complete destructive interference will occur because both elements have the same number of scattering particles. However, for a liquid this is only true for the average number of particles per volume element over a large enough period. This is because of density fluctuations caused by thermal agitation. The result is that the two elements will not necessarily have the same number of scattering particles and therefore the scattering from one element exceeds that of the other. The fluctuation in density is manifested by variation in the dielectric constant. In this case the

relationship between the polarisability α and the dielectric constant ε becomes:

$$\frac{4\pi\alpha}{\Delta v} = \frac{\Delta\varepsilon}{\varepsilon} \qquad (2.16)$$

Using equation (2.8) the Rayleigh ratio, R_θ, can be expressed by

$$R_\theta = \frac{\pi^2 \Delta v \overline{(\Delta\varepsilon)^2} (1 + \cos^2\theta)}{2\lambda_o^4} \qquad (2.17)$$

where $\overline{(\Delta\varepsilon)^2}$ is the mean square change in the dielectric constant. The general equation of the scattering by pure liquids can then be obtained by relating the changes in the dielectric constant to changes in density, which in turn can be related (as for any other thermodynamic quantity) to changes in the system free energy F by the general equation

$$\overline{(\Delta x)^2} = \frac{kT}{(\partial^2 F/\partial x^2)_{x=\bar{x}}}$$

where $\overline{(\Delta x)^2}$ is the mean square change in the thermodynamic quantity from its mean value $\bar{x}$. The equation, so obtained, for $R_{90}{}^o$ (Kerker - 1969) is

$$R_{90} = \frac{2\pi^2}{\lambda_o^4} n^2 \rho_o^2 \left(\frac{dn}{d\rho_o}\right)_T^2 k.T.\beta$$

or

$$R_{90} = \frac{2\pi^2}{\lambda_o^4} \frac{kT}{\beta} n^2 (dn/dP)_T^2 \qquad (2.18)$$

Here β, P and ρ_o are the isothermal compressibility, pressure and density of the liquid respectively at temperature T and k is the

Boltzmann's constant. This allows direct calculation of R_{90} from measurements of β and $(dn/dP)_T$.

2.2.3 Solutions of finite concentration

For solutions of very low concentration, it was possible to consider the particles to be randomly located and independent. In such a case the solution is called an ideal solution and equation (2.14) can be applied directly. But when the concentration is increased the assumption of randomly located particles is not valid. This problem has been solved by Einstein (1910) who extended the method of fluctuation used by Smoluchowski for pure liquid scattering, to include such solutions.

In this case, beside local fluctuations in density, there are local fluctuations in the concentration of the solute. The contribution to the scattering from density fluctuation is usually very small and can be taken as that arising from density fluctuation in the pure solvent. The major contribution arising from fluctuation in the concentration can be accounted for in a treatment similar to that employed by Smoluchowski for scattering from pure liquids, except that the mean square change in the dielectric constant is related to changes in the concentration, which is a thermodynamic quantity. Therefore these changes in the concentration can be related to changes in the free energy which in turn can be expressed in terms of the osmotic pressure P. The equation, so obtained, for R_{90} is

$$R_{90}^{o} = \frac{2\pi^2 \, RTCn_o^2}{\lambda_o^4 \, N_A (\partial P/\partial C)} \left(\frac{\partial n}{\partial C}\right)^2 \qquad (2.19)$$

where R is the gas constant. Equation (2.19) shows that there is a close relation between the scattered light from a solution and its

osmotic pressure. This is to be expected since it is the work done by the osmotic pressure P which causes the fluctuations in the concentration. The molecular weight of the solute can therefore be calculated by using Van't Hoff's general equation for osmotic pressure:

$$\frac{P}{RT} = \frac{C}{M} + BC^2 \qquad (2.20)$$

where B is termed the second virial coefficient. Combining (2.19) and (2.20) and rearranging we obtain the relationship:

$$\frac{K'C}{R_{90}} = \frac{1}{M} + 2BC \qquad (2.21)$$

K' is the optical constant as defined by eqn. (2.15). Equation (2.21) enables us to investigate concentration dependence effects and reduces to eq. (2.14) when ideal solutions are considered.

Thus the scattering from a solution of small isotropic molecules, arises from two independent types of fluctuations. Local fluctuations in the density which give rise to a scattering governed by the scattering equation of pure liquids applied to the solvent, and local fluctuations in the concentration which result in a scattering that follows eq. (2.21). Since we are interested in the solute molecules to which eq. (2.21) applies, therefore the scattering from the pure solvent is usually deducted from that of the solution. Then data obtained at $\theta = 90^{\circ}$ for solutions of different concentrations, allow a graph of $(K'.C/R_{90}$)against C to be plotted from which values of the molecular weight, M, may be found from the intercept and 2B from the slope.

2.2.4 The relationship between turbidity and light scattering

The attenuation of the incident beam due to the loss of light by scattering is given by the relation

$$I_t = I\, e^{-\tau' \ell} \qquad (2.22)$$

where I_t is the intensity of the transmitted beam, τ' and ℓ are the turbidity and the optical path length of the scattering medium respectively. Assuming $\tau' << 1$ and ℓ is unity, then eq. (2.22) gives

$$\tau' = \frac{I - I_t}{I}$$

Provided that elastic scattering is the only process responsible for the decrease in the incident beam intensity, then the intensity of scattered light over all directions is equal to $(I - I_t)$, i.e.

$$\int_0^{\pi} 2\pi r^2 I_s \sin\theta \, d\theta = \frac{16\pi}{3} R_{90} I = I - I_t$$

Therefore

$$\tau' = \frac{16\pi}{3} R_{90}$$

This relationship between turbidity and the Rayleigh ratio as expressed by eq. (2.23) enables us to rewrite all equations expressing R_{90} in terms of the turbidity of the medium. However, it is a common practice to write these equations in terms of Rayleigh ratio.

2.2.5 Scattering by small, optically anisotropic, particles

The dipole moment induced in small optically isotropic particles is parallel to the electric field vector. However, in the case of optically anisotropic particles the induced dipole will be, except at

special orientation, inclined to the direction of the electric field vector. Therefore the light scattered at $\theta = 90^{o}$ will no longer be linearly polarised, but there will be excess scattering from light polarised, perpendicular to it.

A useful method for measuring the deviation from the ideal case is to measure what is usually called the depolarisation ratio ρ_u. For unpolarised light, and if the observation is made as usual in the horizontal plane, ρ_u is found by measuring the ratio of the horizontal to the vertical component of the scattered light at 90^{o}.

The theory for isotropic particles, discussed in the previous sections, can be used to calculate the molecular parameters if the excess scattering caused by the optical anisotropy is corrected for. Martin (1923) found that the observed intensity at an angle θ must be multiplied by a factor $f(\theta)$ where

$$f(\theta) = \frac{6 - 7\rho_u}{6 + 6\rho_u\left(\frac{\sin^2\theta}{1 + \cos^2\theta}\right)} \qquad (2.24)$$

which reduces at $\theta = 90^{o}$ to

$$f(90^{o}) = \frac{6 - 7\rho_u}{6 + 6\rho_u} \qquad (2.25)$$

as found earlier by Cabannes (1920). The factor $f(90^{o})$ is usually known as the Cabannes' correction factor.

2.3 Scattering by Large Particles (Rayleigh-Debye Theory)

2.3.1 The large particle scattering factor $\overline{P(\theta)}$

The following theory has generally been termed Rayleigh-Gans theory. Actually the contribution of Gans in this respect was hardly

significant and it seems more appropriate to call it Rayleigh-Debye theory (Kerker - 1969, p.414). In the Rayleigh-Debye approach, the large particle is subdivided into volume elements which are small enough to be treated as Rayleigh scatterers excited by the electric field of the incident light wave. The light scattered from these volume elements reaches an observer having different phases and as a result destructive interference takes place. Thus a reduction in the scattered intensity takes place. As Fig. (2.2) shows the magnitude of this effect depends on the angle of observation θ. It does not exist at $\theta = 0$ and increases with θ. Thus the scattered intensity at an angle θ is reduced by a factor $\overline{P(\theta)}$ usually called the particle scattering factor. Obviously $\overline{P(\theta)}$ is given by

$$\overline{P(\theta)} = \frac{\text{scattered intensity for large particle}}{\text{scattered intensity without interference}}$$

Since at $\theta = 0$ the scattered intensity is not affected by this intramolecular interference therefore we expect that the equations derived for the scattering by small particles can be used when the results are extrapolated to $\theta = 0$. However while with small particles it is sufficient to measure the scattered intensity at one angle, with large particles it is necessary to measure the scattered intensity at several angles and extrapolate the results to zero angle in order to obtain the molecular weight. Fortunately it turns out that the intramolecular interference depends on the distances between the individual volume elements and on their distribution within the particle , i.e. on the size and shape of the particle. Therefore it is possible to obtain additional information on the shape and size from the angular dependence

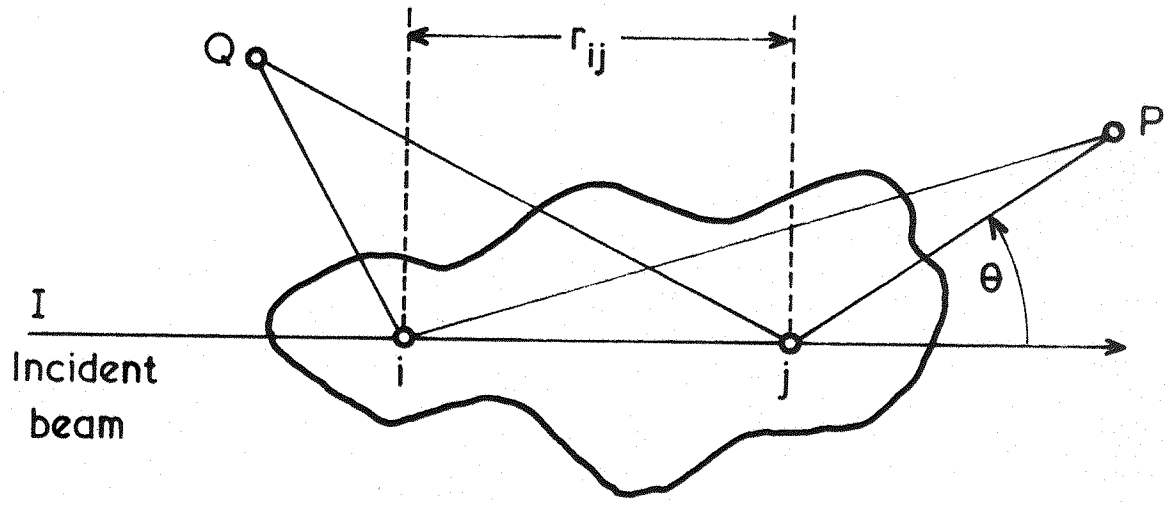

Fig. 2.2 Shown is light scattered from two volume elements (i and j) of a large particle in two directions (P and Q). There is no phase difference between the light scattered from these two elements in the forward direction (i.e. when $\theta = 0$). However there is phase differences (due to the difference in the optical path) in direction P and Q, it is evident that the phase difference increases with the angle of observation θ.

of the scattered intensity.

Within the limits of the Rayleigh-Debye theory, $\overline{P(\theta)}$ decreases smoothly from unity at $\theta = 0^{o}$ to $\theta = \pi$ and is similar in form to that derived by Debye (1915) in connection with X-ray scattering. For an isolated particle fixed in space $P(\theta)$ [$\overline{P(\theta)}$ denotes the average of $P(\theta)$] is given by the Debye equation:

$$P(\theta) = \frac{1}{\sigma^2} \sum_{i=1}^{\sigma} \sum_{j=1}^{\sigma} \cos(k\, \bar{s}.\bar{r}_{ij}) \qquad (2.26)$$

Here σ is the number of scattering elements, $\bar{r}_{ij}$ is the vector leading from the ith to the jth point, k is the wave number and $\bar{s}$ represents a vector of magnitude 2 sin $\theta/2$ and given by

$$\bar{s} = \bar{a} - \bar{b}$$

where $\bar{a}$ and $\bar{b}$, see (Fig. 2.3), are unit vectors in the directions of the incident and scattered beam respectively.

Eq. (2.26) gives $P(\theta)$ for a particle fixed in space. However, in a solution the particles are either randomly orientated relative to a specified direction or orientated to some degree by an external force.

In both cases we are interested in the average value of $P(\theta)$ over all possible orientations. The average of $P(\theta)$, call it $\overline{P(\theta)}$, is obtained by averaging eq. (2.26). Thus

i) For a random distribution the Debye equation is

$$\overline{P(\theta)} = \frac{1}{\sigma^2} \sum_{i=1}^{\sigma} \sum_{j=1}^{\sigma} \frac{\sin(k\bar{s}.\bar{r}_{ij})}{k\bar{s}.\bar{r}_{ij}} \qquad (2.27)$$

ii) For particles partially orientated by an external force, the existing statistical distribution of the particles must be found

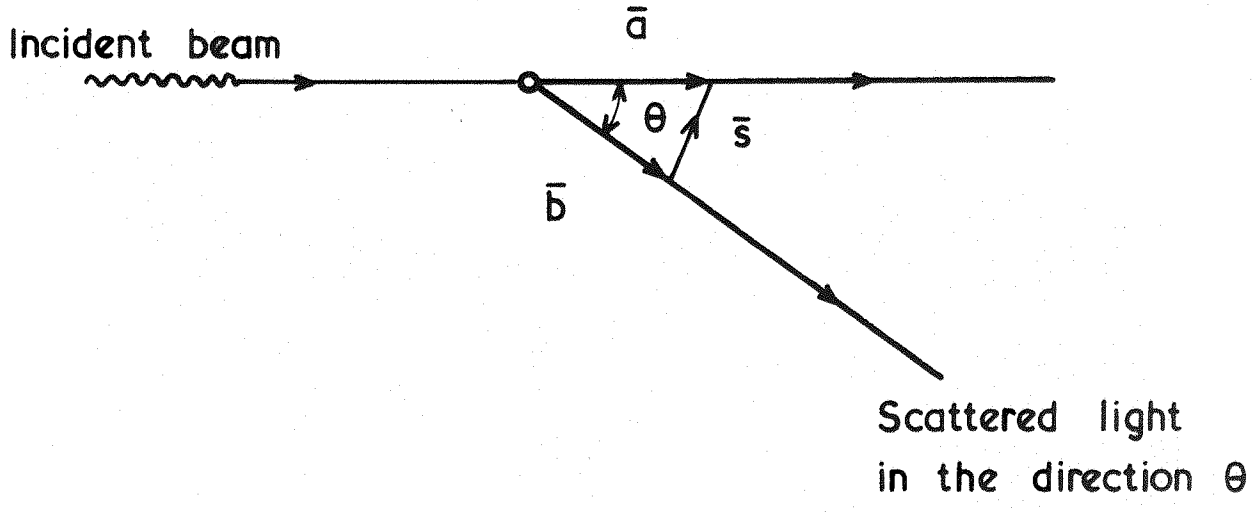

Fig. 2.3 Direction and magnitude of $\bar{s}$ (see text).
$\bar{a}$ and $\bar{b}$ are unit vectors in the direction of the incident and the scattered light respectively.

first and then eq. (2.26) can be averaged to give $\overline{P(\theta)}$. This problem will be the subject of Chapter 3.

The fundamental approximation in the Rayleigh-Debye approach is that the phase difference between light scattered from different parts of the particle be negligible, i.e.,

$$2ka(m-1) << 1 \qquad (2.28)$$

where"a"is the largest dimension through the particle. Therefore neither the particle size nor the relative refractive index can become too large. To be more specific the Debye equation applies only to solutions of low concentrations of mono-disperse optically isotropic particles of size and refractive index governed by eq. (2.28). It also applies to optically anisotropic particles when the optical anisotropy itself is small (Horn -1955).

Most important of all is that the radius of gyration ρ can be determined without any prior assumption regarding the shape of the particle. By expanding the function $\sin \bar{ks}.\bar{r}_{ij}$ in the Debye equation into a power series and dropping higher order terms under the limiting condition of small (θ), Guinier (1939) has shown that

$$P(\theta)_{\theta \to o} = 1 - \frac{k^2 s^2 \rho^2}{3} \qquad (2.29)$$

This is a unique result as there is no other physical technique in which the radius of gyration can be determined precisely without the assumption of any supplementary hypothesis. Since the radius of gyration assumes very different values for particles of different configurations therefore by knowing the radius of gyration the determination of the shape of the particles under investigation becomes relatively simpler.

It is clear that for a very dilute solution of large particles

the reduced intensity R_θ is

$$R_\theta = K'CM\,\overline{P(\theta)}(1 + \cos^2\theta) \tag{2.30}$$

Thus the scattering equation at infinite dilution is

$$\frac{K'C}{R'_\theta} = \frac{1}{M\,\overline{P(\theta)}} \tag{2.31}$$

where $R'_\theta = \dfrac{R_\theta}{1 + \cos^2\theta}$

2.3.2 Methods of investigating large particles by the light scattering technique

The investigation of large particles by the light scattering technique is usually carried out according to one of two widely used methods.

i) The first method was suggested by Zimm (1948b). For solutions of finite concentrations Zimm (1948a) has shown that to a close approximation the scattering equation is:

$$\frac{K'C}{R'_\theta} = \frac{1}{M\,\overline{P(\theta)}} + 2BC \tag{2.32}$$

Therefore in the limit of zero angle where $\overline{P(\theta)} = 1$

$$\frac{K'C}{R'_\theta} = \frac{1}{M} + 2BC \tag{2.33}$$

On the other hand, in the limit of zero concentration and at sufficiently low angles so that Guinier equation, eq. (2.29), is valid

$$\frac{K'C}{R'_\theta} = \frac{1}{M}\left(1 + \frac{k^2 s^2 \rho^2}{3}\right) = \frac{1}{M}\left(1 + \frac{16\pi^2}{3\lambda^2}\rho^2 \sin^2\theta/2\right) \qquad (2.34)$$

Finally, in the limit of both zero angle and zero concentration

$$\frac{K'C}{R'_\theta} = \frac{1}{M} \qquad (2.35)$$

Thus the molecular weight, M, can be evaluated from (2.35), B the second second virial coefficient of interaction can be evaluated from the slope of a plot of $K'C/R'_\theta$ vs. C with the aid of (2.33) and knowledge of M, and ρ can be evaluated from the slope of a plot of $K'C/R'_\theta$ vs. $\sin^2\theta/2$ with the aid of (2.34).

In practice the scattered intensity is measured as a function of the angle θ (usually between 30^o and 145^o) at different concentrations. Then curves representing $K'C/R'_\theta$ vs. $\sin^2\theta/2 + gC$ are drawn. The constant g is chosen to give convenient spread of the results. If the lines which represent observations at constant angle and those which represent observations at constant concentration are drawn, a gridlike plot, known as the Zimm plot (see Fig. 2.4) is obtained. By extrapolating to zero concentration and zero angle and joining the points of zero concentration and separately of zero angle two curves are obtained. The two curves have the same intercept, 1/M, and the initial slope of the curve given by (2.34) gives the radius of gyration while that of the curve given by (2.33) gives B. So it is possible to determine the molecular weight, the radius of gyration which is related to the particle configuration, and the second virial coefficient which indicates the kind of interaction taking place between the particles and the solvent.

The effects of the choice of the value of g upon the precision of the results has been studied by Böel and Elrich (1966). They found that there is an optimal value for "g", g_{opt} , which may be chosen in

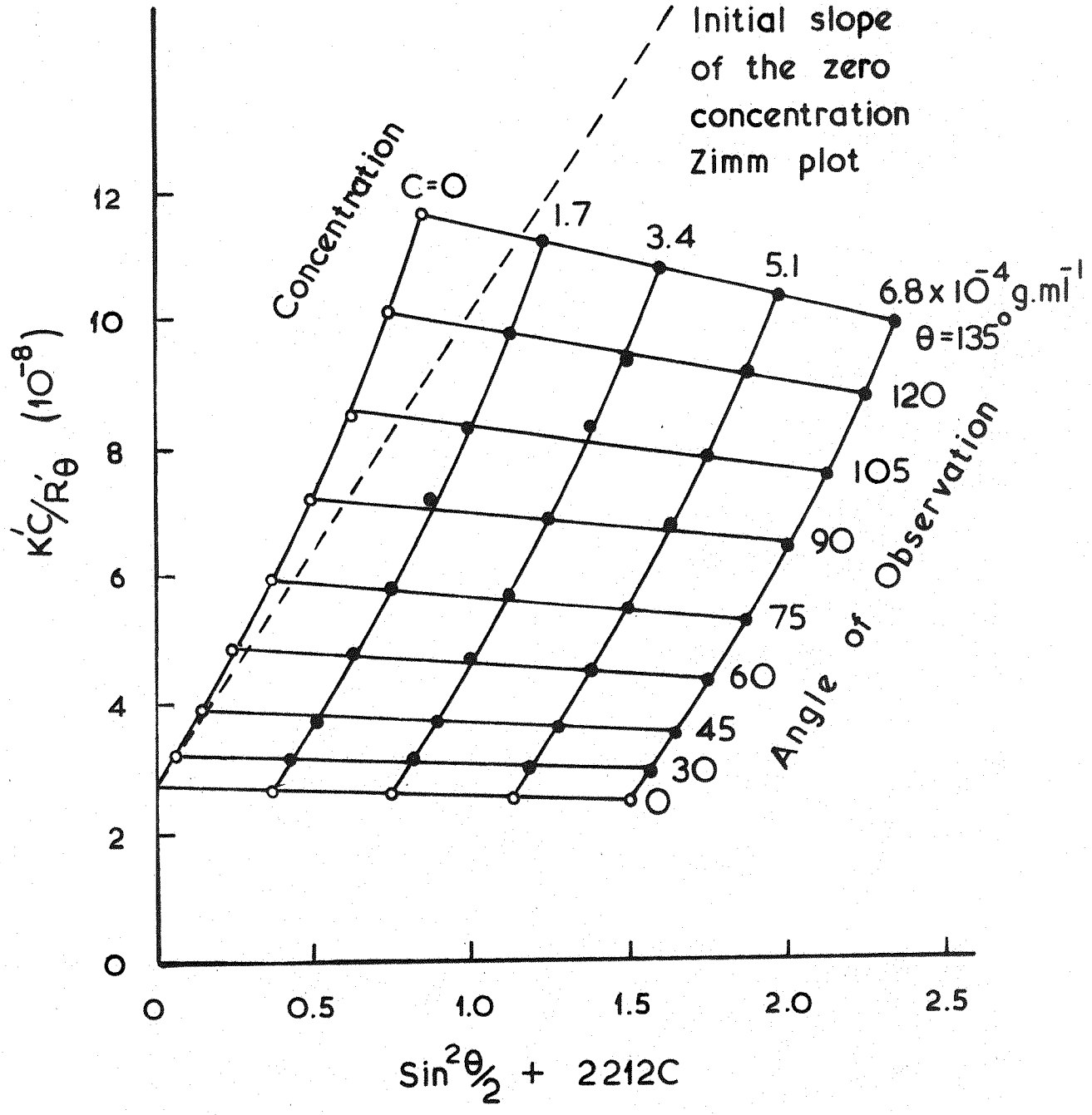

Fig. 2.4 A typical Zimm plot (Details are given in Chapter 7, sec.7.4).

● Experimental o Extrapolated

order to give the best interpretation of the data. However the calculation of g_{opt} is fairly lengthy and its use is not justified with a manually constructed Zimm plot for which it is sufficient to make $gC \simeq \sin^2\theta_{max}/2$.

ii) The second method was suggested by Debye (1947) and known as the dissymmetry method. The dissymmetry Z is defined as the ratio of intensity scattered at two different angles symmetrical about 90^o. Thus

$$Z(\theta) = \frac{R_\theta}{R_{(180-\theta)}} = \frac{\overline{P(\theta)}}{\overline{P(180-\theta)}} \qquad (2.36)$$

The method is based on the fact that $\overline{P(\theta)}$ is a single valued function and two values are enough to characterise it. Therefore, provided we have a previous knowledge of the particles configuration, the measurement of the dissymmetry could give definite information about their size. This can be illustrated with the aid of Fig. (2.5) where the 45^o dissymmetry for spheres, random coils and rods is plotted against a/λ('a'is the particle's largest linear dimension). It is seen that, for a specific shape, $Z(45^o)$ increases rapidly with increasing particle size. Also $Z(45^o)$ assumes very different values for different particle shapes when their characteristic dimensions are the same. Thus measuring Z, the size of the particles in question can be obtained from suitable graphs or tables such as those given by Stacey (1956) or by Beattie and Booth (1960). However these tables are for ideal solutions and therefore the dissymmetry is measured at several concentrations and the results are extrapolated to obtain the value of Z at zero concentration. A drawback of the method described above is that it assumes previous knowledge of the configuration.

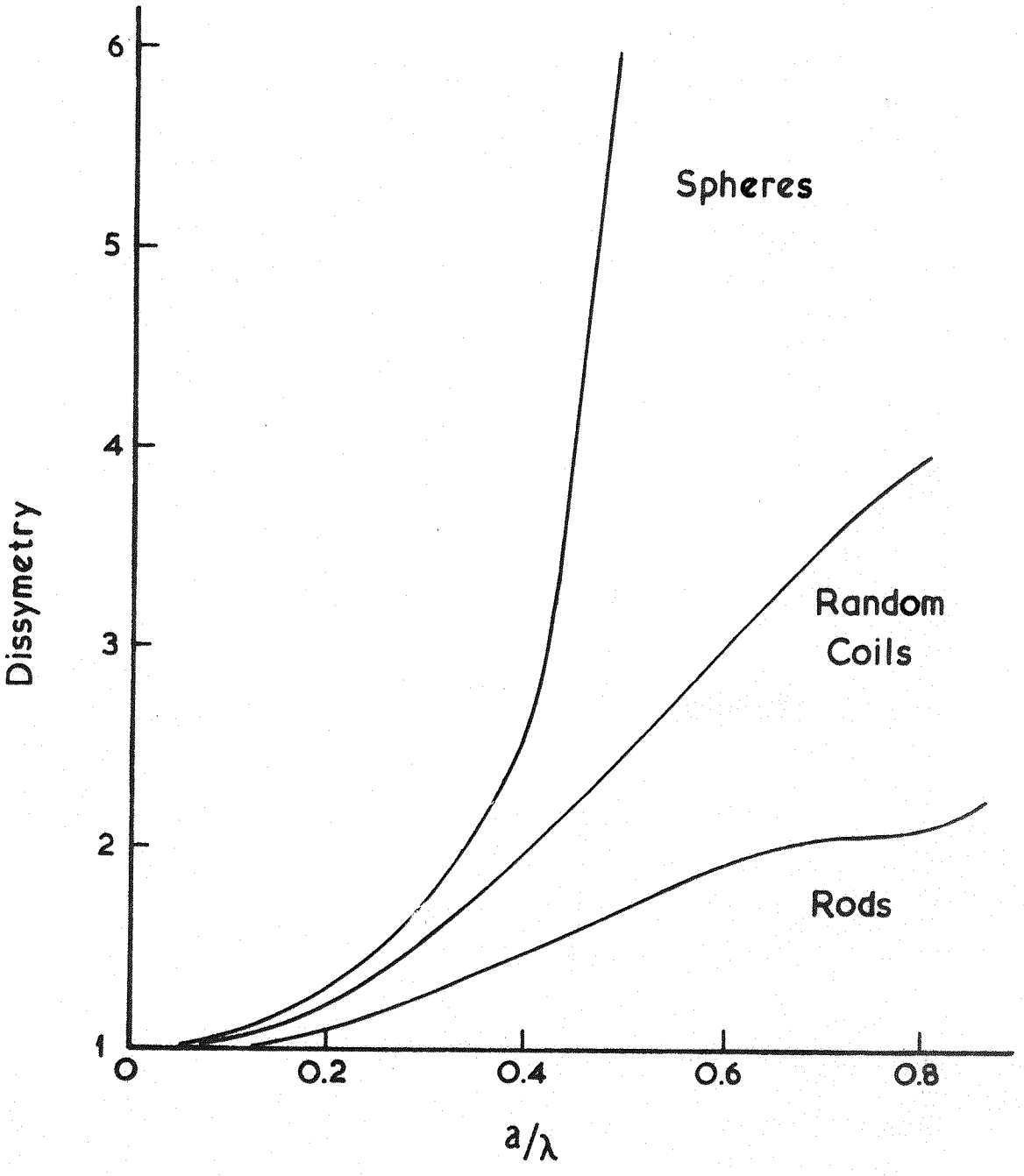

Fig. 2.5 Dissymmetry at 45° relative to 135° plotted against the relative characteristic length a/λ for spheres random coils and rods.

2.3.3 Further information from the light scattering technique: Determination of the particle scattering factor.

It has been shown in the previous section that the zero concentration Zimm plot leads to the evaluation of the radius of gyration and the molecular weight without any supplementary assumption concerning the shape of the particles. Furthermore since this plot is given by

$$\frac{K'C}{R'_\theta} = \frac{1}{M\,\overline{P(\theta)}}$$

the form of the reciprocal of $\overline{P(\theta)}$ is identical to that of the zero concentration Zimm plot and the experimental data can very easily be converted into $\overline{P(\theta)}$ or to its reciptocal $\overline{P(\theta)}^{-1}$. As $\overline{P(\theta)}$ is related to the configuration of the particle, it is possible at least in principle to obtain information about the structure of the particles by direct comparison between the experimental and the theoretical data. This comparison requires the evaluation of the $\overline{P(\theta)}$ function for the system under investigation i.e. solving the general Debye equation that relates $\overline{P(\theta)}$ to the configuration:

$$\overline{P(\theta)} = \frac{1}{\sigma^2} \sum_{i=1}^{\sigma} \sum_{j=1}^{\sigma} \frac{\sin(\bar{ks}.\bar{r}_{ij})}{\bar{ks}.\bar{r}_{ij}} \qquad (2.27)$$

Thus the explicit form of $\overline{P(\theta)}$ has been obtained for a large number of configurations. In fact in this field of the light scattering theory most efforts have been made mainly in this direction and the theory has been developed to a high degree of perfection. (c.f. Kratohvil - 1972)

2.3.4 The $\overline{P(\theta)}$ functions for basic particle shapes

The three basic particle shapes which were considered first are: homogeneous spheres, thin rods and linear Gaussian coils. The latter is the most important in polymer chemistry since a large number of

unbranched chain macromolecules meet to a greater or smaller extent the structural prerequisites of a Gaussian coil.

The explicit form of $\overline{P(\theta)}$ for a sphere of diameter D as given by Rayleigh (1911) and later by Gans (1925), is

$$\overline{P(\theta)} = \left[\left(\frac{3}{x^3} \right) (\sin x - x \cos x) \right]^2 \qquad (2.37)$$

where $x = \frac{2\pi D}{\lambda} \sin \theta/2$

For a thin rod of length L Neugbauer (1943) found

$$\overline{P(\theta)} = \frac{1}{x} \, si(2x) - \left(\frac{\sin x}{x}\right)^2 \qquad (2.38)$$

where $si(2x) = \int_0^{2x} \frac{\sin v}{v} \, dv$

and $x = \frac{2\pi L}{\lambda} \sin \theta/2$

For a flexible unbranched chain Debye (1947) has shown that

$$\overline{P(\theta)} = \frac{1}{x^2} (e^{-x} + x - 1) \qquad (2.39)$$

Here $x = \frac{k^2 s^2 \overline{r^2}}{6}$ where k is the wave number, $s = 2 \sin \theta/2$ and $\overline{r^2}$ is the mean square of the end-to-end distance.

The numerical values of the $\overline{P(\theta)}$ function for these three basic shapes for many different values of the parameter x were calculated by Doty & Steiner-1950(see also Beattie & Booth-1960) and are illustrated in fig.(2.6).

Many other models of compact bodies have also been considered such as: discs (Kratky and Porod - 1949), ellipsoids of revolution (Saito and Ikeda - 1951), cylinders (Saito and Ikeda - 1951 and

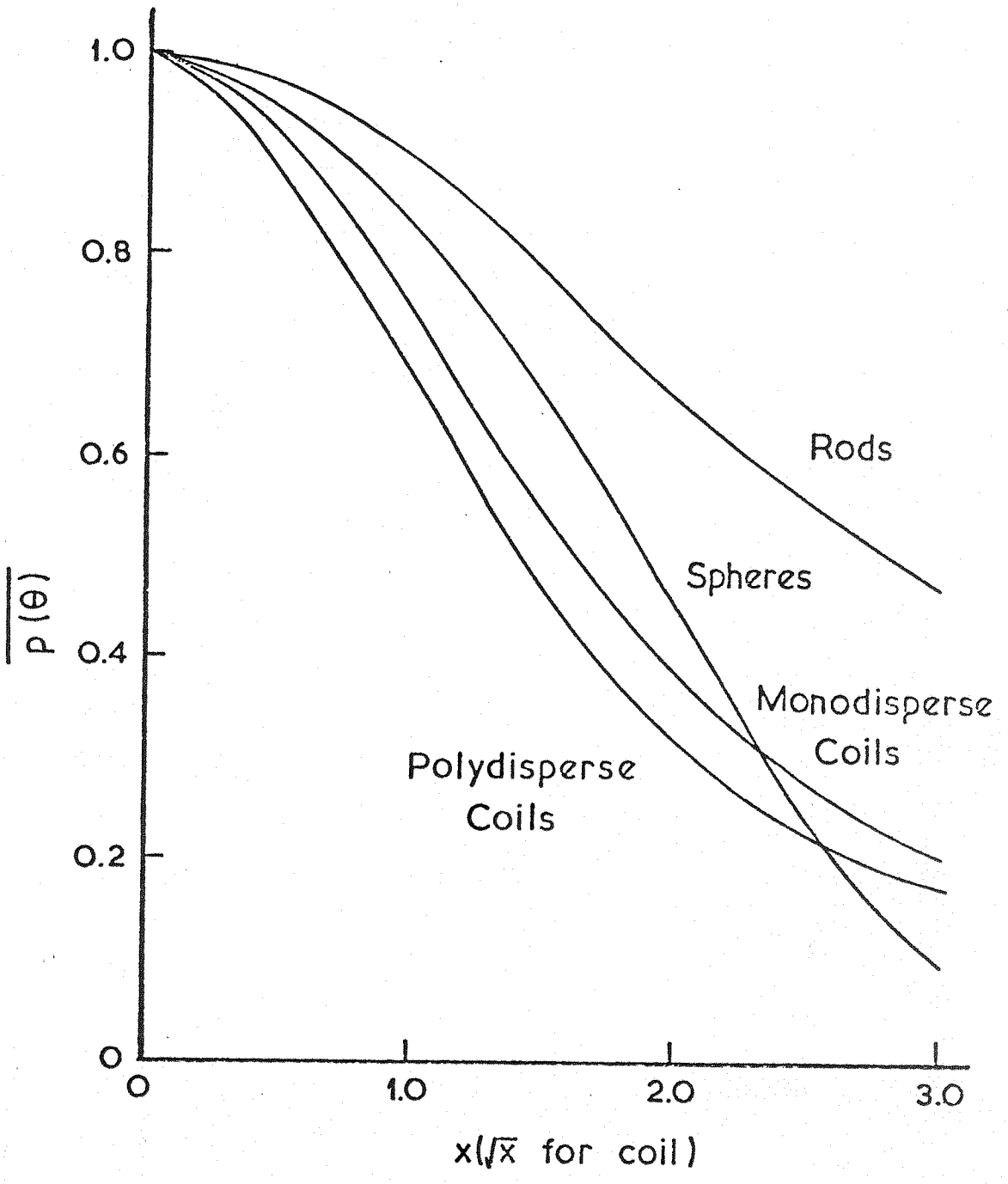

FIG. 2.6 Particle scattering factors for spheres, rods and monodisperse and polydisperse randomly kinked coils

Beidl et al - 1957), cubic particles (Napper and Ottewill - 1963), regular octahedral and square pyramids (Napper - 1968).

Due to a number of factors some polymers do not behave as perfectly flexible chains (Gaussian chains). Hence expressions have also been obtained for several non Gaussian chains. Allowance has been made for the effects on the $\overline{P(\theta)}$ function of chain stiffness, excluded volume, chain branching, polydispersity and optical anisotropy of the individual segments. The analysis of Ptitsyn (1957) shows that the excluded volume when operative causes a downward curvature in the reciprocal of $\overline{P(\theta)}$ at the higher angles of observation. A similar effect can also be introduced by chain stiffness (Peterlin - 1953a, b and 1963) and by polydispersity (sec 2.4). Thus in practice a severe limitation is imposed in the application of the theories discussed so far to experimental results except in the case of very well defined polymer samples.

2.4 Polydispersity

So far it has been assumed that the particles are all alike. However, in most cases the particles under examination are not all of uniform mass and dimensions. Such samples are termed polydisperse. Other sources of polydispersity are aggregation, impurities and dust. Thus the molecular weight obtained is an average molecular weight. The kind of average depends on the technique employed.

The molecular weight common averages are: The number average M_n, the weight average M_w, the Z average and the Z+1 average. These averages are defined by

$$M_n = \sum M_i N_i / \sum N_i$$

$$M_w = \sum M_i^2 N_i / \sum M_i N_i$$

$$M_Z = \sum M_i^3 N_i / \sum M_i^2 N_i$$

$$M_{Z+1} = \sum M_i^4 N_i / \sum M_i^3 N_i \qquad (2.40)$$

where N_i represents the number of gramme molecules per unit volume of molecular weight M_i. These averages can also be defined in terms of the concentration C_i where

$$C_i = M_i N_i \qquad (2.41)$$

For a polydisperse system of infinite dilution the total scattering from all individual species is

$$R'_\theta = K' \sum C_i M_i \overline{P_i(\theta)} \qquad (2.42)$$

where $\overline{P(\theta)}_i$ is the scattering factor for the particles whose molecular weight is M_i. As $\theta \to o$ the scattering factor becomes unity and eq. (2.42) reduces to

$$\begin{aligned} (R'_\theta)_{\theta \to o} &= K' \sum C_i M_i \\ &= K' C \sum M_i^2 N_i / \sum M_i N_i \\ &= K' C M_w \end{aligned} \qquad (2.43)$$

Thus the light scattering technique leads to a weight average molecular weight.

On the other hand for a polydisperse system in the limit $\theta \to o$

$$\overline{P(\theta)} = 1 - \left(\frac{k^2 s^2}{3}\right) \sum \rho_i^2 M_i^2 N_i / \sum M_i^2 n_i$$

Since the radius of gyration is related to the molecular weight in a definite manner for any given shape, therefore the average of the radius of gyration will differ for different shapes. For example, it is a Z average for random coils and thin disclike particles and a $(Z.\overline{Z+1})^{\frac{1}{2}}$ average for thin rods.

A very general effect of polydispersity is to introduce a downward curvature at the higher angles of the zero concentration Zimm plot (or into the reciprocal of $\overline{P(\theta)}$). This is because the light scattered from the larger particles decreases with the angle of observation more rapidly due to stronger intramolecular interference than the light scattered by the smaller particles and the contribution of the latter becomes more significant the higher the angle of observation. As mentioned before (sec. 2.3.4) such a downward curvature might be caused by some other factors which renders the analysis intractable except for very well defined samples.

For the case of polydisperse systems, which effectively can be considered to consist of very large particles, the zero concentration Zimm plot can also be used to obtain the number averages of both the molecular weight and the radius of gyration for certain molecular shapes. Benoit (1953) and Benoit et al (1954) have shown that for a randomly coiled polymer the asymptotic intercept and slope can be used to evaluate both M_n and ρ_n, see fig. (2.7). The asymptotic behaviour of the $\overline{P(\theta)}^{-1}$ function for rods of uniform cross section has also been analysed by Holtzer (1955). However very often the asymptotic part of $\overline{P(\theta)}^{-1}$ cannot be realised experimentally, [Kratohvil (1966b), Carpenter (1966) and Shultz and Stockmayer (1969)] in particular for systems with a rather high polydispersity.

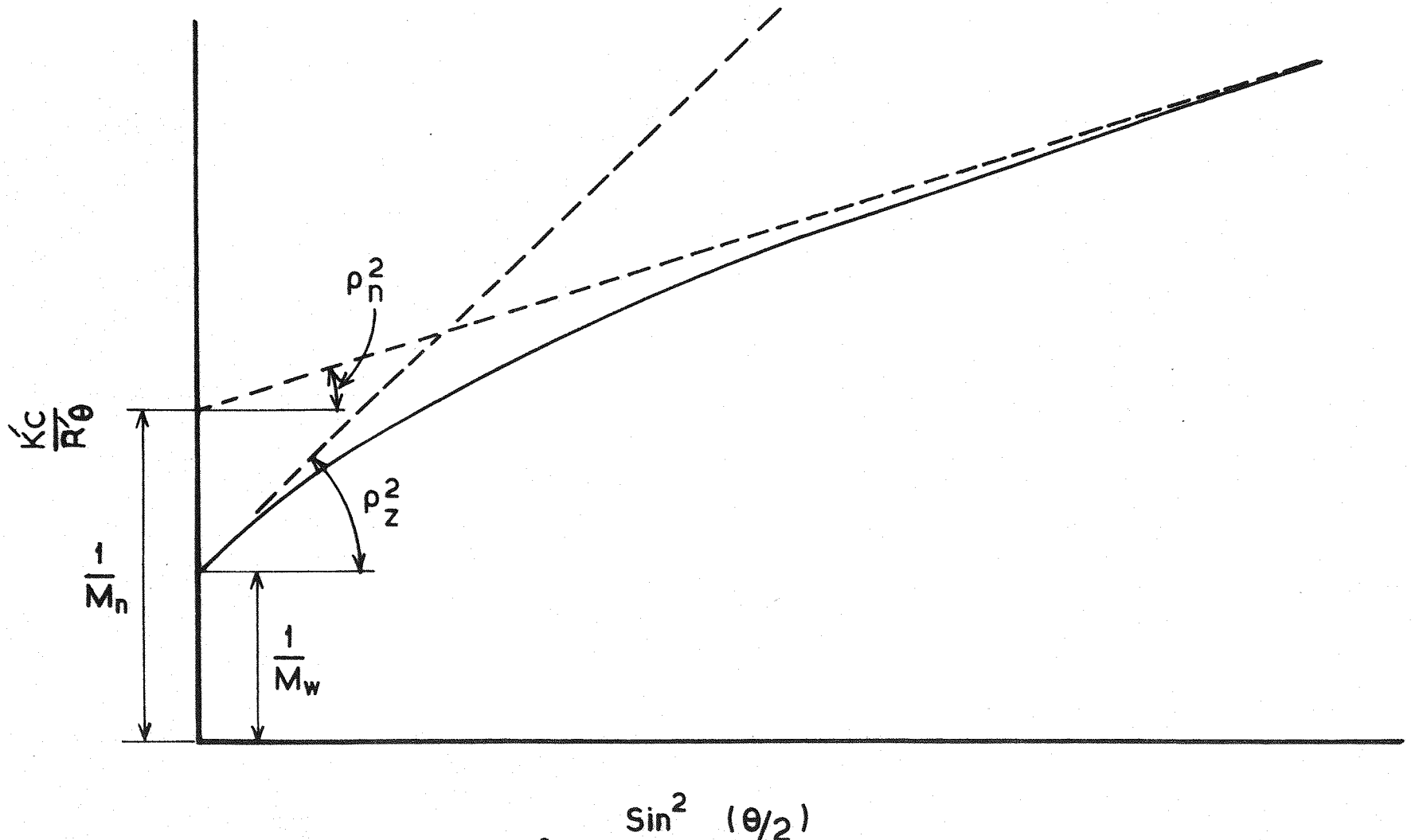

Fig. 2.7 Schematic plot of $K'C/R'_\theta$ against $\sin^2(\theta/2)$ for a polydisperse system at randomly coiled macromolecules. The initial intercept and slope give the weight average molecular weight (M_w) and the Z-average radius of gyration ρ_z. The asymptotic intercept and slope give the number average molecular weight (M_n) and the number average radius of gyration ρ_n (Benoit et al 1954).

CHAPTER III

THEORY OF LIGHT SCATTERED BY MACROMOLECULAR SOLUTIONS IN THE PRESENCE OF ELECTRIC FIELDS

3.1 Introduction

The particle's scattering factor depends on both the shape and the spatial orientation of the particles; and it is a measure of the scattered intensity, (Chapter 2, Section 2.3). Therefore by applying an orientating mechanism capable of altering the normally existing random orientation of the particles in the solution, a change in the scattered intensity (except for spherical particles) takes place. Measurement of these changes enables us to obtain even more information about the particles with little or no more extra treatment of the solution.

Variations in the intensity of scattered light, by macromolecular solutions subjected to the action of an orientating field, have been observed for the first time by Bloch (1908) for an aerosol of aluminium chloride subjected to a direct current electric field. However, Wippler (1953-7) was the first to carry out systematic theoretical and experimental work when molecular orientation was due to electric fields. By using the theories of Peterlin & Stuart (1943) and Benoit (1951) of macromolecular orientation by electric fields of low intensity, Wippler developed expressions for changes in the scattered intensity for rigid rods when subjected to d.c. or a.c. fields and for rigid and flexible macromolecular chains (in which the dipole moment of each segment of the chain follows the chain contour)when subjected to d.c.

fields. Wippler also gave a formula for the decay of the scattered intensity after the removal of the electric field which is similar to that given by Benoit for the birefringence decay of rigid spheroids.

More recently, the theory for rigid rods was extended by Stoylov (1966) to include the use of d.c. electric fields of sufficiently high intensity to cause complete orientation and by Sokerov and Stoimenova (1974) who derived expressions for the transients arising from the sudden application and removal of such electric fields. Also the theory of macromolecular chains was extended by Wallach and Benoit (1966) to include the case where the dipole moments of the segments are no longer reconstrained to follow the chain contour. Furthermore, expressions were developed for the scattered intensity from thin discs when subjected to d.c. and a.c. fields of low intensity by Stoylov (1967) and Jennings et al (1970) respectively.

In all the previous theories the solutions are assumed to be mono-disperse (or poly-disperse if modifications are made) and sufficiently dilute so that the interaction effects between the particles can be neglected. It is also assumed that the particles are optically isotropic and their size and refractive index obey the restrictions imposed by the Rayleigh-Debye theory. Furthermore these theories are for electrically non conducting solutions in which case the orientation of the particles is due to the interaction of the applied electric field with either/both a permanent dipole moment associated with the particles or/and a dipole induced in the particles by the electric field itself because the particles are electrically anisotropic.

Another recent development is the analysis by many workers of the intensity changes arising from the application of electric fields on solutions of optically anisotropic particles [Picot et al (1968), Stoylov and Sokerov (1969) and mainly Ravey (1970 and 1972)]. However, the

theory of optically anisotropic particles will not be discussed here since the results to be reported in this work are for particles which have a relatively small optical anisotropy.

The determination of the electric properties and the diffusion constants of particles in solution by measuring the changes in the light scattered intensity have been reported by a number of workers. Wippler (1956 and 1957), Wallah and Benoit (1962 and 1966), Stoylov and Sokerov (1967 and 1968), Hornick and Weill (1971) and Jennings et al (1965 - 1974). This technique has become almost standard for the determination of these parameters and its theory and practice has been reviewed by Stoylov (1971) and by Jennings (1972).

3.2 Scattering by Orientated Rigid, Rod-like Particles

3.2.1 Orientation by d.c. electric fields of low intensity.

In a solution, in the absence of the electric field, all orientations are equally probable. However, when the field is applied, the particles try to align themselves in the direction of minimum potential energy. This is opposed by the Brownian motion and a statistical distribution is achieved. As the scattered intensity, I_s, is proportional to the particles' scattering factor $\overline{P(\theta)}$, which itself is dependent on the statistical distribution of the particles, then a change in the scattered intensity takes place. If $\overline{P_E(\theta)}$ and $\overline{P(\theta)}$ are the values of the particles' scattering factor when it is under the action of the electric field and when there is no field, respectively, then it is seen that

$$\frac{\Delta I_s}{I_s} = \frac{\overline{P_E(\theta)} - \overline{P(\theta)}}{\overline{P(\theta)}} = \frac{\Delta\overline{P(\theta)}}{\overline{P(\theta)}} \qquad (3.1)$$

By using the value of the distribution function,* derived by Benoit (1951), for a suspension of rigid rods subjected to low intensity** d.c. fields, Wippler derived an expression for the change in the particles' scattering factor.

$$\Delta\overline{P(\theta)} = \frac{E^2}{4}(1-3\cos^2\Omega)\left(\frac{\mu^2}{k^2T^2}+\frac{\alpha_1-\alpha_2}{kT}\right)\left[\frac{\overline{P(\theta)}}{3}+\frac{\sin^2 x}{4x^3}-\frac{1}{2x^2}\right] \qquad (3.2)$$

where E is the field strength, μ is the effective permanent dipole moment along the symmetry axis of the rod, α_1 and α_2 are excess electrical polarizabilities along the symmetry and transverse axes respectively and Ω is the angle between the direction of the field and the direction of $\bar{s}$. The direction $\bar{s}$ is the bisectrix to the angle external to the scattering angle θ. Also, $x = 2\pi L/\lambda \sin\theta/2$ where L is the length of the rod.

More recently, Plummer and Jennings (1968) have shown that if the particles have also a considerable permanent dipole moment along the transverse axis, then the term μ^2 in eq. (3.2) should be replaced by $\mu_1^2-\mu_2^2$. Here again, indices 1 and 2 denote symmetry and transverse axes respectively. Thus the contribution to $\Delta\overline{P(\theta)}$ when the orientation is due to a dipole along the symmetry axis (i.e. μ_1) is of opposite sign to that when it is due to a diple across the particle (i.e. μ_2). The same reasoning applies to α_1 and α_2.

Eq. (3.2) indicates that:

1) The changes in the scattered intensity arising from the application of d.c. fields of low intensity are proportional to the square of the

---

* This is the probability of finding a particle in a specified direction at a given time t.

** i.e. where the potential energy caused by the electric field is much less than the thermal energy, kT, of the particles in the solution.

intensity. Thus, the theory is not applicable when these changes show any sign of saturation effects.

2) They also depend on the direction of the applied field through the factor $(1-3\cos^2\Omega)$. Thus the values of $\Delta\overline{P(\theta)}$, $\left[\Delta\overline{P(\theta)}\right]_{\Omega=o}$ and $\left[\Delta\overline{P(\theta)}\right]_{\Omega=90^o}$, under the condition $\Omega = 0$ and $\Omega = 90^o$, respectively, have a ratio R of (-2), i.e.,

$$R = \frac{\left[\Delta\overline{P(\theta)}\right]_{\Omega=o}}{\left[\Delta\overline{P(\theta)}\right]_{\Omega=90}} = -2 \qquad (3.3)$$

This is no longer valid if the particles are deformed in the presence of the field, so that this criterion can be used to distinguish between flexible and rigid particles. The ratio R is known as the rigidity parameter.

3) The measurement of the changes in the scattered intensity due to static fields can not be used for the determination of the electrical parameters (μ and $\alpha_1-\alpha_2$) except when either μ dominates (polar electrically isotropic particles) or when it is absent (non polar electrically anisotropic particles). However, for both of these two special cases it is possible to determine whether the dipole moment (being permanent or induced) is acting along the major axis or perpendicular to it, from the sign of the changes. Jennings (1972) has shown that under the condition of $\Omega = 90$ when the term $(1-3\cos^2\Omega)$ in eq. (3.2) has a value of unity, then $\Delta\overline{P(\theta)}$ is positive if the orientation is due to a dipole moment along the major axis, and negative if it is due to a dipole across that axis. Fortunately, as will be seen immediately, when sinusoidal electric fields are used, then the contribution to the changes in the scattered intensity from both dipoles (permanent and induced) can be separated and thus it is possible to evaluate their

magnitudes and determine their direction relative to the major axis of the rod.

3.2.2 Orientation by sine wave electric fields of low intensity

By using the value of Peterlin and Stuart (1943) for the distribution function in a sinusoidal electric field represented by $E = E_o \sin \omega t$, Wippler derived expressions for $\overline{\Delta P(\theta)}$ in terms of the changes observed in an equivalent d.c. field. Wippler considered two specific cases. In the first case the orientation is due only to the effect of a permanent dipole moment μ along the major axis of the rod (i.e. the case of polar electrically isotropic particles where $\alpha_1 - \alpha_2 = 0$). On the other hand, in the second case the orientation is due only to the effect of an induced dipole moment since the particles are assumed to be non polar ($\mu = 0$) but electrically anisotropic.

The corresponding value of $\overline{\Delta P(\theta)}$ for the case where $\alpha_1 - \alpha_2 = 0$ is given by

$$\overline{\Delta P(\theta)} = \left[\overline{\Delta P_o(\theta)}\right]_\mu \left\{\left(1 + \frac{\omega^2}{4D_\mu^2}\right)^{-1} - \left[\left(1 + \frac{\omega^2}{4D_\mu^2}\right)\left(1 + \frac{\omega^2}{9D_\mu^2}\right)\right]^{-\frac{1}{2}} \sin(2\omega t - \varepsilon_\mu)\right\} \qquad (3.4)$$

Here $\left[\overline{\Delta P_o(\theta)}\right]_\mu$ is the value of the change for such polar particles when a static field of the same effective field intensity (root mean square) is applied (i.e. eq. 3.2 under the condition $\alpha_1 - \alpha_2 = 0$), D_μ is the rotary diffusion constant of these particles, ω is the frequency of the sinusoidal electric field and ε_μ is the phase angle where

$$\tan(\varepsilon_\mu) = \left[\left(\frac{\omega^2}{D_\mu^2}\right) - 6\right]\left(\frac{D_\mu}{5\omega}\right) \qquad (3.5)$$

Similarly the value of $\overline{\Delta P(\theta)}$ for the case where $\mu = 0$

$$\Delta\overline{P(\theta)} = \left[\overline{\Delta P_o(\theta)}\right]_\beta \left[1 - \left(1 + \frac{\omega^2}{9D_\beta^2}\right)^{-\frac{1}{2}} \sin(2\omega t - \varepsilon_\beta)\right] \qquad (3.6)$$

where $\left[\overline{\Delta P_o(\theta)}\right]_\beta$ is the value of the change for a static field of equivalent intensity under the condition $\mu = 0$, D_β the rotary diffusion constant for these non polar particles and ε_β is the phase angle where

$$\tan(\varepsilon_\beta) = -\frac{3D_\beta}{\omega} \qquad (3.7)$$

Thus for these two specific cases the changes in $\overline{P(\theta)}$ consist of both a steady component and a double frequency alternating component. Eq. (3.4) shows that the steady component of the polar particles is frequency dependent through the term $(1 + \omega^2/4D^2)^{-1}$. Thus it has the limiting values of $\left[\overline{\Delta P_o(\theta)}\right]_\mu$ and zero for d.c. and high frequency fields respectively. On the other hand, the steady component for the non polar particles is independent of frequency. Therefore, the frequency dependence of the steady component is an indication of the presence of a permanent dipole moment whose contribution becomes negligible at a high enough frequency. Thus it is possible to determine $\alpha_1 - \alpha_2$ from the asymptotic value of the steady component at high frequency. Jennings and Plummer (1969) have shown that the steady component for the general case when the particles are both polar and electrically anisotropic is the sum* of the two steady components for the two specific cases considered by Wippler. Therefore, it is possible to separate the contribution of each mechanism to the steady component, and so determine μ when the frequency dependence of the steady component is measured. The sign of the changes can also be used to determine the direction of the dipole moments relative to the major axis of the rod.

The frequency dependence of the steady component can also be used to determine D_μ from analysis of the nature of this dependence, or by

* Such summation does not apply to the alternating components given by eqs. 3.4 and 3.6 because they have different phases.

determining the critical frequency F_c at which the frequency dependent contribution to $\overline{\Delta P(\theta)}$ is half of its maximum value. A simple relation exists between F_c and D :

$$F_c = D/\pi = 1/3\pi\tau \qquad (3.8)$$

where τ is the molecular relaxation time.
Clearly, in the case where the particles are non polar then D_β can be obtained only from the frequency dependence of the alternating component.

Of some interest is the case of a mixture of both polar electrically isotropic particles and non polar electrically anisotropic particles, where each type will contribute to the changes in the scattered intensity. However, the contribution to the alternating component from the non polar electrically anisotropic particles predominates at high frequency (see equations 3.4 and 3.6). Thus, the diffusion constant for the polar particles can be obtained from the frequency dependence of the steady component and that of the non polar particles from the measurements of the alternating component at relatively high frequencies.

Finally, the rigidity parameter has a value of -2 as in the case of d.c. fields. It should be noticed that the changes are proportional to E^2. The theory cannot be applied when this criterion is violated.

3.2.3 Scattering from fully orientated rod-like particles

Scheludko and Stoylov (1964) developed a theory for the dependence of the relative changes in the scattered intensity on the strength of the applied electric field. The solution of the resulting general equation, which does not apply to transients of the electric field, is rather complicated and for a full solution computation must be used. However, the rigid rods approximate solutions were obtained by Stoylov

(1966) for several special cases. Of particular interest is when fields of high enough intensity as to cause complete orientation of the particles are used. In this limiting case and when the electric field is perpendicular to the plane of observation, Stoylov found that:

$$\left(\frac{\Delta I_s}{I_s} \right)_{E\to\infty} = \frac{1}{\overline{P(\theta)}} - 1$$

or

$$\left[\overline{P(\theta)} \right]^{-1} = 1 + \left(\frac{\Delta I_s}{I_s} \right)_{E\to\infty} \qquad (3.9)$$

Hence $(\Delta I_s/I_s)_{E\to\infty}$ depends only on the length of the particles L. Therefore, Stoylov proposed the use of the previous relation for the determination of the length of the particles. Clearly, the electric properties of the particles cannot be determined by the use of such high intensity electric fields.

3.3 Scattering By Orientated Disc-shaped Particles

A formula for the changes in the scattered intensity from thin disc-shaped particles caused by the application of low intensity d.c. electric fields has been derived by Stoylov (1967). He found that:

$$\Delta\overline{P(\theta)} = \frac{k^2 s^2 r^2}{180} (1 - 3\cos^2\Omega) \left(\frac{\alpha_2 - \alpha_1}{kT} - \frac{\mu_1^2}{k^2 T^2} \right) E^2 \qquad (3.10)$$

where μ_1 is the permanent dipole moment along the minor (symmetry) axis of the disc, α_1 and α_2 are excess polarizabilities along the minor and the longitudinal axes of the disc, respectively, and r is the radius of the disc. The other symbols (Ω, s and E) have exactly the same meaning as in the case of rod-like particles.

The changes arising from the application of sinusoidal fields have been considered by Jennings et al (1970), who derived the follow-

ing expression for the steady component:

$$\overline{\Delta P(\theta)} = \frac{1}{180}\frac{k^2 s^2 r^2 E^2}{kT}(1 - 3\cos^2\Omega)\left[(\alpha_2-\alpha_1) - \frac{\mu_1^2}{kT(1+\omega^2/4D^2)}\right] \quad (3.11)$$

where ω is the frequency of the applied field and D is the rotary diffusion constant.

There is no equivalent expression for the alternating component which so far has been given only for rigid rods.

Here again, as with rod-like particles, the changes are proportional to E^2, depend on the direction of the field through the term $(1-3\cos^2\Omega)$ and the contribution due to the induced dpiole moment is frequency independent. Also the rigidity parameter, R, has a value of (-2). However, the contribution to these changes from a dipole moment along the symmetry axis is negative in this case, while it is positive for rod-like particles.

It can be easily seen that, as for rods, the dispersion of the steady component can be used for the determination of the parameters: $\alpha_2-\alpha_1$, μ_1 and D. The method of analysing the results is identical to that outlined in Sec. 3.2.2 in connection with rod-like particles.

3.4 Scattering by Particles Subjected to Pulsed Fields

If a step function field is applied on a macromolecular solution, the molecules will attempt to line up to a state of minimum potential energy. On reaching this state they will stay aligned while the field amplitude is constant and return to a state of disorder when the field is removed. If the degree of orientation is sufficiently large, a change in the scattered intensity will take place. However, the molecules take time both to become aligned and also to return to their state

of random orientation. Thus the build up of the change in the scattered intensity and its decay will lag behind that of the field,as shown in fig.3.1. For a mono-disperse solution, Wippler, following the procedure of Benoit (1951),has shown that on removal of the applied field the change in the scattered intensity, $\Delta I_s(t)$, at a given time t, is given by

$$\Delta I_s(t) = \Delta I_s(o)e^{-6Dt} \qquad (3.12)$$

where $\Delta I_s(o)$ is the change in the scattered intensity when the field is cut off, which is taken to be zero time, and D is the rotary diffusion constant. Clearly, a plot of $\ln \Delta I_s(t)/\Delta I_s(o)$ against t will be a straight line with a gradient of -6D from which D may be found.

The effects occurring immediately after the electric field is applied can be described by relationships similar to those obtained for the Kerr effect which will be discussed in the next chapter. The decay of the change in the scattered intensity from poly-disperse solutions is also considered.

Stoylov and Sokerov (1967 and 1968) were the first to report light scattering experiments using pulsed fields to measure the rotational diffusion constant of the tobacco mosaic virus (T.M.V.). The technique has the advantage of eliminating heat and depolarisation effects that accompany the use of a.c. fields with conductive solutions.

3.5 Macromolecular Chains Subjected to Low Intensity d.c. Fields

Two extreme models have been considered by Wippler. The first a Gaussian chain with perfect flexibility so that each segment in the chain can take any orientation with respect to its neighbours. In this

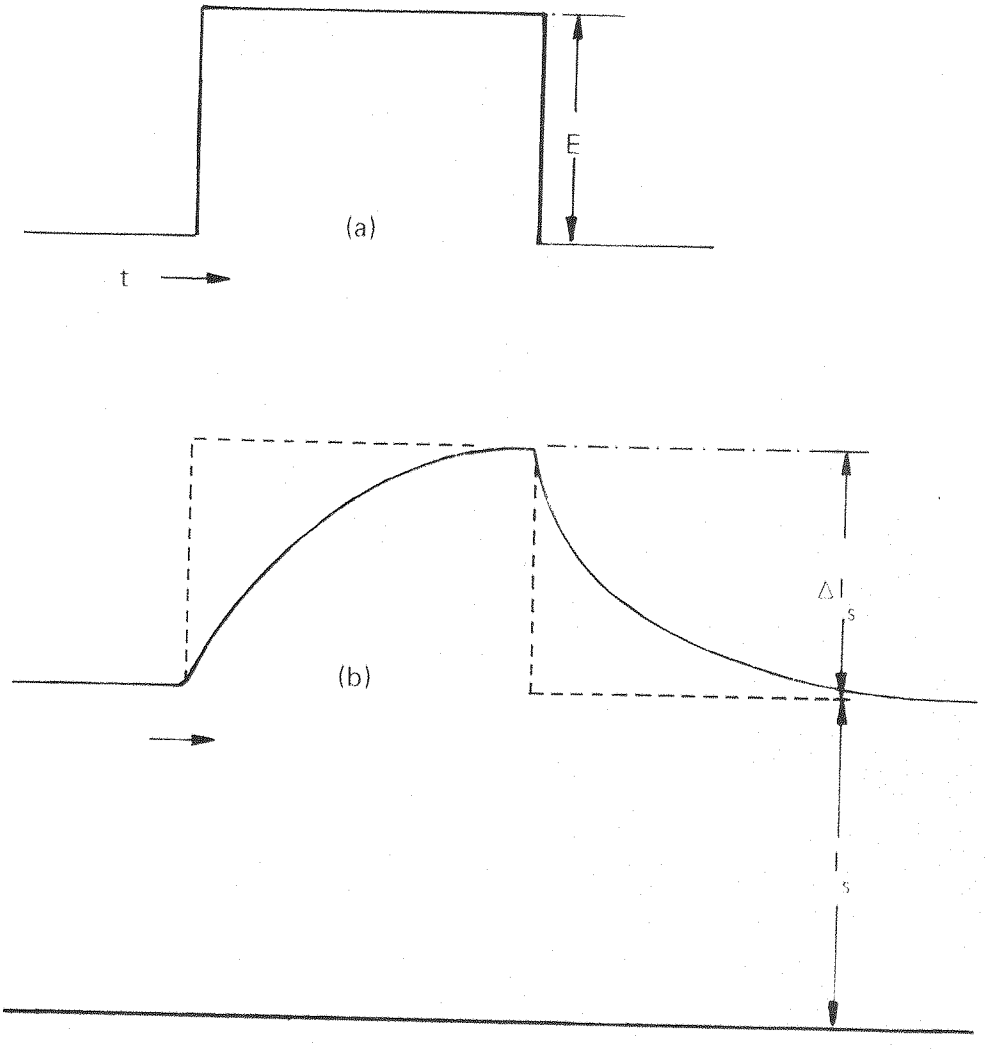

Fig. 3.1 a - Applied electric pulse

b - Rise and decay of the electric light scattering

I_s - scattered intensity in absence of the field

ΔI_s (t=o) - electric light scattering at start of decay

A_1 - area over the rise

A_2 - area under the decay

case, the applied electric field orientates each segment individually and causes a modification of the statistical configuration of the chain. The second is that of a rigid chain in which the rotations of individual segments are completely hindered and the electric field acts on the chain as a single unit. In both models it is assumed that the chain is composed of N identical segments of length b which is small compared to the wave length of light. It is further assumed that for flexible chains the segments are either polar (i.e. having a segmental dipole μ_o which coincides with the major axis of the segment) but electrically isotropic, or non polar but having an electrical anisotropy α_o along the major axis. In addition, for rigid chains, where consideration is restricted to polar types only, it is assumed that the dipole moment μ is proportional to the separation between the ends of the chain.

The expressions derived by Wippler for the changes in the scattered intensity due to the application of weak d.c. electric fields on solutions of such chains are now given:

(a) Rigid chains.

$$\Delta\overline{P(\theta)} = \frac{N^2 b^4 k^2 s^2}{324}(1 - 3\cos^2\Omega)\left(\frac{\mu E}{kT}\right)^2 \qquad (3.13)$$

where k, s and Ω have the same meaning as before. Thus, as with all rigid particles, R = -2.

(b) Flexible polar electrically isotropic chains.

$$\Delta\overline{P(\theta)} = -\frac{N^2 b^2 k^2 s^2}{108}\left(\frac{E\mu_o}{kT}\right)^2 \qquad \text{when } \Omega = 0 \qquad (3.14)$$

$$\Delta\overline{P(\theta)} = \frac{N\, b^2 k^2 s^2}{270}\left(\frac{E\mu_o}{kT}\right)^2 \qquad \text{when } \Omega = 90 \qquad (3.15)$$

Thus R = -5N/2. Since R is proportional to N, which is usually large, then the changes at $\Omega = 90$ are negligible.

(c) Flexible non polar electrically anisotropic chains

$$\overline{\Delta P(\theta)} = \frac{N b^2 k^2 s^2}{270} (1 - 3\cos^2\Omega) \frac{\alpha_o E^2}{kT} \qquad (3.16)$$

Here again as for rigid particles R = -2. However the changes in this case are proportional to N and thus to the molecular weight, M, while for rigid chains it is proportional to the square of M. Therefore by taking measurements on two samples of different molecular weight it is then possible to distinguish whether the chains are rigid or flexible. Usually with flexible chains the changes are small.

More recently Wallah and Benoit (1966) extended Wippler's treatment of polar flexible chains to include firstly the case where the segmental dipole μ_o makes an angle β_o with the segmental major axis, and secondly where the segments are notlonger identical but have alternating dipoles μ_o and μ_1 at orientations β_o and β_1 respectively, with their major axes. They found that for the first model

$$R = -\frac{5N}{2} \frac{1}{1 - \frac{1}{2}\tan^2\beta_o} \qquad (3.17)^*$$

and for the second model

$$R = -\frac{5N}{2} \frac{(\mu_o \cos\beta_o + \mu_1 \cos\beta_1)^2}{\mu_o^2(3\cos^2\beta_o - 1) + \mu_1^2(3\cos^2\beta_1 - 1)} \qquad (3.18)$$

* This is the expression given by Jennings (1972) because that of Wallah and Benoit was found to be incorrect.

Thus for all the models of polar flexible chains that have been considered R is proportional to N, which is a direct result of the fact that $\Delta\overline{P(\theta)}$ is proportional to N^2 when $\Omega = 0$ and to N when $\Omega = 90$. For most polymers N is large and therefore R is usually also large except in special cases e.g. if in eqn. 3.17 $\beta_o = \pi/2$, then R is zero .

It is clear from the previous discussion that the parameter R can be used to indicate the flexibility, and this can be achieved by carrying out two measurements only.

CHAPTER IV

THEORY OF THE KERR EFFECT

4.1 Introduction

Kerr (1875) observed that on the application of an electric field at certain dielectrics, liquids and solutions, they become double refracting. This phenomenon is known as the electro-optic effect, and the substances behave optically like uniaxial crystals with optical axes parallel to the field direction. Double refraction in uniaxial crystals is known to arise from two facts: Firstly the crystal is a very regular well ordered structure and secondly the crystal is built up of units which are optically anisotropic. Both of these conditions must be fulfilled simultaneously as although the optical anisotropy is the cause of the birefringence unless all the units producing this effect are in a regular array their individual contribution may be mutually cancelled. Therefore liquids and solutions cannot normally cause birefringence even if they consist of optically anisotropic matter because of the absence of a regular ordered structure. On the application of the electric field the molecules tend to line up in the field and some degree of order is achieved. This degree of order in a system depends on the field strength and the electric properties of the molecules in the system.

The most important feature of this ordering process is that large molecules take a finite time to line up, when the field is applied, and to return to a state of random array when the field is removed. Therefore the build up and the decay of the birefringence will lag behind that of the applied field. In general therefore, if an electric field in the form of a rectangular pulse is applied, a gradual increase in the

birefringence occurs which may reach a steady value if the pulse duration is long enough, followed by a decay. The observation of the rise and decay can give very useful information. For example, Benoit (1951) related the time taken for the decay of the birefringence to the rotary diffusion constant which in turn is dependent on the molecular size and shape, Perrin (1934). Also a comparison of the decay and the rise time can be used to investigate the mechanism of orientation. Moreover the magnitude of the steady birefringence induced by the electric field will depend on the optical and the electrical properties of the molecules. Theories relating these quantities for fields of low intensity i.e., when the birefringence magnitude is proportional to the square of the electric field intensity, have been given by Langevin (1910), Born (1918), Peterlin and Stuart (1943) and a later theory is due to Benoit (1951). Saturation birefringence theories have been put forward by O'Konski et al (1959) and Shah (1963).

A theory of the Kerr effect which applies to very dilute suspensions of rigid monodisperse unionised molecules in an insulating medium was proposed by Peterlin and Stuart (1943) and has been extended by Benoit (1951) and Tinoco (1955). In those treatments the orientation of the macromolecules is considered to arise from the interaction of the electric field with either/(both) a permanent dipole moment μ associated with the molecule or/(and) a dipole induced by the electric field itself. The macromolecular model for the general case is an ellipsoid of revolution of principal axes a_1, a_2, a_3 along which the refractive indices are n_1, n_2, n_3, the dielectric constants are ε_1, ε_2,ε_3 and the dipole moment, components are μ_1, μ_2, μ_3. The solvent is treated as an insulating isotropic medium of refractive index n_o and dielectric constant ε_o. The electric birefringence arising from the application of sinusoidal

fields was treated by Peterlin and Stuart (1943), Benoit (1951) treated the build up and decay in square pulsed fields for ellipsoids of revolution when the permanent dipole moment is directed along its major axis. This treatment was extended by Tinoco (1955) to include the possibility of a permanent dipole acting across the molecule. Benoit treatment was also extended by Nishinari and Yoshioka (1969) who proposed a theory for the rise of the birefringence which holds for arbitrary field strength. Expressions for the birefringence arising from the action of a reversing* pulse were also obtained by Tinoco and Yamaoka (1959) and by Matsumoto et al. (1970).

For some comprehensive reviews see O'Konski (1968) and Yoshioka and Watanabe (1969).

4.2 The Kerr Law

The electric birefringence, Δn, of a medium is conventionally defined by relation (4.1).

$$\Delta n = n_{\parallel} - n_{\perp} \tag{4.1}$$

where $n_{\parallel}$ and $n_{\perp}$ are the refractive indices for linearly polarised light with its direction of vibration parallel or perpendicular to the applied electrical field respectively. If the wave length of the light in vacuum is λ_o, the corresponding difference of optical path length in wave lengths is given by

$$\frac{L}{\lambda_o}(n_{\parallel} - n_{\perp})$$

where L is the length of the path in the birefringent medium.

Accordingly the optical retardation, δ, in radians, is given by eq. (4.2)

$$\delta = 2\pi L \frac{\Delta n}{\lambda_o} \tag{4.2}$$

For most substances at low electric field intensities Kerr found that

* A square pulse is applied to a macromolecular solution and, after the steady-state birefringence is achieved, the field is rapidly reversed in sign.

the birefringence, at a specified wave length, is proportional to the square of the electric field strength. This relation is known as the Kerr law and can be expressed by eq. (4.3).

$$\Delta n = K\, n\, E^2 \tag{4.3}$$

where the proportionality constant K is known as the Kerr constant and n the mean refractive index of the medium.

The specific Kerr constant K_{sp} of a solution is given by $(K-K_o)/C$ extrapolated to zero concentration, where K_o is the Kerr constant of the solvent, K is the Kerr constant of the solute and C is the concentration. However, if the solute particles are large it is possible to ignore K_o and write

$$K_{sp} = \left(\frac{K}{C}\right)_{C \to o} \tag{4.4}$$

4.3 The Kerr Effect Theory

4.3.1 Rectangular pulses (fields of low intensity).

The most widely used equations are those of Benoit (1951). These equations are:

i - Steady state

$$K_{sp} = \frac{2\pi}{15n^2}(g_1 - g_2)\left\{\frac{\mu^2}{k^2T^2} + \frac{\alpha_1 - \alpha_2}{kT}\right\} \tag{4.5}$$

ii - Birefringence decay*

$$\Delta n(t) = \Delta n(o)\, e^{-t/\tau} = \Delta n(o)\; e^{-6Dt} \tag{4.6}$$

* Benoit suggested that eq. (4.6) is very general, being dependent only on the validity of the diffusion equation. This has also been verified by O'Konski et al (1959).

iii - Birefringence rise

$$K_{sp} = \frac{2\pi}{15n^2}(g_1-g_2)\left[A+B-\frac{3}{2}A\,e^{-r_1Dt} + (\frac{A}{2}-B)e^{-r_2Dt}\right] \quad (4.7)$$

where $\Delta n(t)$ is the birefringence at any time t after the field is cut off, $\Delta n(o)$ is the birefringence at t = 0,

$$r_1 = 2 + E^2(\frac{A}{5} - \frac{2B}{5}) \quad ,$$

$$r_2 = 6 - E^2(\frac{A}{5} + \frac{2}{7}B) \quad , \quad (4.8)$$

$$A = \frac{\mu^2}{k^2T^2} \text{ and } B = \frac{\alpha_1 - \alpha_2}{kT}$$

μ effective dipole moment, k Boltzmann constant, T absolute temp., D rotational diffusion constant and related to the relaxation time τ by

$$\tau = \frac{1}{6D} \quad (4.9)$$

(g_1-g_2) is the optical anisotropy factor. Subscript 1 and 2 refer to the symmetry and transverse axes respectively.

$(\alpha_1 - \alpha_2)$ is the excess polarisability of the solute particles in the solvent.

It is clear from eq. (4.6) and eq. (4.7) that the rise and the decay of the birefringence will be symmetrical when the molecules are non polar (i.e., only distortion polarisation is taking place). This fact can be used in investigating the polarisation mechanism. Moreover, the ratio of the permanent to the induced dipole can be calculated by finding the areas A_1 and A_2 over the rise and under the decay respectively. According to Yoshioka and Watanabe (1963):

$$\frac{A_1}{A_2} = \frac{4r+1}{r+1} \qquad (4.10)$$

where r is

$$r = \frac{\mu^2}{(\alpha_1-\alpha_2)kT} \qquad (4.11)$$

4.3.2 The Kerr effect in a.c. fields of low intensity

For an electric field, represented by $E = E_o \sin \omega t$, the most general expression for the birefringence can be given by

$$\frac{\Delta n}{\Delta n_o} = \left[X + Y \cos(2\omega t - \phi) \right] \qquad (4.12)$$

where ϕ the phase shift is a function of ω and D, Δn_o is the birefringence exhibited under the influence of a static field of the same effective field intensity (root mean square). Eq. (4.12) shows that the birefringence consists of both a steady component X which is time independent and an alternating component Y which alternates at twice the frequency of the applied field. The amplitude of the alternating component Y is always frequency dependent, whereas the component X is frequency dependent only when the molecules are polar. This behaviour is analogous to the behaviour of the changes in the scattered intensity arising from the application of sinusoidal fields. The latter has been discussed earlier, at length (Chapter 3, sec. 3.2.2). There it was noted that the measurement of the frequency dependence of the steady component can be used for the determination of the electrical parameters of the molecules. The dispersion of both the steady and alternating components also leads to the evaluation of the relaxation time of the molecules.

4.3.3 Saturation birefringence

O'Konski et al (1959) have developed the theory of saturation birefringence which like benoit's is based on the work of Peterlin and Stuart.

The expression for the saturation birefringence, Δn_s, derived by O'Konski et al is given by

$$\frac{1}{C}\ \frac{\Delta n_s}{n} = \frac{2\pi}{n^2}(g_1 - g_2) \qquad (4.13)$$

i.e., the saturation birefringence depends only on the optical anisotropy as would be expected.

In their analysis, O'Konski et al assumed that both the permanent and the induced dipole moments were aligned in the same direction. Shah (1963) extended this treatment to the case where these two dipole moments are at right angles to each other. His analysis is for a disc shaped particle which has its permanent dipole moment along the particle symmetry axis and its induced dipole along the semi major axis. His results show that for certain values of the ratio of the permanent dipole to the excess polarisability of the particle, the birefringence undergoes a minimum and, furthermore, exhibits a reversal of the sign of birefringence with increasing field strength.

4.4 Poly-Disperse Systems

For a mono-disperse system of rigid axially symmetric particles the birefringence decay is given by eq. (4.6).

$$\Delta n(t) = \Delta n(o) e^{-t/\tau} \qquad (4.6)$$

$$\text{Hence } \ln \Delta n(t) = -\frac{t}{\tau} + \ln \Delta n(o) \qquad (4.14)$$

Therefore a graph of $\ln \Delta n(t)$ against t (which will hereafter be implied

when reference is made to "log plot" in this work) will be a straight line of slope $-1/\tau$. However, for a poly-disperse system the decay is no longer exponential. The decay for a system composed of k types of particles can be described (Benoit 1951) by the following expression*

$$\Delta n(t) = \sum_{i=1}^{k} \Delta n(o)_i e^{-t/\tau_i} \qquad (4.15)$$

where $\Delta n(o)_i$ is $\Delta n(o)$ for species i whose relaxation time is τ_i. Thus curvature in the log plot indicates poly-dispersity of the sample. Schweitzer and Jennings (1972) have discussed the methods used in analysing these plots, the two most common of which are now described below.

In the first method, the relaxation times determined from the slopes of the initial and end tangent, of the log plot are considered somewhat representative of the smallest and largest particles in the sample respectively; e.g. Golub (1964), Stoylov and Sokerov (1967 and 1968) and Brown et al (1969).

The second method is based on Benoit's equation for the birefringence decay from a poly-disperse system. In this method the non-linear log plot is decomposed into several linear curves each of which leads to the determination of the relaxation time of one of the species in the sample. This method is best explained by considering a system of two components with relaxation times τ_1 and τ_2 ($\tau_2 > \tau_1$): The non-linear curve in this case can be decomposed into two linear curves. The first linear curve is found by extrapolating the end tangent to t = 0 and represents the contribution of the particles with relaxation time τ_2. The second linear curve is obtained by subtracting the first linear curve from the original

---

* For a continuous distribution of rigid macromolecules, or for a flexible macromolecule, an integral form of this expression should be used.

non-linear curve. The method can be generalised to a system composed of more than two components by repetition of the procedure outlined above. However, in practice it is found to be difficult to obtain more than two relaxation times. This method has been used by O'Konski and co-workers (1959a and b) and by Ingram and Jerrard (1963).

The decay of the changes in the scattered intensity for a poly-disperse system can also be described by an equation similar to that of Benoit, viz.

$$\Delta I_s(t) = \sum_{i=1}^{k} \Delta I_{si}(0)\, e^{-t/\tau_i} \qquad (4.16)$$

where $\Delta I_{si}(0)$ is $\Delta I_s(0)$ for species i whose relaxation time is τ_i, $\Delta I_s(0)$ itself is the value of the change in the light scattered intensity at $t = 0$ and $\Delta I_s(t)$ is the value of the change at any time t after the field is cut off.

The methods of analysing such non-exponential decay curves are identical to those used for birefringence decay. However, Schweitzer and Jennings (1972) found that the initial slope determined when using the electric birefringence technique is different from that determined using the electric light scattering technique, and hence the two techniques yield different values of τ.

Finally it should be noted that it is not only poly-dispersity that can cause the decay not to be represented by a single exponential. Both lack of symmetry [Ridgeway (1966 and 1968)] and flexibility of the particles lead to a non-exponential decay. Recently Sokerov and Stoimenova (1974) investigated the transients of the changes in the light scattered intensity for a mono-disperse solution of rigid rods at complete orientation. In this case, the decay is represented by a sum of time

exponentials. This reduces to a single exponential when the particles are relatively short. Thus care must be exercised when applying equations (4.15 and 4.16) to ensure that the type of particles in the solution fulfil the assumptions of the theory.

4.5 Electrically conducting solutions (polyelectrolytes)

So far only electrically non-conducting solutions have been considered. For such solutions it was assumed, by Peterlin and Stuart (1943), that the dipole moments induced in the particles, by the application of the electric field, are the result of local distortion of the charges at various sites within the bulk or body of each particle. i.e. In this case the induced dipoles arise from electron polarisation only.

However, with electrically conducting solutions induced moments may result from charge displacement either on the molecular surface or within any solvent layer which is bound to the particles. This was experimentally verified by several workers (see, O'Konski and Haltner - 1957, Jennings and Jerrard - 1966 and also Stoylov review - 1971). For these solutions the magnitude of the polarisability is considerably greater and has a much larger relaxation time (10^{-5} - 10^{-8} sec. compared to 10^{-14} sec. for the electronic electric polarisability of non conducting solutions).

At present, there is no general theory which can satisfactorily explain the interaction of the applied electric field with the ion atmosphere present around the macromolecules. However, some progress has been made in this direction. Using different procedures both O'Konski (1960) and Schwarz (1962) extended the well known Maxwell-Wagner (1892-1914) theory of dielectric polarisation and dispersion of spherical suspensions to account for the surface conductivity resulting from the displacement of the counter ions under the effect of the electric field. Also a thermo-

dynamic approach was suggested by Oosawa (1970) who calculated the mean square electric dipole moment due to the thermal fluctuation of the bound counter ions.

CHAPTER V

PART A THE LIGHT SCATTERING APPARATUS

PART B THE KERR EFFECT APPARATUS

PART A

5.1 Introduction

The study of a macromolecular solution by the light scattering technique requires the measurement of the Rayleigh ratio, R_θ, defined by eq. (2.13). Numerous light scattering-photometers have been designed and built for this purpose by several workers, e.g. Brice et al (1950), Oster (1953), Wippler and Scheibling (1954), Jerrard and Sellen (1962), Froelich et al. (1963), Chu (1964 and Harpst et al (1968). All these instruments consist basically of an intense light source, some means of collimation or focusing to obtain a well defined or parallel light beam, a cell containing the solution under study, a collimation system for the scattered intensity, and some means of comparing the intensity of the incident and scattered beams.

The light scattering apparatus that was used in this work is essentially that designed and built by Jerrard and Sellen. The description of this apparatus and its operating procedure have been given in detail by Sellen (1962). Therefore it is sufficient here to explain the basis of the method of measuring R_θ using this apparatus, with a brief description of the apparatus itself and the modifications made to it by the present worker.

5.2 Method of Measuring the Rayleigh Ratio R_θ.

In the afore-mentioned apparatus both the incident and the scattered beam are allowed to fall upon the same photomultiplier, P.M. The method of measuring the angular scattered intensity is illustrated in fig. (5.1). The collimated incident or primary beam of intensity I is allowed to pass straight to a collimating unit where it is linearly polarised by a polariser P_1 in the direction 90^o to that of the scattered beam of intensity I_s. The latter is in general partially polarised and since the degree of polarisation is dependent upon the angle of scattering a polariser P_2 is used to completely linearly polarise the scattered beam. P_2 will however attenuate the scattered intensity by different proportions for each angle of observation. To overcome this difficulty a quarter wave plate Q is inserted before P_2 at azimuth of 45^o to the plane of partial polarisation. Finally the two beams pass through a third polarising disc P_3 which rotates with an angular frequency ω. The resultant intensity at the P.M. is given by I_r, Sellen (1962), where

$$I_r = \frac{I + I_s}{2} + \frac{I - I_s}{2} \cos 2\omega t \qquad (5.1)$$

In eq. (5.1) there is a d.c. component and an a.c. component: it suggests the use of the null modulation method of detection. The a.c. component is proportional to the difference in intensities of the two signals. In practice the incident beam is some 10^6 times more intense than the scattered beam. To achieve partial equality in intensity a neutral filter N and a polariser P are inserted before P_1 in the path of the incident beam. The filter plays the role of a coarse attenuator and the polariser is used as a fine attenuator to give equality of the two signals. The attenuation of the beam by P_1 is a function of the angle ϕ between the vibration directions of the two polarisers P and P_1. The

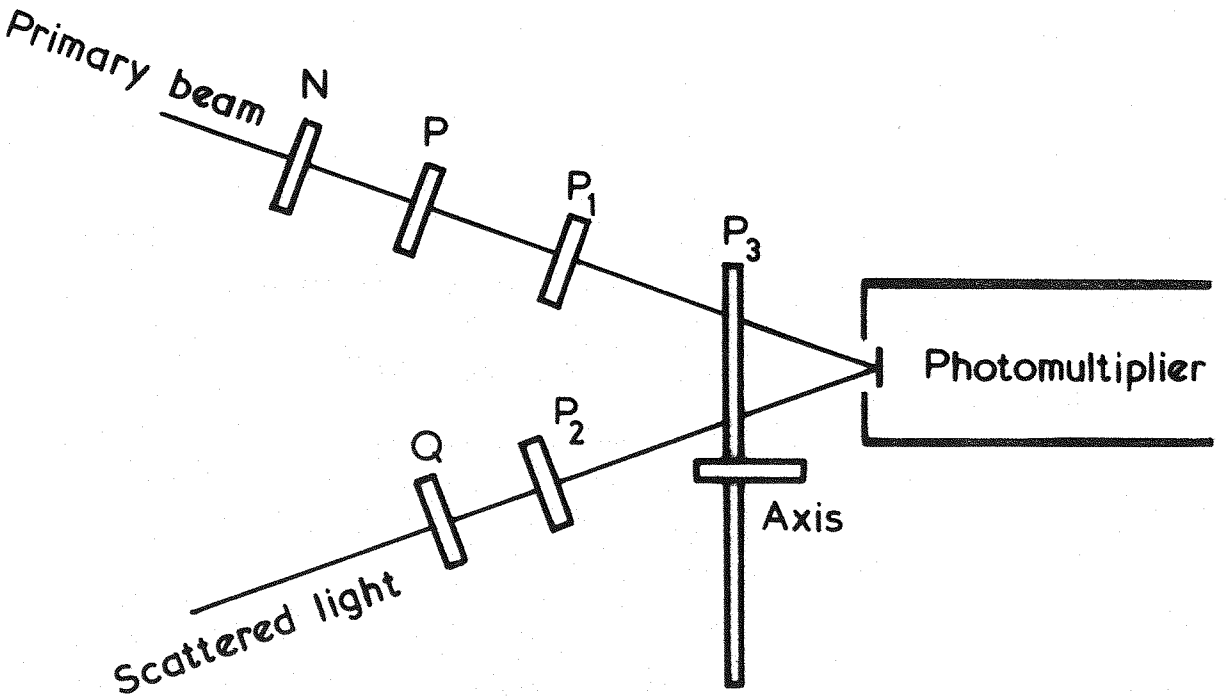

Fig. 5.1 Method of measurement

relative values of I_s are obtained in terms of a function of ϕ, $F(\phi)$, which is not a simple $\cos^2\phi$ law because it also accounts for the attenuation which is due to the partial polarisation caused by the neutral filter N. This is at 45^o to the incident beam so that the reflected beam is prevented from passing through the cell containing the solution. The function $F(\phi)$ against (ϕ) is shown in fig. (5.2).

The absolute values of I_s and hence also those of R_θ are determined by calibration of the apparatus. This is the subject of chapter six.

5.3 The Apparatus

The apparatus is shown in fig. (5.3). For the purpose of description it can be divided into three parts: a, b, c; the optical system, the electrical system and the cells respectively.

a. The optical system.

This consists of a collimating arrangement to produce an intense incident light beam, two units for collecting the transmitted and the scattered light, hereafter referred to as the primary and viewing unit respectively, and a depolarisation unit P" that can be fitted to the viewing unit.

b. The electrical system.

This is designed to detect the alternating component in the P.M. output and thus determines when it is zero. Fig. (5.4) shows a block diagram of the electrical system. The P.M. output is passed into a selective amplifier, and the amplifier output is, in turn, fed into a phase sensitive detector (P.S.D). The P.S.D. is also supplied with a reference signal and it gives a d.c. output (proportional to the level of the output signal of the selective amplifier) only if the signal is of the same frequency and has the correct phase in relation to the reference

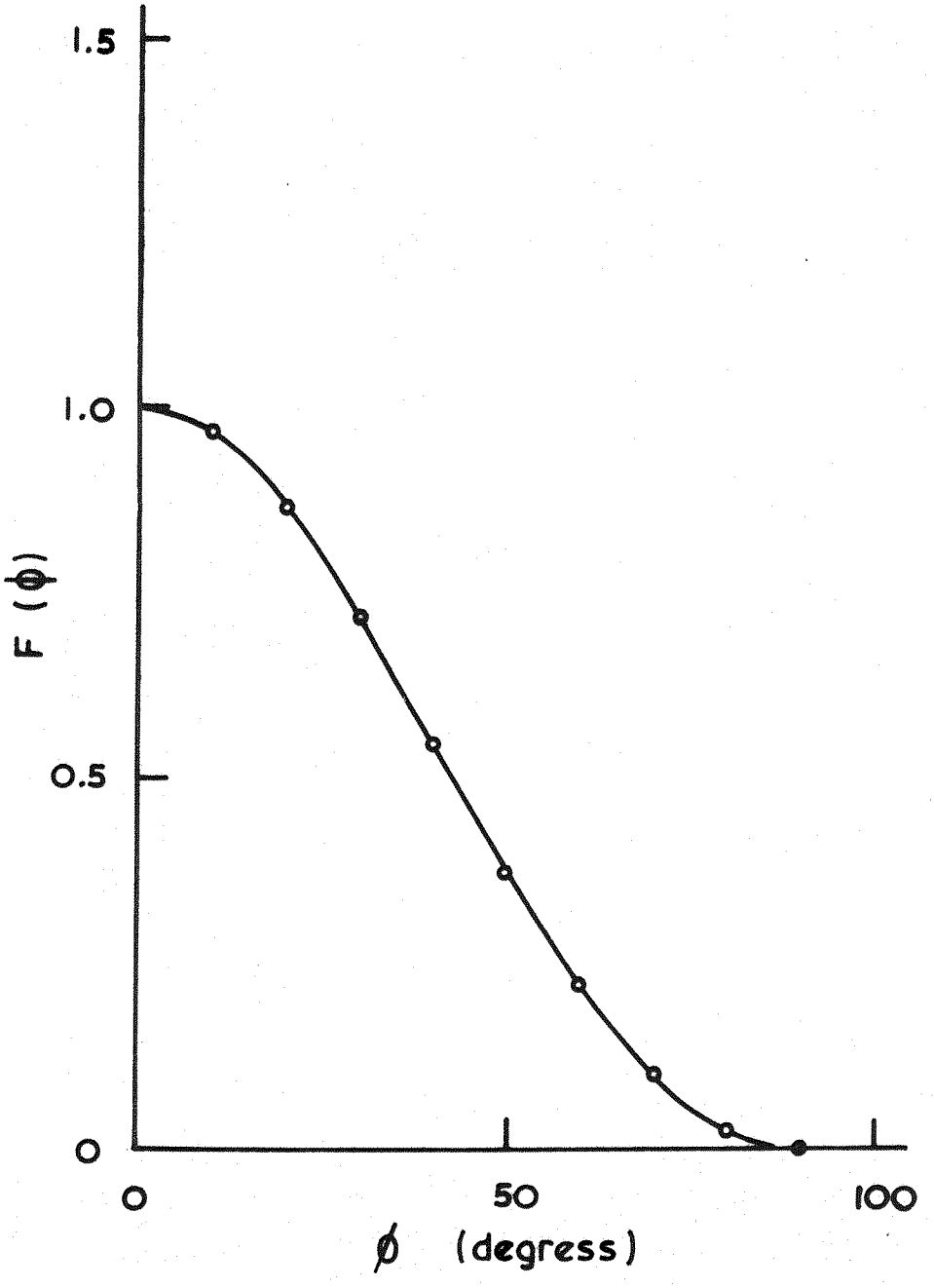

Fig. 5.2 Apparatus calibration curve

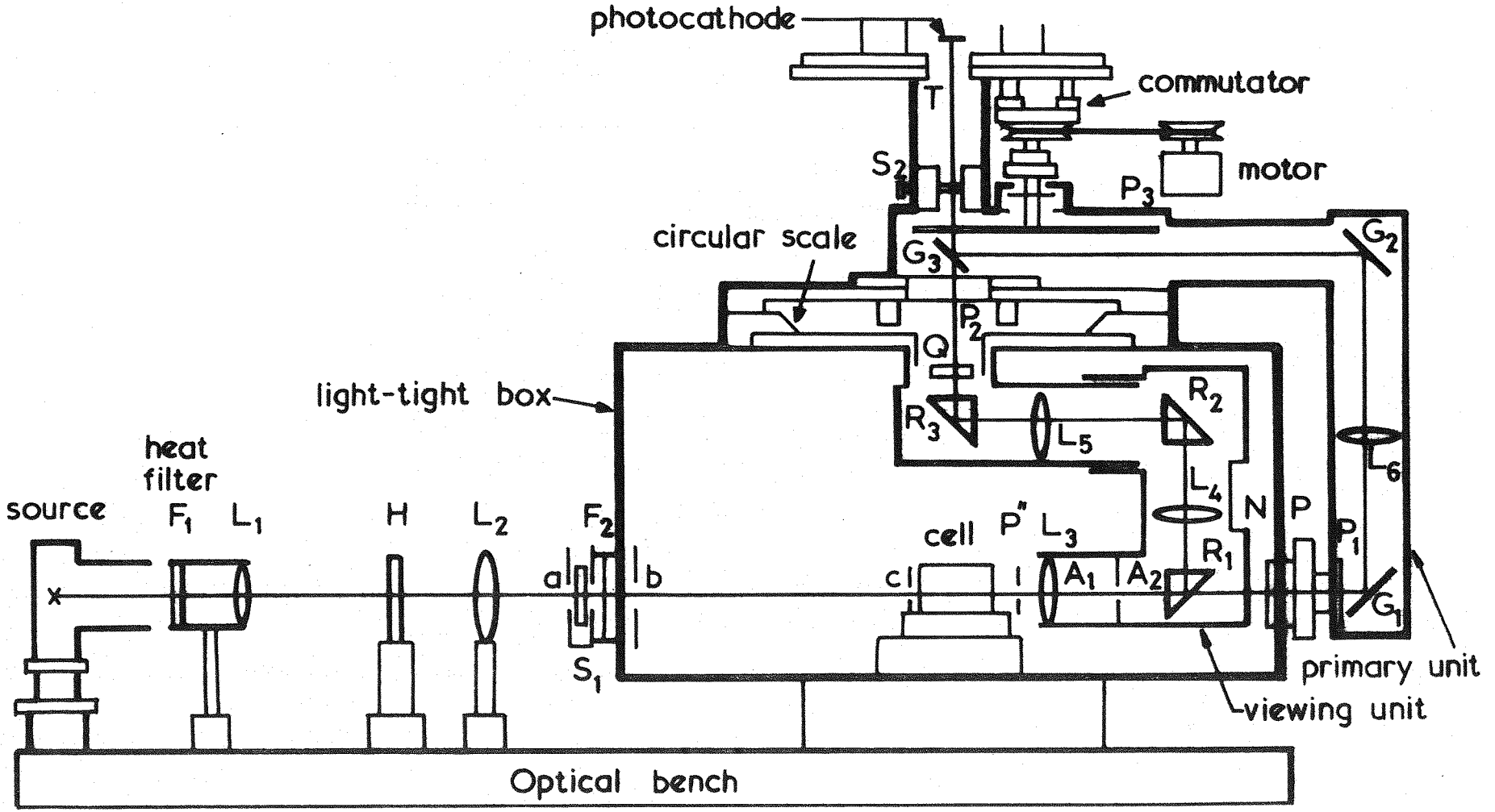

Fig. 5.3 Diagrammatic view of apparatus

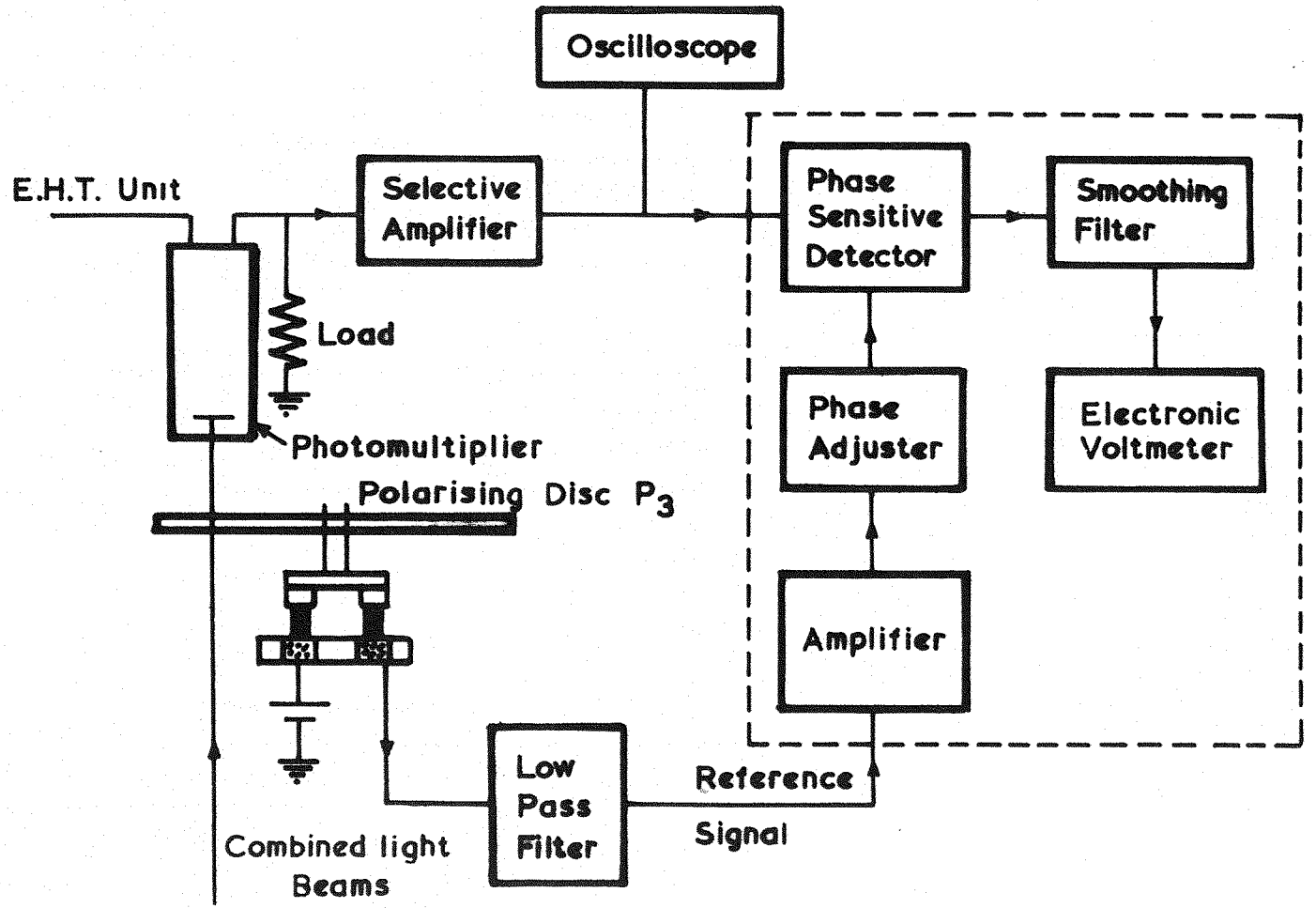

Fig. 5.4 Block diagram of electrical system

signal. This output is fed into a smoothing filter which removes the alternating voltages and the noise. The d.c. voltage is then displayed on a meter. The reference signal applied to the P.S.D. is generated from a commutator mounted on the same shaft as the rotating polariser P_3. This gives a square wave of the desired frequency which then passes through a low pass filter, an amplifier and a phase adjustor so that a sine wave of the required amplitude and phase is obtained.

c. The cells.

Two types of cells were available with this apparatus. The first is a semi-cylindrical cell and can be used for measuring the scattered intensity at different angles, with or without the presence of electrical fields. The other cell is designed for the measurement of the rigidity parameter, R, (see chapter 3, sec. 3.2.1). Although both cells have been previously described by Jennings (1964), it is felt that their description here will show the modification made on the cells which were used in this work.

i) The Semi Cylindrical Cell.

A horizontal cross section of the semi cylindrical cell is shown in fig. (5.5). The components of this cell (7 altogether, lid is not included) are cemented together by using araldite. The two parallel electrodes are cemented to the back wall, facing the semi cylindrical face, and the incident beam passes in the gap between them. A wire is connected to each electrode, the wire leading to the upper electrode passes through a notch ground in one of the top edges of the cell and the wire leading to the bottom electrode passes through a notch in one of the bottom edges. The latter notch is ground and the wire placed in position before the base of the cell is cemented and both notches are sealed with araldite. Finally a cooling compartment made of perspex is cemented to the back wall of the

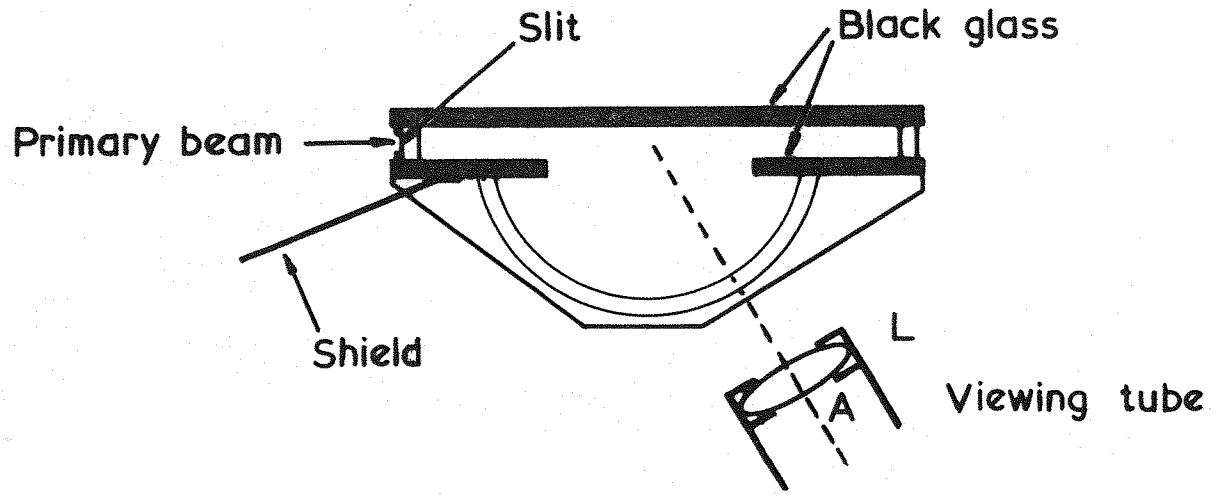

Fig. 5.5 Horizontal section of light scattering cell

cell. The terminals of the wires are attached to the sides of this cooling jacket and held by grub screws.

ii) The Rigidity Parameter Cell.

This cell which is rectangular consists of four glass sides mounted, using araldite, on a flat glass base. Also on this base there are two terminals from which connecting wires run through holes into the cell and to the electrodes where they are held by grub screws. These electrodes are cemented to the cell in diametrically opposite corners. The cell has a square glass lid which holds a small glass chimney over which fits a rubber sealing cap and no cooling is provided.

The rigidity parameter, R, is the ratio of the change in the scattered intensity, ΔI_s, when $\Omega = 0^o$ to that when $\Omega = 90^o$. Ω is the angle between the direction of the electric field and the vector $\bar{s}$. $\bar{s}$ is in the direction of the bisector of the angle external to the angle of observation θ. Using this cell R was then obtained by measuring I_s at the positions marked I and II in fig.(5.6) which correspond to $\Omega=0^o$ and $\Omega=90^o$ respectively. It is evident that this method of measuring R prevents any of the faces of the cell to be used for its cooling through a cooling jacket.

5.4 Modifications

5.4.1 The new cells

The cells used and constructed by the present worker, except for one, were improved versions of the cells described earlier, which, among other things, were difficult to fabricate. These cells are now described:

Cell A: A semicylindrical cell, with two electrodes and is a copy of the one described in section (5.3.c).

Cell B: A semicylindrical cell and similar to cell A. One major difference is that the glass lid in cell A is replaced by a teflon cover that holds the two electrodes, see fig. (5.7). This makes the construc-

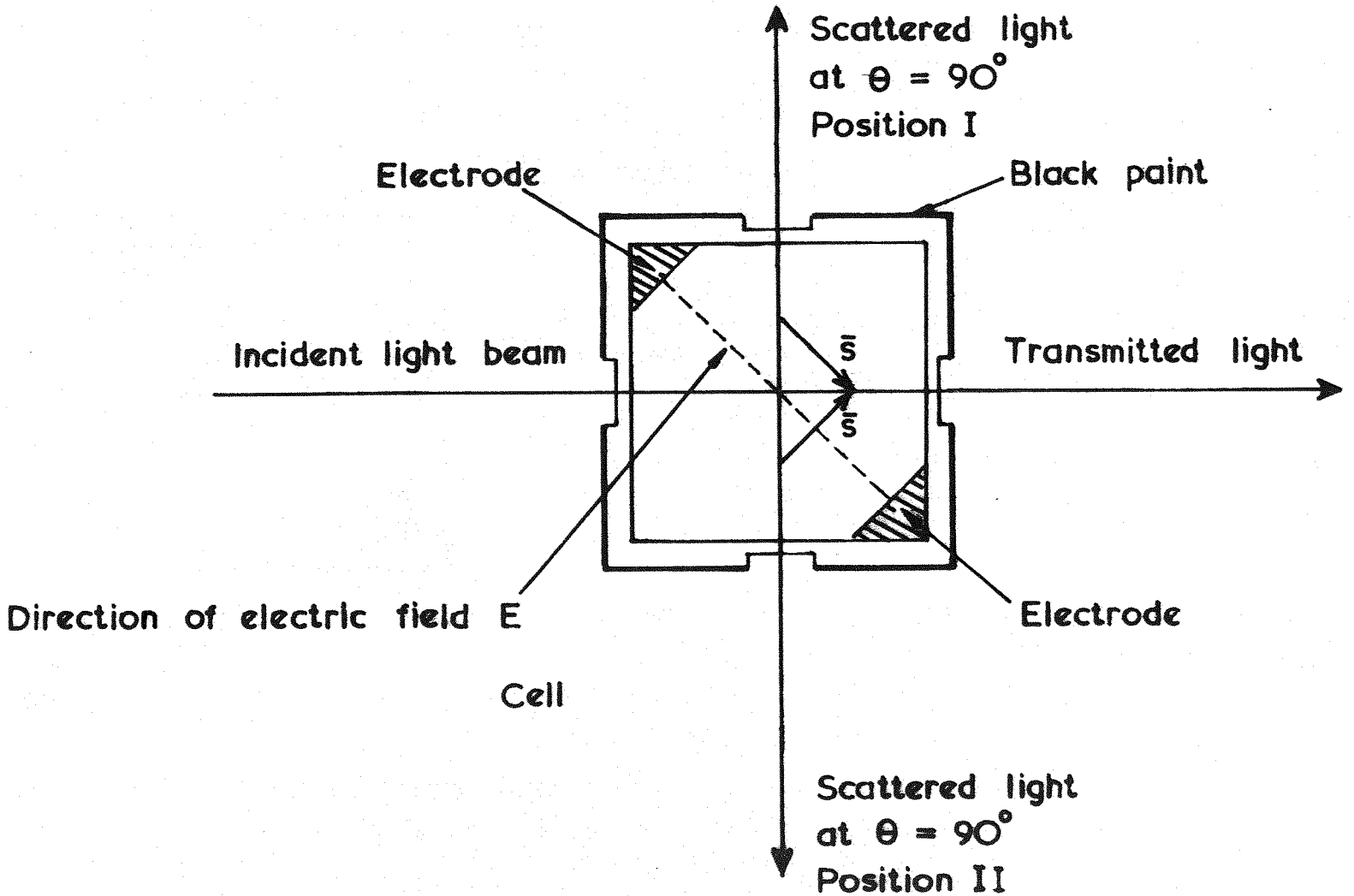

Fig. 5.6 Method of measuring the rigidity parameter R when using a fixed pair of electrodes

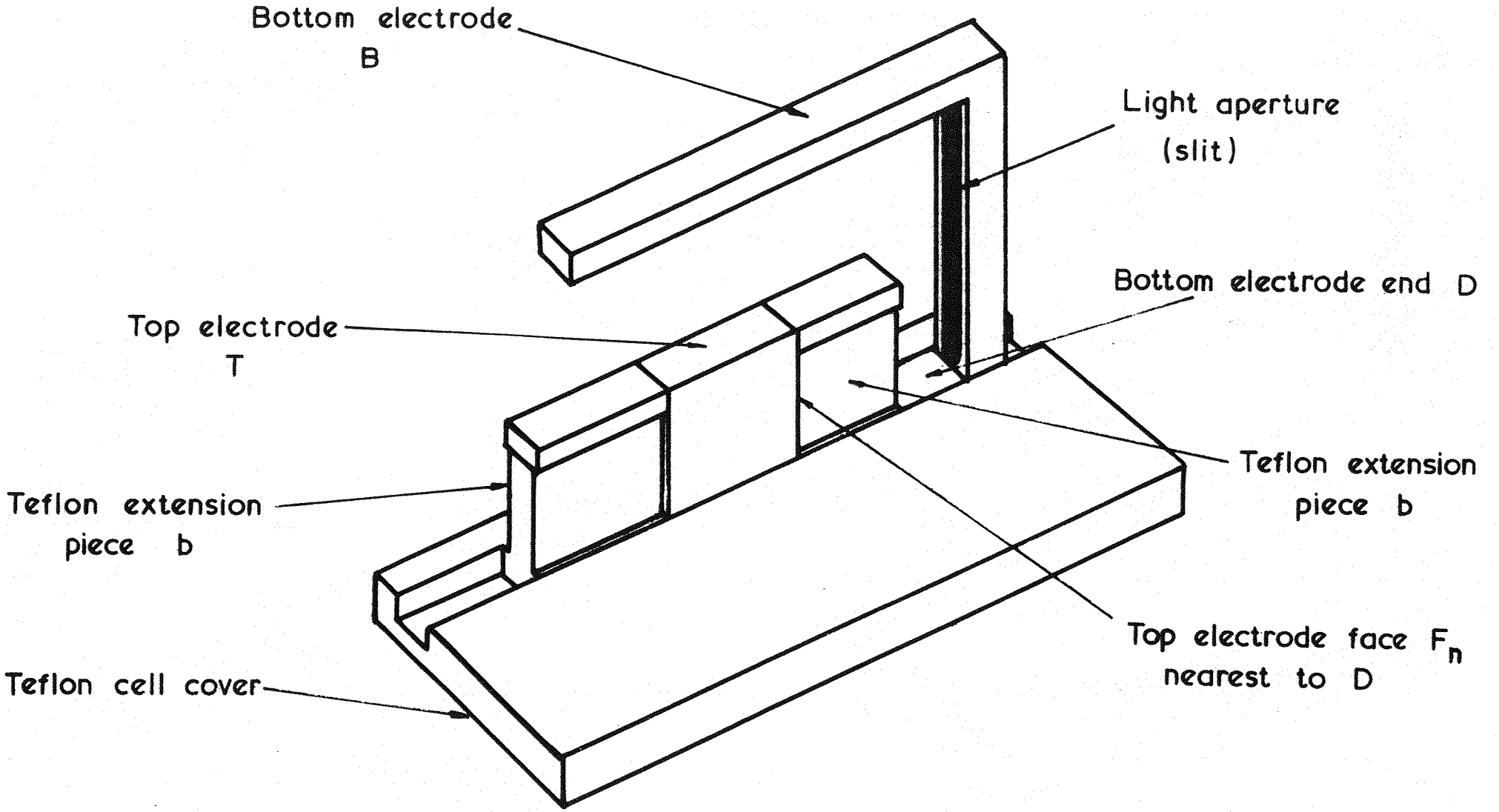

Fig. 5.7 Cylindrical cell cover showing electrode assembly

tion easier. The electrodes were of stainless steel, the top electrode T extends 0.5 in. along the rectangular part of the cell and is located at its centre. This is not long enough to cover the rectangular part, see fig. (5.5), extending along the semicylindrical piece, therefore two teflon pieces b, b were placed, one on each side, for that purpose. Although this can be done by having a longer electrode which is the arrangement adopted in cell A, it is undesirable to do so,firstly because more heat will be produced in the solution, which is to be avoided and secondly because face F_n of the top electrode and the end D of the bottom electrode B become very near. The bottom electrode is a right angled piece of which one arm is facing the upper electrode and the other arm extends along the entrance window of the cell. A wide slit is made in the latter arm to allow the incident beam to pass through the cell. The pieces of teflon and electrodes are fixed to the cover by screws and nuts. To prevent any slight rotation of the teflon pieces or the electrodes and so misalignment, a groove was made in the cover which located them and kept them aligned. Since the width of the electrodes and the teflon piece matches that of the rectangular part of the cell it was always possible to get the electrodes in the same position.

Cell C: This is a rectangular cell and similar to that described in section (5.3.c). The major difference is that a teflon cover is used to hold four triangular electrodes, one on each corner, as in fig. (5.8), where only two electrodes are shown.

The rigidity parameter, R, is obtained by measuring the changes in the scattered intensity at $\theta = 90^{\circ}$ with the electric field applied diametrically across the cell, firstly using one pair of electrodes and then the other. These two directions of the applied electric field are shown in fig. (5.9) as positions (I and II), and correspond to the conditions of

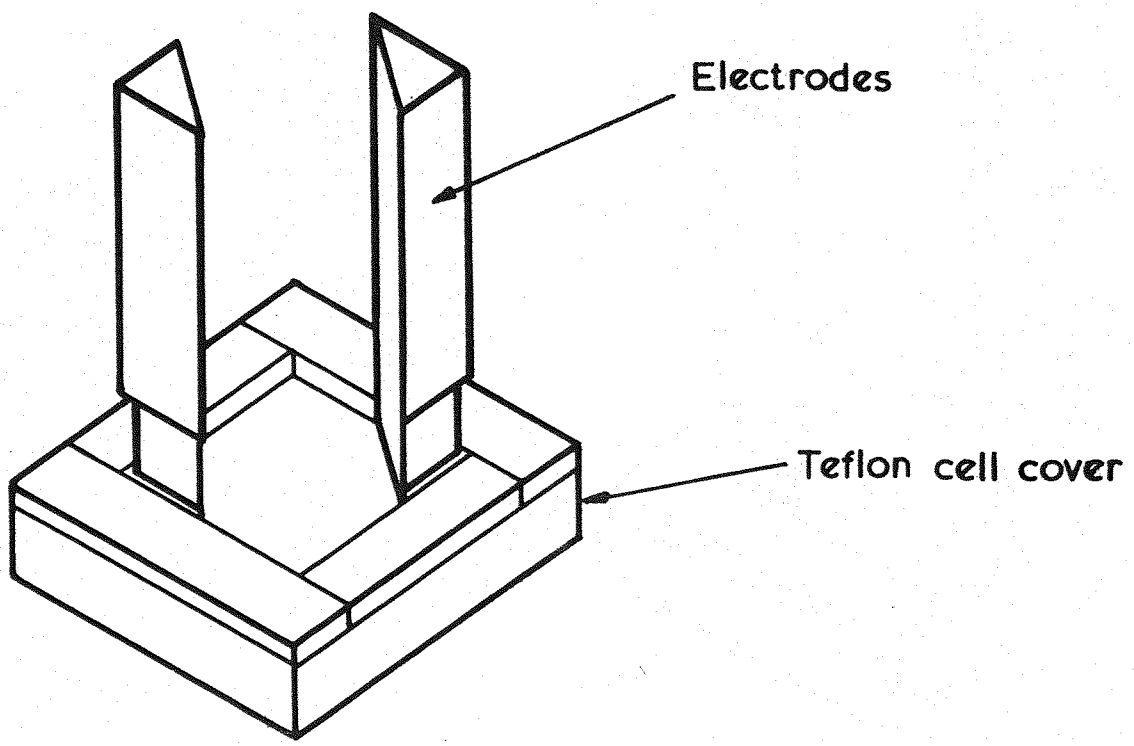

Fig. 5.8 Rigidity parameter cell electrode assembly

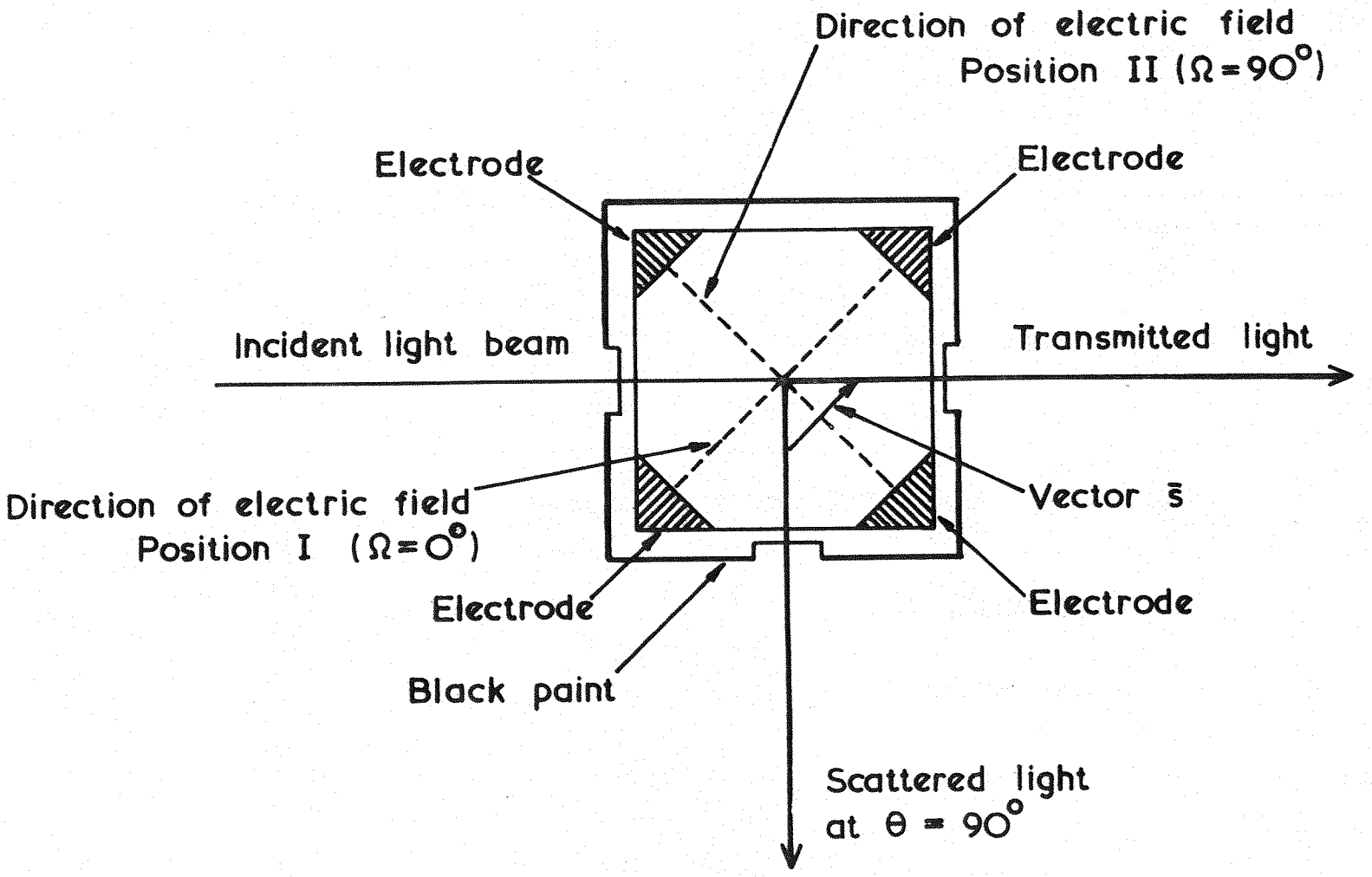

Fig. 5.9 A method of measuring the rigidity parameter R when using two pairs of electrodes

$\Omega = 0^{o}$ and $\Omega = 90^{o}$ respectively.

This method of measurement permits cooling of the cell using a water jacket on the side of the cell opposite to that where the scattered light is measured.

5.4.2 Two shutters to protect the photomultiplier

Frequently the light tight box, see fig. (5.3), has to be opened for various reasons, for example when placing the cell in the box or inserting the depolarisation unit P". The effect of exposing the P.M. to light was usually reduced by switching the power supply off. To protect the P.M. from being exposed to the light unnecessarily, a shutter S_2 was placed immediately after the polariser P_3, see fig. (5.3). This is a 0.5" diameter screw that can completely block the passage of light through the tufnol tube T so that the light is prevented from reaching the P.M. However this shutter was used only when the box has to be opened, because it needs to be rotated 13 turns to shut/open the reduced cross section of the tube through which the two beams, (the scattered and the transmitted), passes. Therefore another shutter S_1, which is easier to operate, was cemented at the entrance of the light tight box to stop the incident beam when unnecessary.

5.5 Method of Measuring the Changes in the Scattered Intensity

The changes in the scattered intensity arising from the application of alternating electric fields to certain solutions have been discussed in chapter 3 sec. (3.2.2). These changes are composed of both an alternating signal of a frequency which is twice that of the electric field, and a constant component. The electrical system, fig. (5.4), can be used for measuring the direct component without any modification. To detect

the alternating component the rotating polariser P_3 must be kept stationary and its plane of polarisation adjusted so that the maximum amount of scattered light is transmitted through it. Also the transmitted beam must be prevented from reaching the P.M. The electrical system can be used for the detection of the alternating component if a new reference signal of a frequency which is twice that of the applied electric field, is provided. In the first instance the reference signal was obtained by splitting the output from the selection amplifier into two components one of which was used as the reference. However such a signal is rather noisy, and a clearer signal is needed. A better reference signal has been obtained by feeding a small fraction of the electric field signal, applied to the solution, through a device which doubles the frequency.

This device doubles a set of selected frequencies in the range of 30 c/s - 30 Kc/s which is the range of the Airmec power oscillator(type 254)used in this work. The circuit of this frequency doubler* and the set of the selected frequencies are shown in fig. (5.10).

---

* Designed and constructed for the author in the Physics Dept.'s electronic workshop.

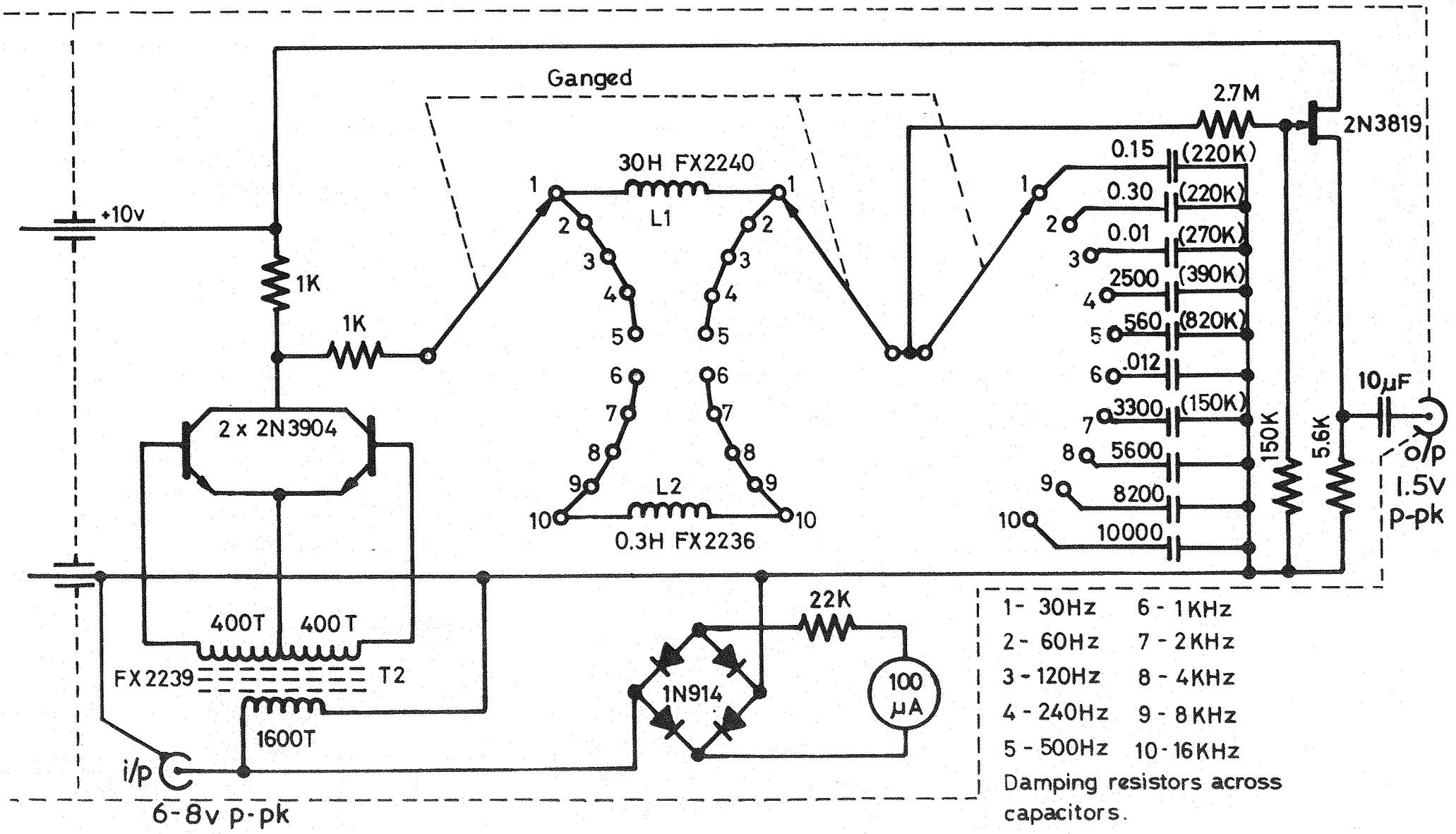

Fig. 5.10 Frequency doubler

PART B

THE KERR EFFECT APPARATUS

5.6 Introduction

Numerous instruments have been built in the past to study the optical response of a macromolecular solution to the application of a transient electric field, e.g. Benoit (1949), Okonski and Zimm (1950), Krause and Okonski (1959) and Jerrard et al. (1969). The similarity in the basic components in these instruments is very clear. These are: An optical system to produce a parallel beam of linearly polarised light, a cell to contain the solution, two parallel electrodes placed inside the cell, a pulse generator to produce a special electric field and a detector. The detector is always a P.M. with a fast responding circuit. The signal from the P.M. is fed to an oscilloscope and recorded by a camera. Added to these components an analyser is usually placed after the cell so that the linearly polarised light can be extinguished and so prevent the light from reaching the detector except when the electric field is applied. If the electric field is applied the solution becomes bire fringent, the linearly polarised light becomes elliptically polarised thus it can reach the P.M. and a signal recorded.

The apparatus that has been used by the present author is that of Jerrard et al. (1969). The description of this apparatus and the method of operating it have been given in detail by Riddiford (1968). As the apparatus was used only for measuring the relaxation time, therefore it is sufficient here to give a brief description of this instrument and also explain the method of determination of the relaxation time.

5.7 Description of Apparatus

The apparatus is shown in fig. (5.11). For the purpose of description it can be divided into the optical system, the electrical system and the cell.

a) The optical system:

A laser (Spectraphysics type 132) is mounted on an optical bench at one end. This provides a narrow beam of unpolarised light of 6328 Å wave length. The light beam transverses the polariser P, the cell C containing the solution under investigation, the quarter wave plate Q and then passes through an analyser A before impinging on the photomultiplier, mounted at the other end of the optical bench. A, P and Q are each mounted on a divided circle provided with a vernier to enable rotation to be read to within 2' of arc. In the present experimental arrangement A and P are crossed, the direction of the electric field applied to the solution in the cell, is approximately 45^{o} relative to the vibration directions of P and A and the azimuth of Q is zero with respect to the vibration direction of P. The purpose of Q is to convert the elliptically polarised light leaving the cell into a linear vibration. However, this is not necessary when measuring the relaxation time.

b) The electrical system.

This consists essentially of a detection unit synchronized to a pulse generator. The pulse generator produces, as shown in fig. 5.12.a, rectangular field pulses of duration of 2.5 μ.sec. (with a rise and decay time of 60 ns and 80 ns, respectively) and having amplitudes variable up to 8 KV. The pulses are generated by discharging a high voltage in a length of transmission cable acting as a delay line through a hydrogen thyratron T_1. The birefringence arising from the application of such pulses was detected by a P.M. (Mullard 56 TVP) with a fast responding

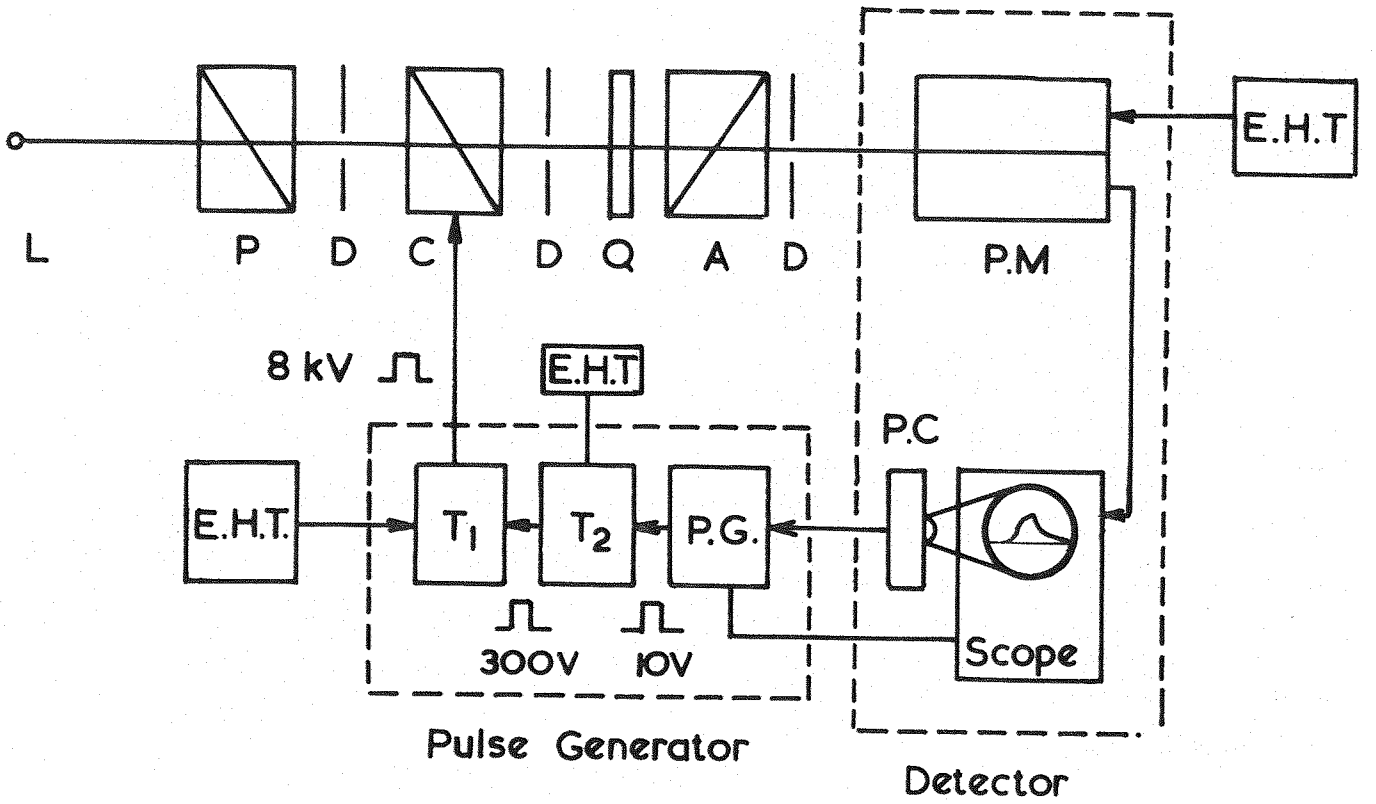

A - Analyser
C - Cell
D - Diaphragm
L - Light source
P - Polariser
Q - Quarter wave plate
P.C - Polaroid camera
P.M. - Photo multiplier
P.G - Pulse generator
T - Thyratron

Fig. 5.11 The Kerr Effect apparatus

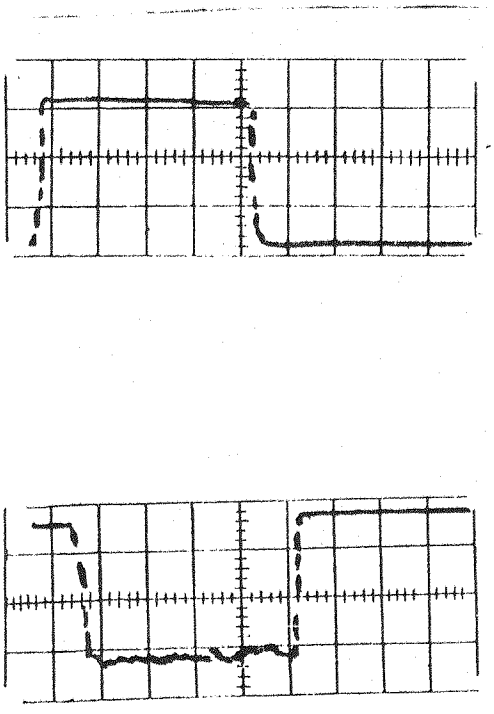

Fig. 5.12 Response of photomultiplier

a) Electric field pulse (8 Kv/cm)

b) Birefringence of nitrobenzene time scale ($0.5\ \mu.sec.cm^{-1}$)

circuit, fig. (5.13). The P.M. output was displayed on a cathode ray oscillograph (Tetronix 585) able to show fast rise times. The traces on the cathode ray oscillograph were photographed by a camera using a 10,000 ASA high speed polaroid film. Fig. (5.12.b) shows a trace of the birefringence of nitrobenzene, obtained using this apparatus when an 8 KV/cm pulse was applied. Nitrobenzene has a very small relaxation time (10^{-11} sec.) and has been used to check the response of the detecting system.

c) The cell

The cell is machined of stainless steel and teflon. As can be seen from the cross sectional diagrams shown in figs (5.14 and 15), it consists of a teflon annulus which is clamped between two pieces of stainless steel of rectangular cross section. The electrode's assembly is a push fit into the centre of the teflon annulus. The electrodes are 5 cm. long, parallel and separated by 0.317 cm. by two teflon spacers. Two stainless steel end plates seal the two ends of the annulus. The end plates are quite complicated, as in them were mounted the end windows of the cell, and also the inlet and exit ducts to the cell. Teflon plugs extending from the exterior of the cell to the teflon annulus are used for inserting a metal rod that can be screwed to the electrodes and this provides the lead to the cell. Finally the cell can be mounted accurately in a brass case around which cooling water is circulated for the purpose of thermal control.

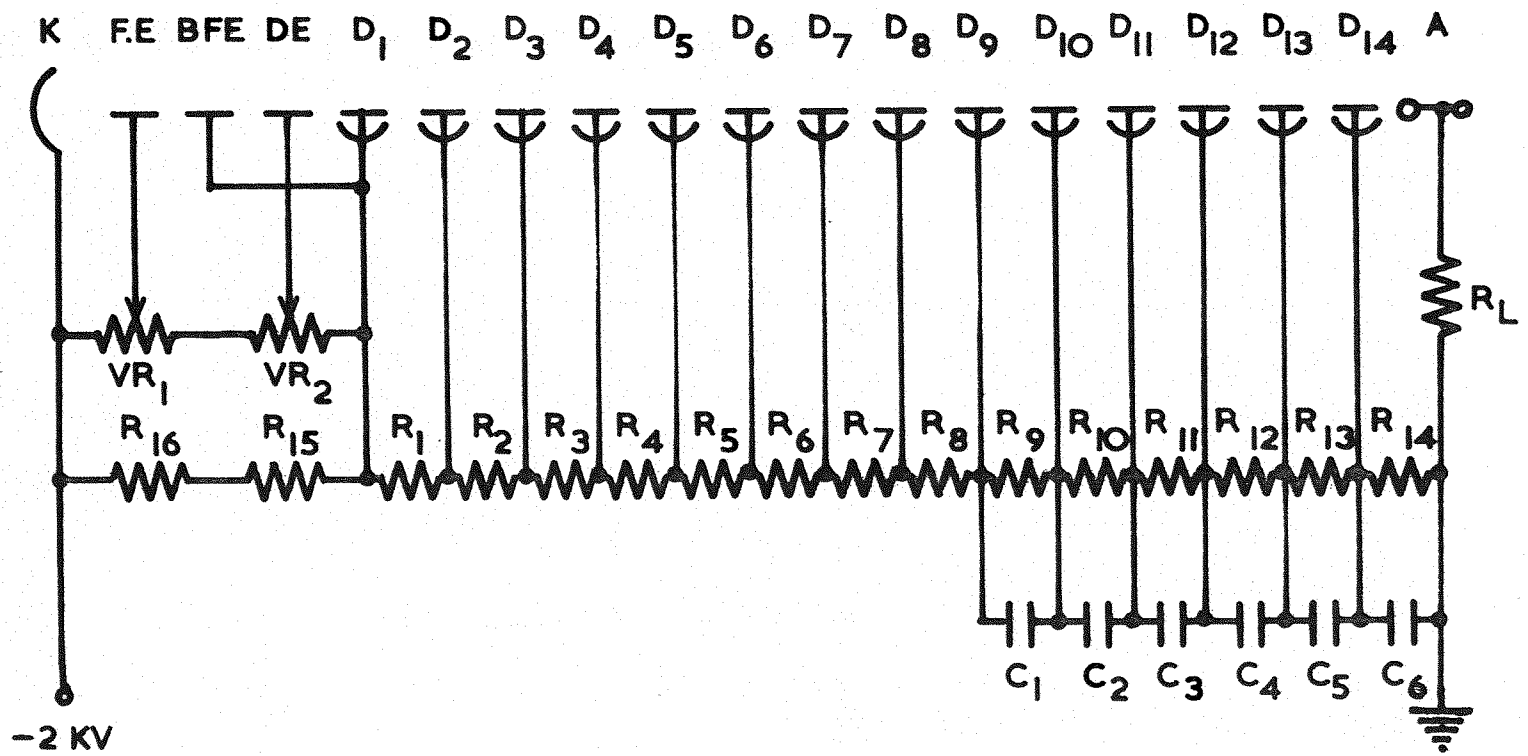

Fig. 5.13 The Photon multiplier circuit diagram

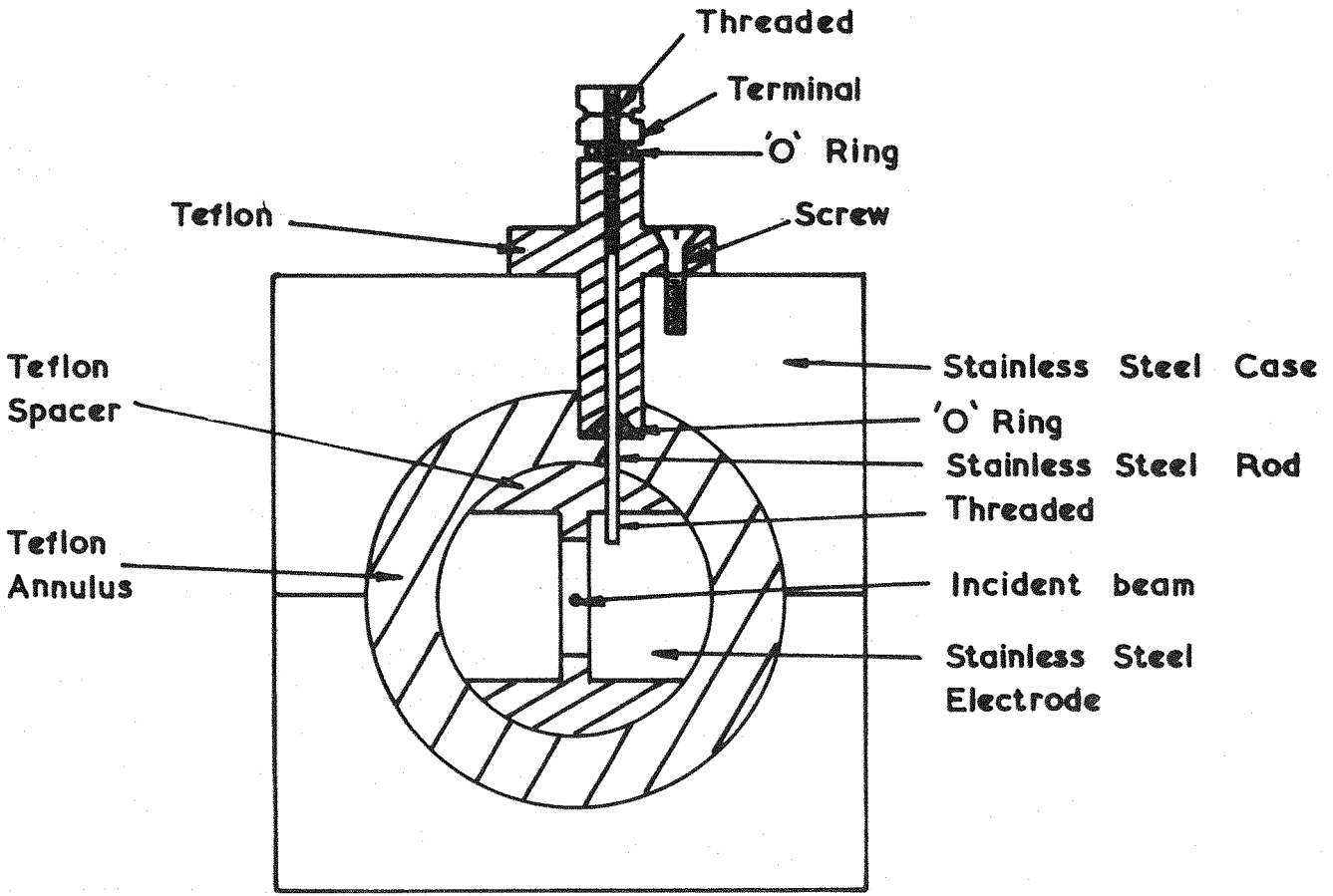

Fig. 5.14 Vertical cross-section of Kerr cell perpendicular to incident beam

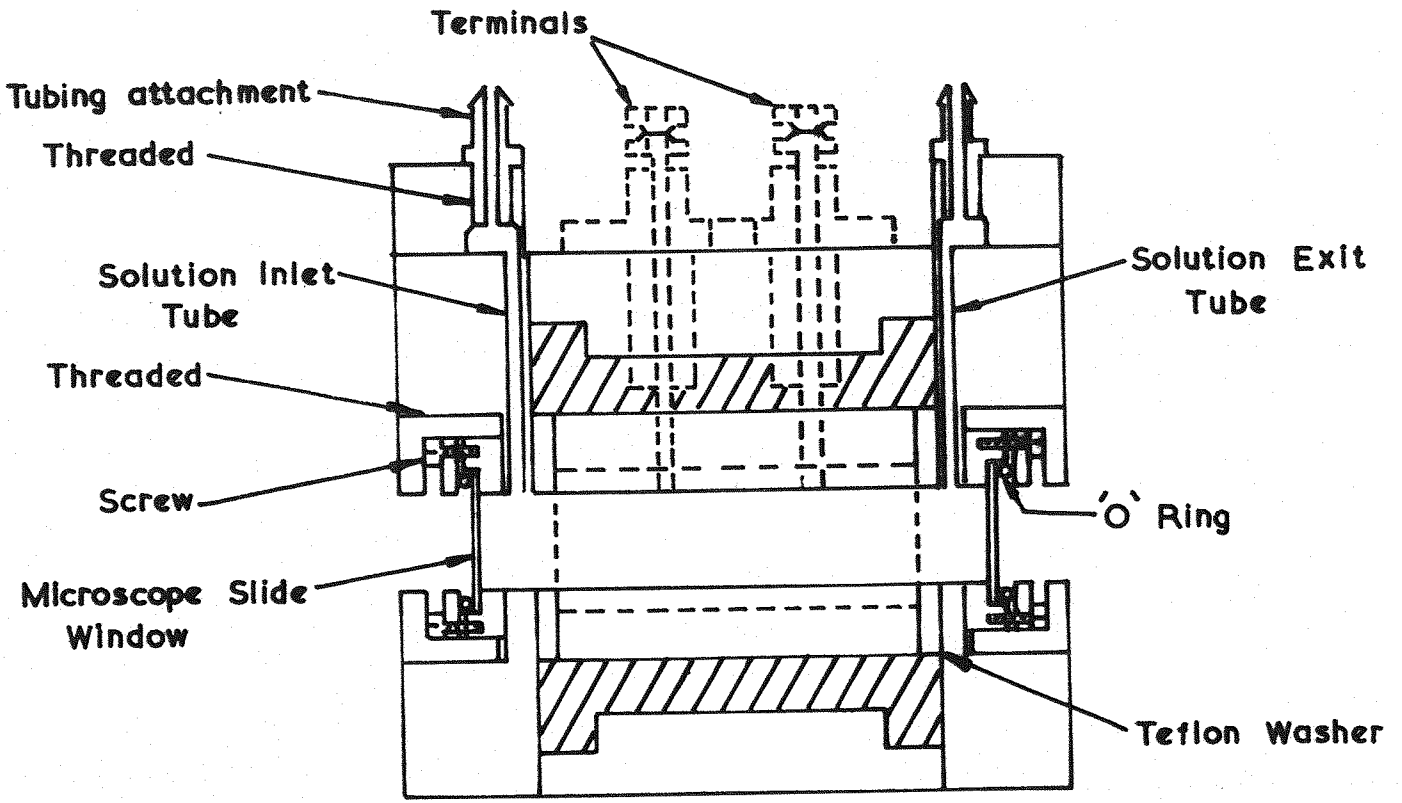

Fig. 5.15 Kerr cell.

(Vertical cross-section parallel to incident beam)

5.8 Method of determining the relaxation time and accuracy

The theory of electric birefringence (discussed in Chapter 4) is for infinitely dilute solutions. Thus for each sample, the measurements must be repeated on solutions of different dilution under similar conditions (such as solution temperature and intensity of the applied electric field). This enables the results to be extrapolated to zero concentration if necessary. Thus several transient traces were obtained for each sample at different concentrations (usually four in this work). These traces were obtained at a solution temperature of $20^{\circ}C$, which is the same as the temperature for the light scattering experiment.

The relaxation times were obtained from the decay curves of the traces by first measuring the height of each of these curves as a function of time t. These measurements were made using a double traverse travelling microscope which could read to ± 0.001 cm. The relative values of the height, which are proportional to the square of the birefringence because the "quadratic method" of detection was employed, were then plotted on a $\log_{10}$ axis against the time t on a linear axis. The initial and end tangents of the resultant log plot were used to determine the relaxation times of the smallest and largest particle species respectively (c.f. sec. 4.4). Both the fact that the quadratic method of detection was employed, and that the traces on the oscilloscope were obtained reduced in size were taken into account when determining the absolute values of the relaxation time to be reported in chapter 7.

Jerrard et al. (1969) reported that for a monodisperse sample and under favourable conditions τ can be estimated to an accuracy of 4% (2% of which is the calibration accuracy of the oscilloscope time base. For a mixture of two components or more the relaxation times will have slightly larger errors.

Chapter VI

CALIBRATION OF THE LIGHT SCATTERING APPARATUS

6.1 Introduction

The molecular weight M of a sample is one of the parameters that can be obtained from the light scattering measurements. However, for the determination of the absolute value of M the instrument must be calibrated. The method of calibration adopted and the experimental procedure that was followed will be given in this chapter after discussing the following points:

a) Preparation of solutions.

b) The correction factors.

c) Testing the alignment and geometry of the apparatus.

d) Background scattering.

6.2

a) Preparation of Solutions

A considerable amount of dust exists in all untreated solutions. Therefore the solutions must be clarified from dust particles before doing any measurements. Without doing so the light scattering data can be misleading for two reasons: firstly the intensity of the scattered light may be greater than that due to the scattering by the particles alone and secondly the scattered light intensity will show higher dissymmetry because most dust particles will in general be larger than the particles under investigation. The most effective way of removing the dust is to expose the solution to a high enough gravitational force for a long enough time and then filter it through special filters. Furthermore, in many cases the clarification process serves as a means

of removing impurities, aggregated particles and also enables, under favourite conditions, to obtain a nearly mono-disperse solution which is easier to analyse from a theoretical point of view.

In this work the solution was always centrifuged and when possible filtered by using Millipore cellulose filters and a Millipore filter unit (Millipore Filter Corporation, Bedford, Massachusetts, U.S.A. English agents, V.A. Howe and Co. London) and then injected into the cell with an all glass hypodermic syringe fitted with an inlet/outlet valve. Another small Millipore filter unit was put in between the syringe body and the hypodermic needle for further clarification of the solution. In order to minimise the exposure of the solution to air a small hole was made in the rubber cap and also in the teflon cover. When the needle was removed the hole was sealed. The previous method* in which the needle was inserted into the cell by forcing it through the rubber cap (although preventing the solution from any exposure to air), was avoided. This was because rubber particles were occasionally driven by the needle into the solution.

b) The correction factors

The light scattering intensities, taken at different angles, must be corrected by a number of optical and geometrical factors before being correlated. The factors which are most relevant to the measurements reported here are:

(i) Backface scattering: The incident light beam passes through the central part of the rectangular section of the cell, see fig.(5.5). At any point, in its path in the cell, part of this light beam is scattered in all directions. A fraction of this is reflected at the backface of the cell and augments the scattered intensity. However

* The method used by Sellen (1962) and Jennings (1964).

the use of black glass limits the reflection to the glass solution interface. The correction is negligible at $\theta = 90^{o}$ and about 3% at $\theta = 30^{o}$ or 150^{o}.

(ii) Fresnel effect: This correction, given by Seffer and Hyde (1952), accounts for the fact that the incident beam is reflected at the exit window of the cell and passes through in the reverse direction. The reflected beam will thus increase the scattered intensity by a fraction, R, which is a function of the refractive index of the medium inside the cell. This increase in the scattered intensity is the same at all angles when the molecules are too small to exhibit a dissymmetry of scatter and therefore it can be accounted for by the calibration factor. However,when the particles are large enough to exhibit dissymmetry then a fraction R of the scattered intensity at an angle θ must be subtracted from that at $(180^{o} - \theta)$ and vice-versa. The results should then be multiplied by $(1 + R)$ so that the calibration factor is not changed.

The fraction R is the total intensity reflection coefficient of the exit window and has the theoretical value of

$$R = (1-r)^2 R_1 + r$$

where

$$R_1 = \left(\frac{n_g - 1}{n_g + 1} \right)^2, \quad r = \left(\frac{n_g - n_L}{n_g + n_L} \right)^2$$

and n_g and n_L are the glass and liquid refractive indices respectively. The value of R for aqueous solutions is about 4%. However, since the incident beam diverges along its path, the reflected fraction that can contribute to the scattering is much less. The value of R actually applied in this work was 2%.

(iii) The scattering volume correction: When the scattered intensity is observed at different angles, the scattering volume varies as $(\sin\theta)^{-1}$. Therefore the scattered intensity must be multiplied by $\sin\theta$.

(iv) Correction due to difference in the path length. If the path of the transmitted beam within the cell, is different from that of the scattered beam then allowance must be made for the extra attenuation. According to Maron and Lou (1954) this attenuation can be accounted for by multiplying the calibration factor by $\exp(-\tau'\ell)$ where τ' is the medium turbidity and ℓ is the difference in the paths length of the two beams.

c) Testing the alignment and geometry of the apparatus

After carrying out the alignment of the optical components of the viewing unit and of the primary unit, the angular dependence of the fluorescent intensity of a dilute aqueous solution of fluorescein was studied. The fluorescent intensity should be independent of the angle θ, if both the alignment and geometry of the apparatus (including the cell) are satisfactory. The solution was exposed to the blue line 4358 $\mathring{A}$, a yellow filter of low attenuation was used in front of the viewing unit to stop any stray reflections or scattered light from reaching the viewing unit and the lateral position of the semi-cylindrical cell was adjusted until the reduced intensity was independent of θ. The range covered due to the physical size of the viewing unit was 30° - 145°. A plot of $F(\phi)\sin\theta$, which can be taken as a measure of the angular fluorescent intensity, against θ is shown in fig. (6.1). The standard deviation of $F(\phi)\sin\theta$ about its mean value was 0.48% over the angular range mentioned earlier. The above procedure does not

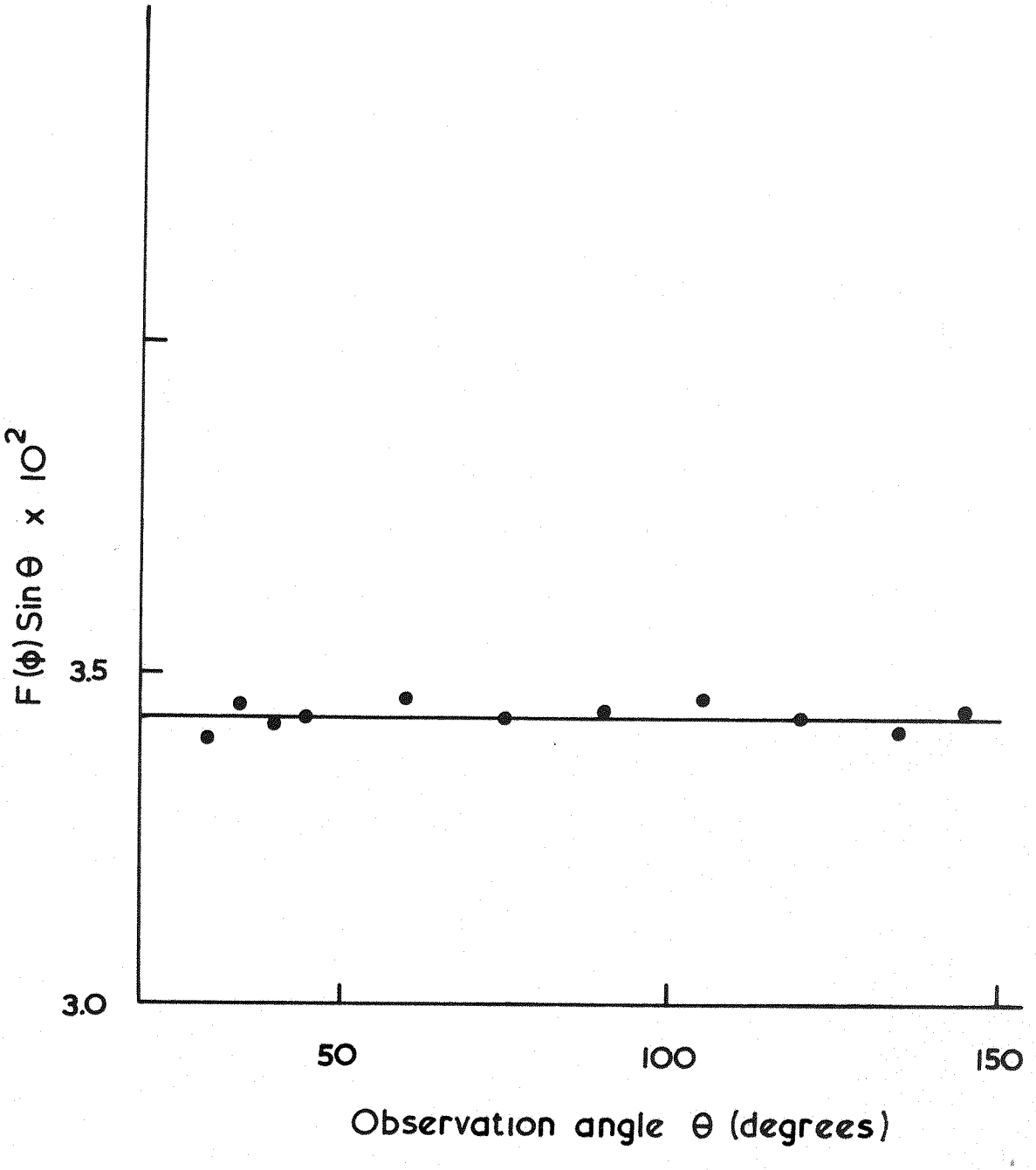

Fig. 6.1 Fluorescence of Fluorescein excited by 4358 A°

test the performance of the quarter wave plate Q (see fig. 5.3) as the fluorescent light is unpolarised.

d) Background scattering

To obtain the scattering caused by the macromolecules, the scattering by the solvent (usually called background scattering) must be subtracted from that of the solution. A plot of R'_θ for freshly double distilled water, which has been passed through a 0.45 μ filter, is shown in fig. (6.2). The incident beam was the blue line of the mercury lamp (4358 Å). The quantity R'_θ can be found from the relation:

$$R'_\theta = \frac{JF(\phi)_B \sin\theta}{1 + \cos^2\theta}$$

where J is the calibration constant of the apparatus, the determination of which will be described in the next section. In the same manner R'_θ for the macromolecules is given by

$$R'_\theta = \frac{J\left[F(\phi)_S - F(\phi)_B\right] \sin\theta}{1 + \cos^2\theta}$$

where $F(\phi)_S$ and $F(\phi)_B$ represent the relative scattering by the solution and the solvent respectively.

In theory the scattered intensity, for pure liquids, should be independent of the angle of observation θ. The rise in R'_θ in fig. 6.2 at low angles is mainly due to the presence of dust particles and that at the higher angles is caused by spurious reflections. Thus it is to be expected that the magnitude of R'_θ will depend on the method of preparation of the liquid. This should not be worrying since the background is always small when compared with that of the particles.

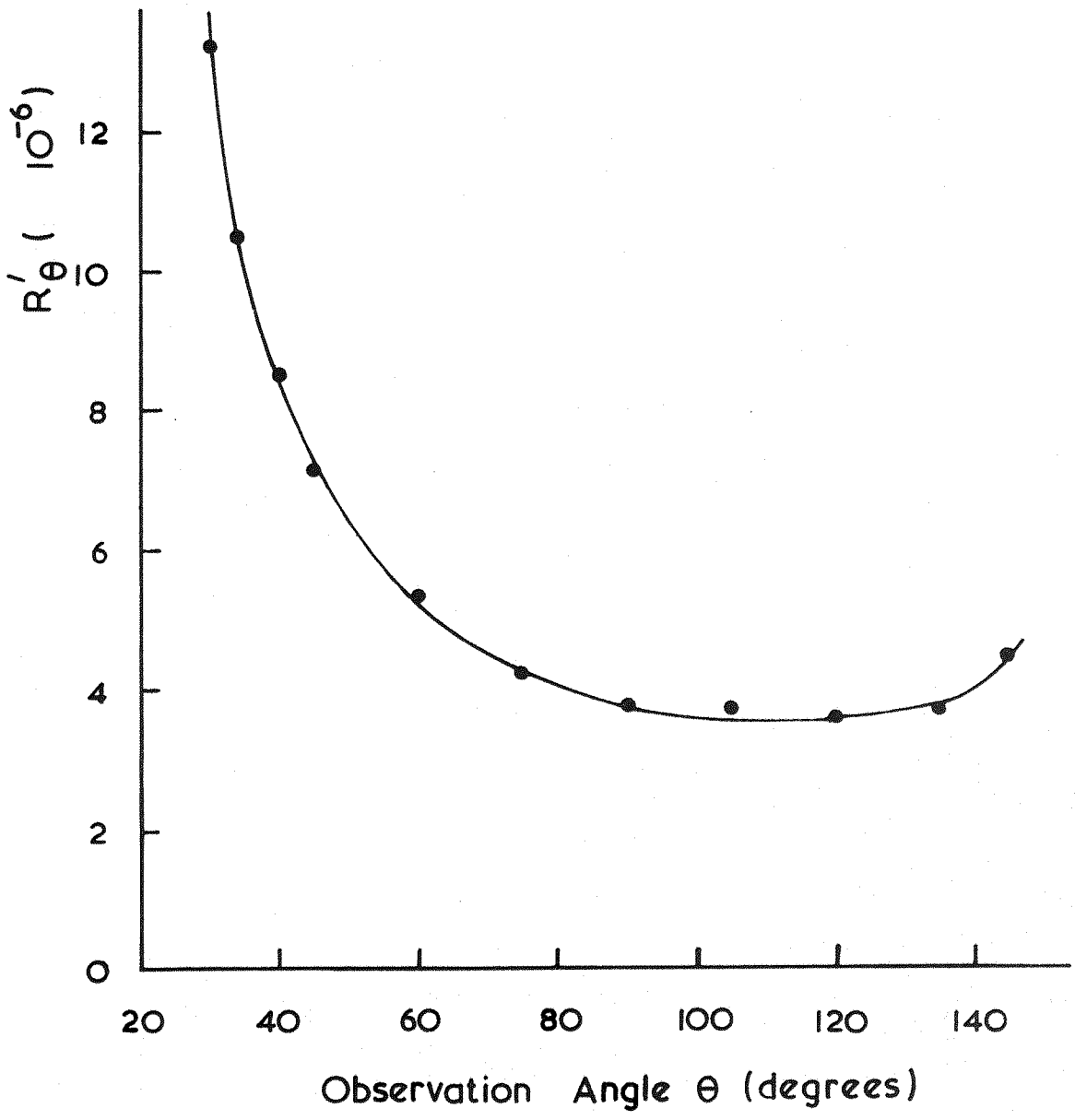

Fig. 6.2 Background scattering from Distilled water at $\lambda_0 = 4358\,A^\circ$

6.3 Calibration of the Apparatus

a) Method

A number of methods, Utiyama (1972), have been used for the calibration of light scattering instruments. A very reliable and widely used method is based on the relationship between the turbidity, τ', and the reduced intensity of a Rayleigh point scatterer at $\theta = 90^{\circ}$, i.e. the following relationship

$$\tau' = \frac{16\pi}{3} R_{90} \qquad (6.1)$$

Eq. (6.1) applies (see Chapter 2 sec.2.2.4) to solutions of low concentration of small optically isotropic particles provided the turbidity of the solution is due to scattering and none due to absorption. Moreover for calibration purpose the solution must be stable over a long enough period to carry out all the necessary measurements and the particles must be dense to give reasonably high turbidity values at low concentrations to avoid secondary scattering and particle interaction.

An aqueous colloidal dispersion of amorphous silica known as Ludox, has been widely used for the calibration of light scattering instruments. This is because it is very stable and the particles are known to be spherical, dense and small. Ludox and Syton 2X (another aqueous colloidal dispersion of silica) have both been used successfully by Jennings and Jerrard (1964) for calibrating the present apparatus, and according to them syton 2X is as good as Ludox and therefore it has been used here.

For the purpose of calibration eq. (6.1) is rewritten in the following form:

$$\tau' = \frac{16\pi}{3} F(\phi)_M \, e^{-\tau' \ell} \, J \qquad (6.2)$$

Thus J is given by

$$J = \frac{3}{16\pi} \left[(C/I_{90})/(C/\tau') \right]_{C \to o} \qquad (6.3)$$

In eq. (6.2) J is the calibration constant of the apparatus, $e^{-\tau' \ell}$ is the Maron and Lou correction arising from cell geometry, $F(\phi)_M$ is a measure of the scattered intensity by the macromolecules and in eq. (6.3)

$$I_{90} = e^{-\tau' \ell} \, F(\phi)_M$$

By measuring $F(\phi)_M$ and τ' for a given solution at different concentrations the value of J can be determined.

b) Experimental

i) Preparation of solution.

An oil free sample of syton 2X was obtained, as a stock solution of 30% concentration at pH 9, from Monsanto Chemicals Ltd. Freshly double distilled water was used to dilute the stock solution to the approximate concentration when required. The diluted solution was clarified by centrifugation at 17,000 g for two hours in an M.S.E. preparative centrifuge. The super-natant from the centrifuged 100 ml plastic tubes was then recentrifuged at about 20,000 g for two hours and the top of the solution from each tube was removed carefully by a syringe. The purpose of this double centrifugation is to ensure that large dust particles and aggregated syton particles are removed from the solution. The solution was further clarified by filtering it

through 1.2 μ and 0.45 μ filters. The concentration of this solution was 3.4510^{-2} $g.ml^{-1}$. This was determined by using a Rayleigh differential Refractometer* and a value of 0.064 for the refractive index increment, dn/dC, at the wave length 4360 Å as given by Jennings and Jerrard (1964).

ii) Optical density measurements.

The optical density was measured for four different concentrations at the 4358 Å wave length and for the solution of the highest concentration measurements were made over the range 4300-6000 Å. These measurements were carried out by using Unicam SP600. The reference solution was filtered freshly double distilled water. Care was taken to replace the 4 cm cells always in the same position. The manufacturer's advice of interchanging the solution and the solvent in the cells and averaging the results was followed. The last procedure eliminates any errors that may occur because the cells are not perfectly matched. From these measurements a graph of D,(the optical density which is linearly related to τ') against the reciprocal of the fourth power of the wave length,and another of C/D against C were plotted. The first graph is shown in fig. (6.3). Since it is linear over the wave length range mentioned earlier therefore all the loss of light is due to elastic scattering. The other graph, shown in fig. (6.4),enables us to get the value of C/D when $C \rightarrow o$ by extrapolating the results to zero concentration. A third graph of D against C, which is shown in fig. (6.5), can be used for the determination of D, for any concentration which is smaller than that of the mother solution.

iii) Light scattering measurements.

These measurements on syton 2X and all the other light scattering measurements reported in this work were obtained while the solution

* This instrument has been described in most standard text-books on optics. A more detailed description has been given by Candler (1951).

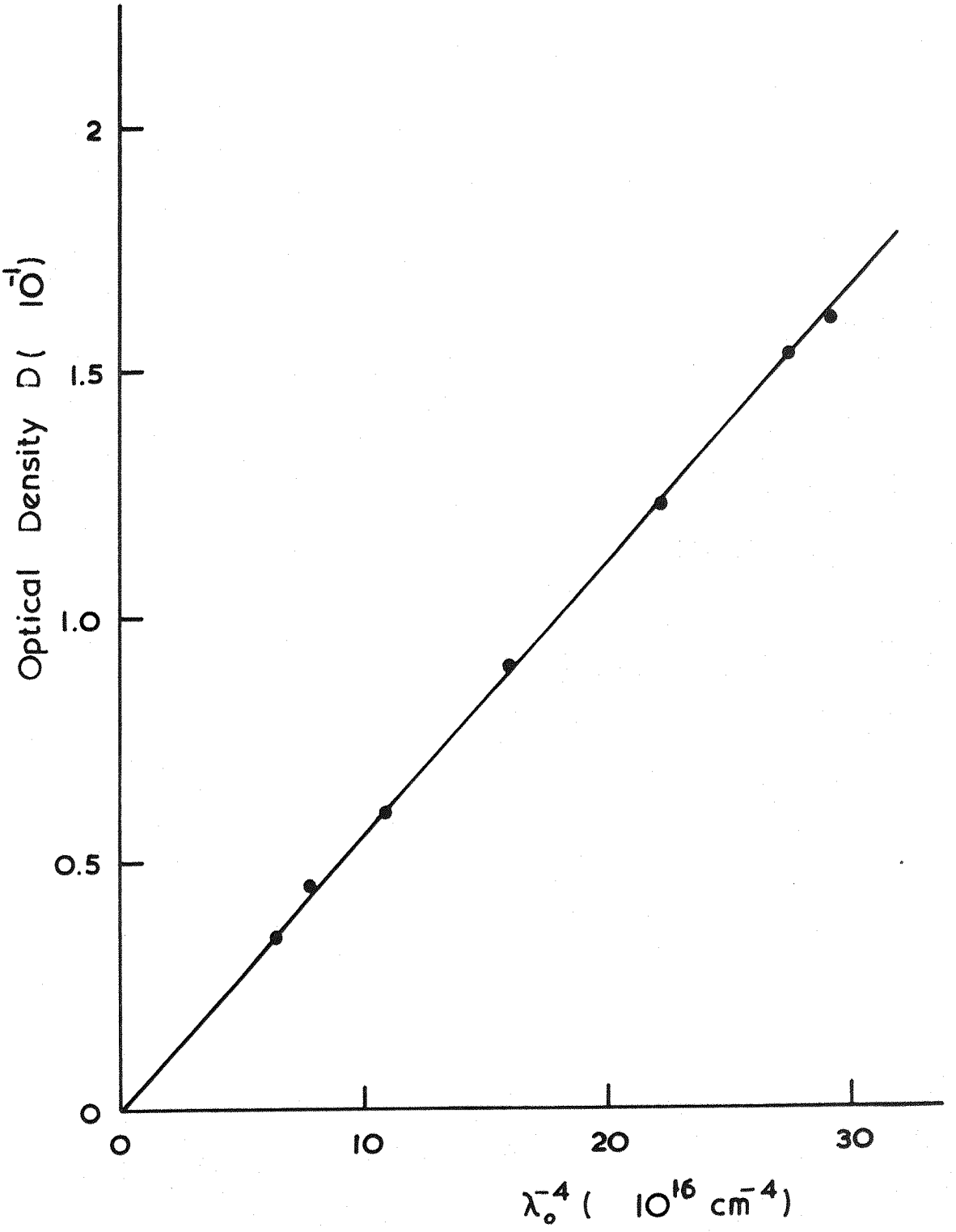

Fig.6.3 Optical density v. λ_o^{-4} for Syton 2X at $C = 3.45 \times 10^{-2}$ g.ml^{-1}

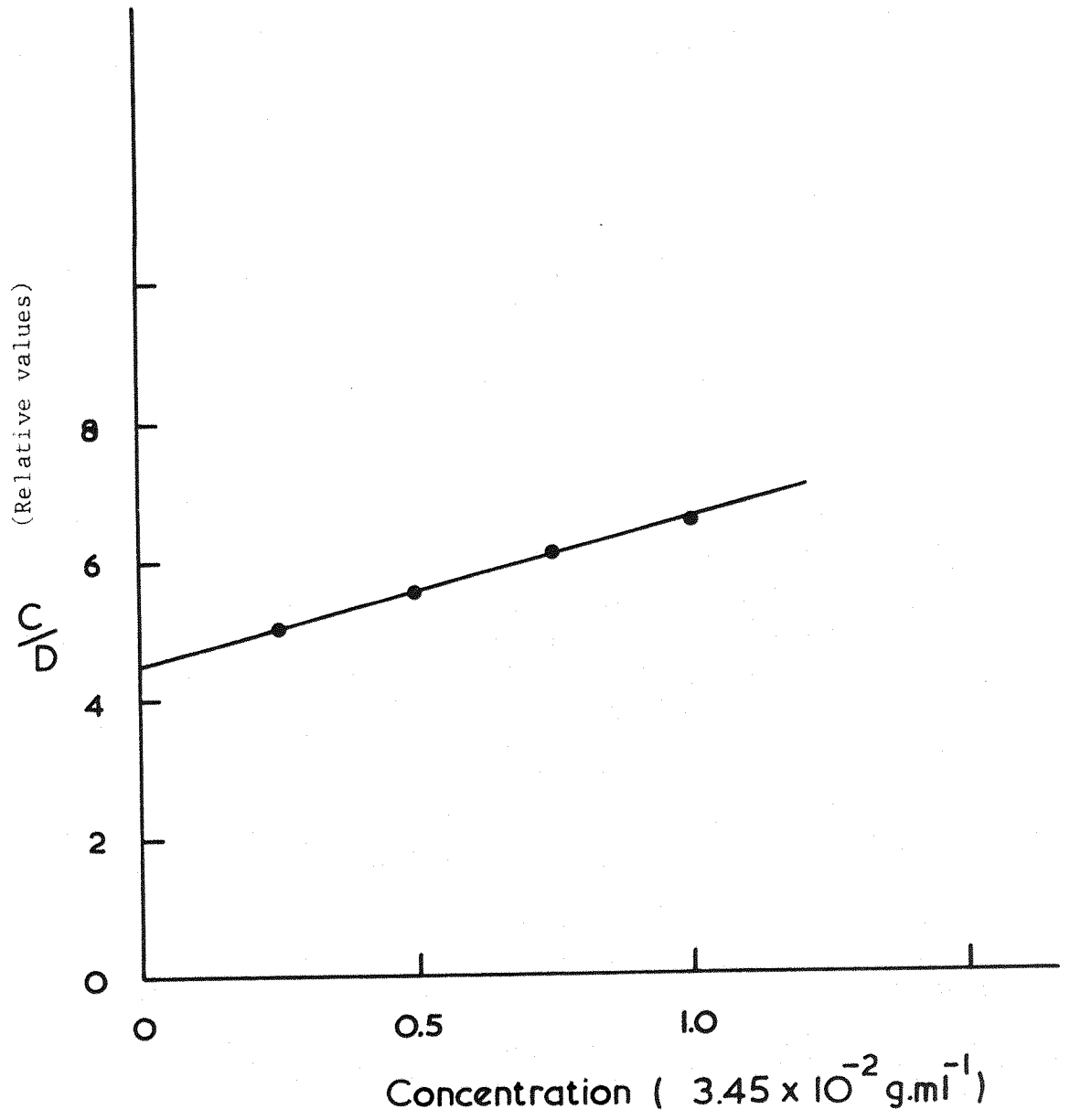

Fig. 6.4 Concentration/Optical Density v. Concentration for Syton 2X at $\lambda_o = 4358\,A^\circ$

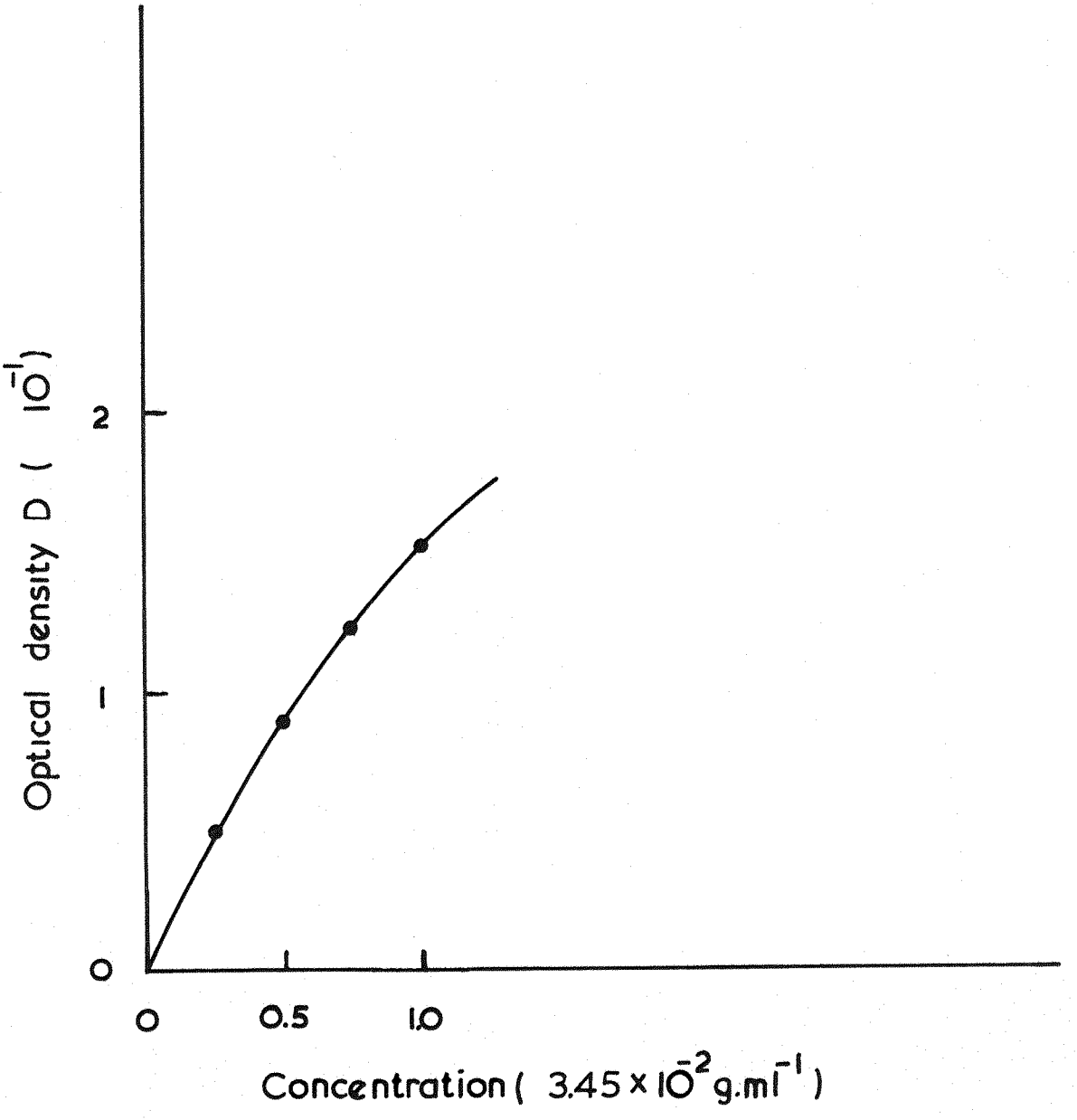

Fig. 6.5 Optical Density v. Concentration for Syton 2X at $\lambda_o = 4358\,A^{\circ}$

inside the cell was kept at a constant temperature of 20 ± 0.5°C. The incident light beam, when measuring the angular scattered intensity, was always the blue line (4358 Å) from the mercury lamp. This is preferable to the green line because it is stronger, the scattered intensity is proportional to the reciprocal of the fourth power of the wave length and the sensitivity of the photocathode of the P.M. is about double for the blue relative to the green. In order to measure the depolarisation ratio* ρ_u with greater accuracy, the blue filter is removed from the path of the incident beam, as this value is independent of wave length. The removal of the filter results in a better signal to noise ratio which is important when measuring the horizontally polarised component, as this is relatively small in all cases.

In the measurements on syton 2X, the angular distribution of the scattered intensity for the solution having the highest concentration (5.4×10^{-3} g.ml^{-1}) was measured over the range 30°-145°. A plot of $F(\phi)_M \frac{\sin\theta}{1+\cos^2\theta}$ against θ is shown in fig. (6.6). No dissymmetry was observed, indicating that the quarter wave plate (in the apparatus) was functioning correctly and that the particles were very small compared to the wave length of the incident beam. The standard deviation in $F(\phi)_M \frac{\sin\theta}{1+\cos^2\theta}$ expressed as a percentage of its mean value was 0.52%. On measuring the depolarisation ratio, ρ_u, for four concentrations, it was found that ρ_u is independent of C and has an average value of 0.0065, as shown in fig. (6.7). This is very small and gives a Cabanne's correction factor* of almost unity. Thus the particles are optically isotropic. The stability of these solutions was confirmed by both turbidity and scattering measurements at the start and the end of the experiment on two solutions. Thus syton 2X can be considered as an ideal material for calibration purpose as reported by Jennings and Jerrard. From the measurements of the scattered intensity at $\theta = 90°$

---

* (c.f. sec. 2.2.5)

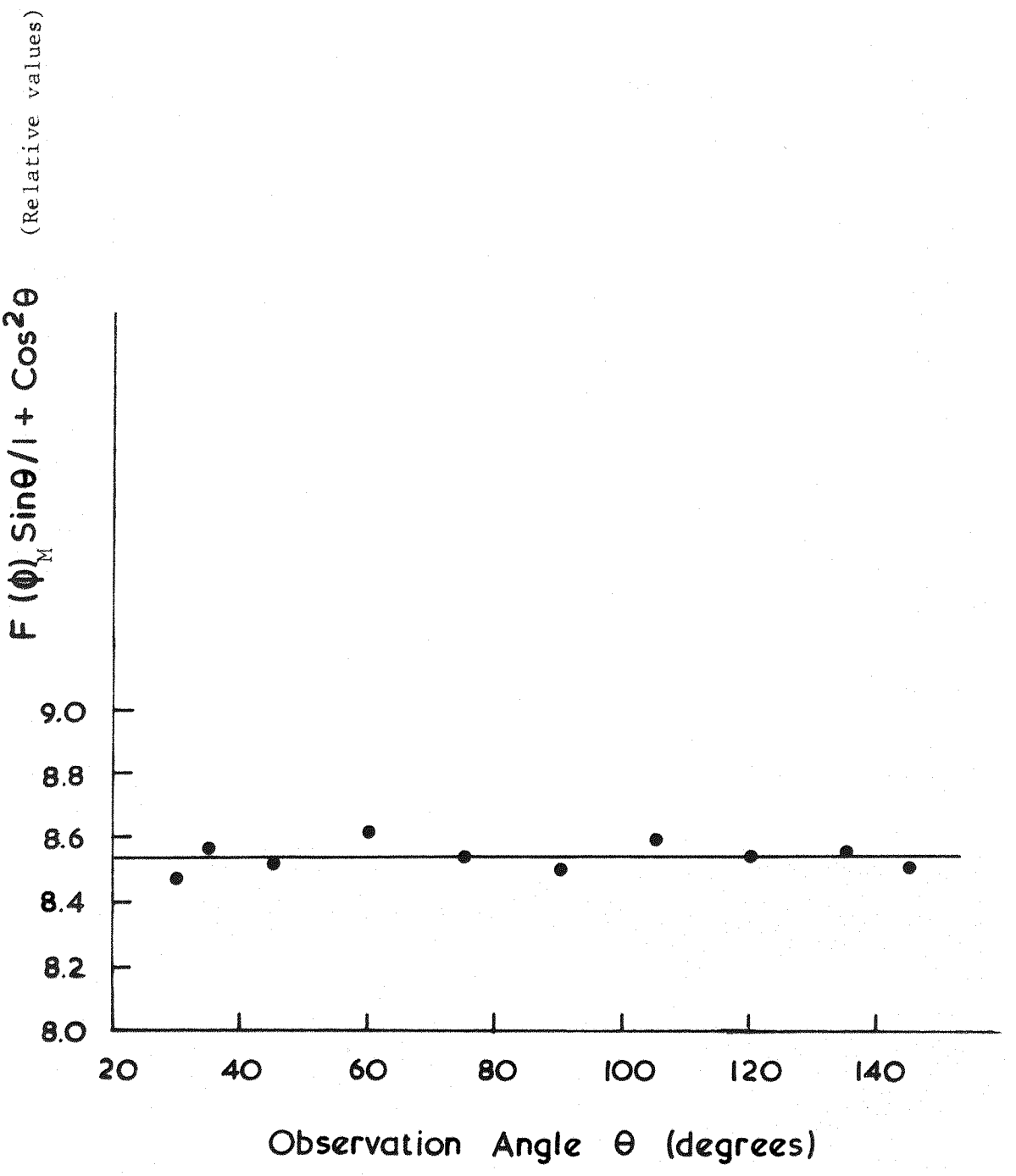

Fig. 6.6 Angular distribution of the scattered intensity for Syton 2X at $\lambda_o = 4358\,A^\circ$ & $C = 5.4 \times 10^{-3} g.ml^{-1}$

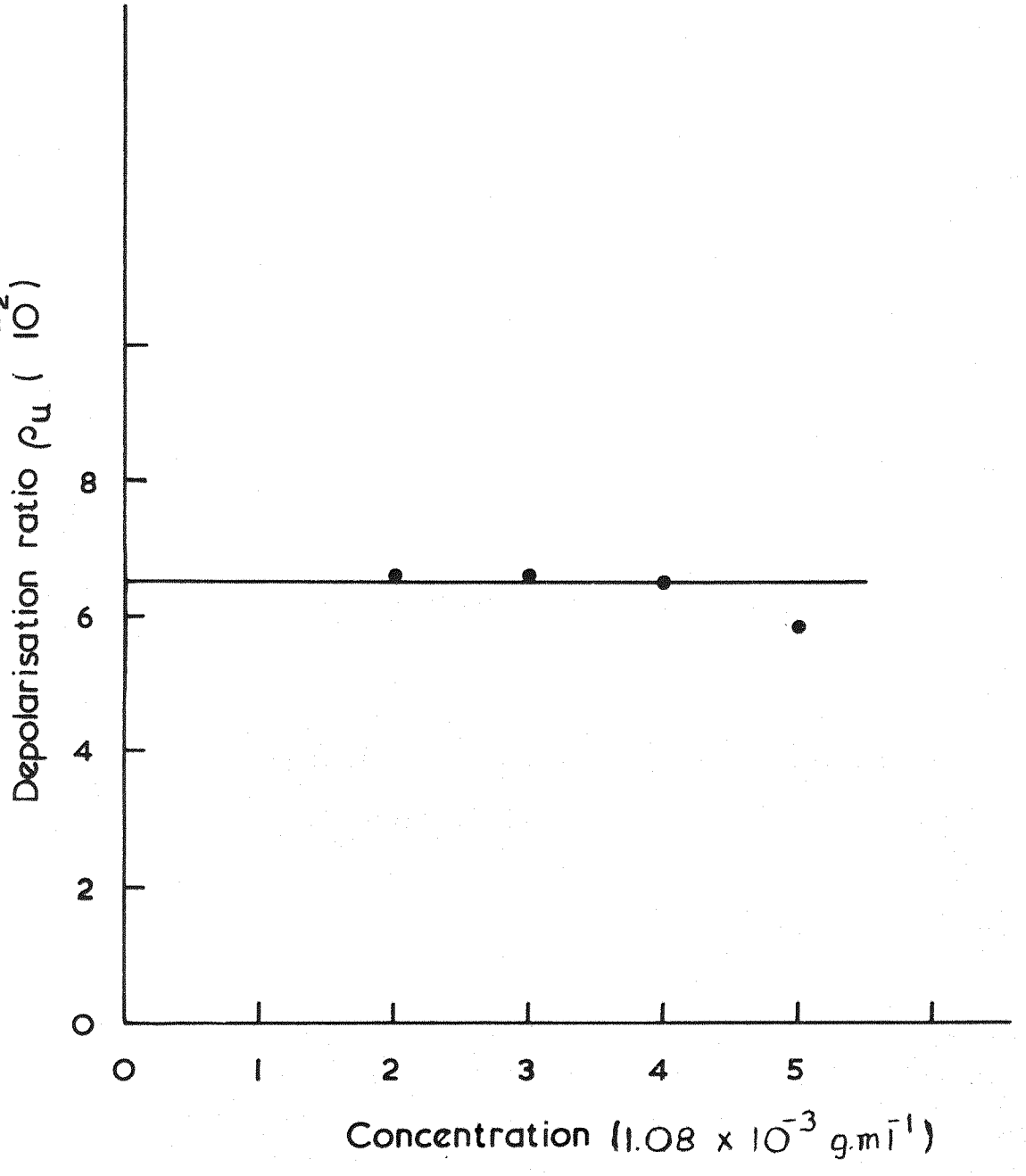

Fig. 6.7 Depolarisation ratio of Syton 2X v. Concentration

for five concentrations, and from the turbidity measurements, it was possible to find (C/I_{90}) for these concentrations. A plot of (C/I_{90}) against C from which the value of $\left|C/I_{90}\right|_{C \to o}$ can be obtained, is shown in fig. (6.8).

iv) Calibration constant determination.

From the previous light scattering measurements a value of 2.95 for $\left|C/I_{90}\right|_{C \to o}$ was obtained when a neutral filter (see fig.5.3) of a nominal optical density of 2 was in the path of the transmitted beam. The value of $\left|C/\tau'\right|_{C \to o}$ was 4.5. By substituting in (6.3) a value of $1.95 \times 10^{-2} \pm 2\%$ was obtained for J.

Other neutral filters of nominal optical densities of 1, 3 and 4 were also needed in this work. The filters were calibrated relative to each other. It can be seen that this is sufficient for the determination of J for these other filters. The values of J for the different filters are given in Table I. These were first obtained for cell A. For cell B it was found that J has different values and these are also shown on the same table. The reason for this difference is mostly due to the presence of araldite upon the edges of the exit window of the two cells. This causes a difference in the width of the transmitted beam on emerging from the cells.

In order to check any variation in the calibration constant, a rectangular glass block was used. This has two slits cemented on the front and the back face, relative to the incident beam, for the entrance and the exit of this beam. The slits are in the same position, relative to the incident beam, as those of the light scattering cell. The back face of the block, facing the viewing unit, was blackened to minimise back face scattering. By measuring the scattered intensity at 90^{o} at the time of the calibration (at the beginning and the end of the run) a

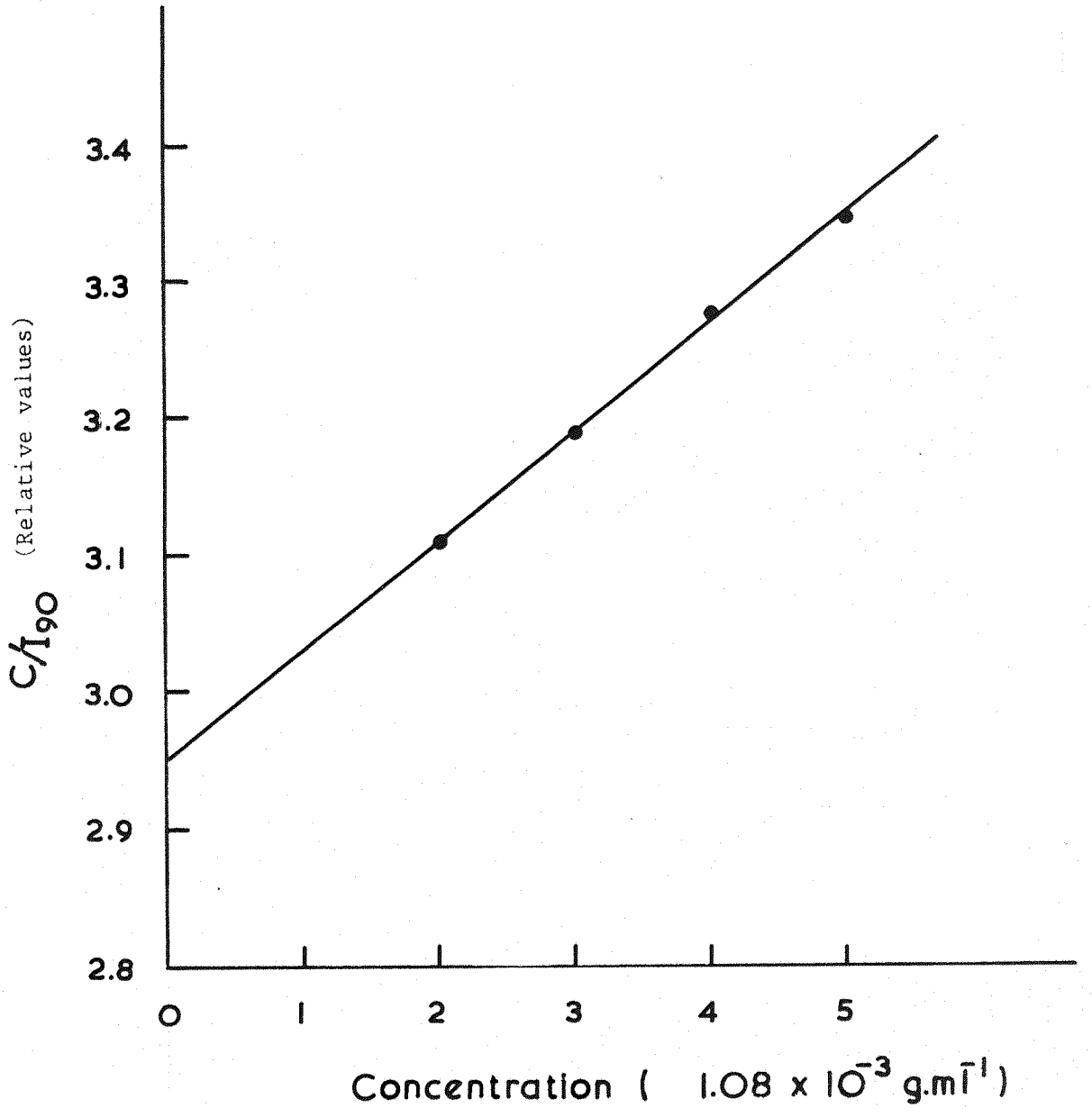

Fig. 6.8 C/I_{90} v. Concentration for Syton 2X at $\lambda_o = 4358\ A^\circ$

value of 0.173 for $F(\phi)$ was obtained. Changes in $F(\phi)$ reflect changes in the calibration factor which are related by

$$JF(\phi) = R_{90^\circ} = 3.86 \times 10^{-3} \text{ cm}^{-1}$$

This value of R_{90° is uncorrected for the refractive index* or the geometry of the block. During the period in which the results, presented in the next chapter, were obtained the changes in $F(\phi)$ were within the experimental error and no corrections were needed.

Table I

Values of the calibration factor J, for cells A and B at a wavelength of 4360 Å, for neutral filters of different optical densities

Neutral filter optical density	J x 10^5 cell A	J x 10^5 cell B
1	17600	19100
2	1950	2230
3	54.6	62.4
4	2.57	2.93

* This is due to the fact that the glass block has a refractive index different from that of the solution used to obtain the calibration constant (see Hermans and Levinson - 1951).

CHAPTER 7

Results

7.1 General Remarks on Procedure of Measurements and Accuracy of Results

In investigating a sample solution using the conventional light scattering technique (i.e. in the absence of any orientating force), it is necessary to measure the light scattered intensity at various angles and concentrations. These measurements must be carried out at a specific light wave length and at constant temperature. In addition to the angular scattered intensity, the depolarisation ratio ρ_u must also be measured. As ρ_u is a ratio (that of the horizontally to the vertically scattered light at $\theta = 90^o$) the incident light beam does not have to be monochromatic.

In the present light scattering measurements the mercury blue line (4358 Å) from a 250 Watt mercury lamp was selected by a suitable filter as the incident light beam. However, when measuring ρ_u the filter was removed from the path of the incident light beam. This was because the horizontal component of the scattered light at $\theta = 90^o$ is usually very small and the presence of the filter would further reduce it.

Depolarisation and angular scattering measurements were made on solutions of bovine albumin, Wyoming sodium bentonite, North African calcium bentonite, hectorite, acid soluble calf skin collagen and the sodium salt of deoxyribonucleic acid (DNA). For each of these substances the scattered intensity was measured at eight angles in the angular range 30^o - 135^o for several solutions of predetermined concentration. The solutions used in these measurements were obtained by volumetric dilution from an already prepared sample solution, known as the mother solution, the preparations of which will be described in due

course. The concentration of these solutions were chosen so that they were in the ratio 1:2:3:4. For all of the samples the procedure being to obtain first the solution of lowest concentration, and then solutions of successively greater concentration. This procedure reduces the errors from contamination of the mother solution due to handling as handling would introduce the largest error in the most diluted solution. Each time after cleaning and drying the cell, solutions of successively greater concentration were investigated.

The angular measurements were analysed using the Zimm plot method except for those of bovine albumin (because it was found to be composed of particles of small size). In this method (chapter 2 sec. 2.3.2) the quantity $K'C/R'_\theta$ is plotted against $\sin^2\theta/2 + g.C$, where g is a constant chosen to give sufficient spread of the results and K' is an optical constant which is proportional to $(dn/dC)^2$ as given by eq. 2.15 Thus for the evaluation of $K'C/R'_\theta$ it was necessary to measure C, and also dn/dC if no value for this parameter was available.

If a value for dn/dC was available (from the present measurements or from the literature) then C, for a given solution, was determined by measuring* Δn, the difference between the refractive indices of the solution and of the solvent. If dn/dC was unknown, it was obtained by measuring Δn for several dilute solutions obtained from the mother solution. The concentration of the mother solution was determined by a 'dry to constant weight' method and permitted $\Delta n/C$ for the diluted solutions to be obtained. The dilution of the mother solution was continued untill $\Delta n/C$ became independent of concentration and it was then assumed that

---

* As with Syton 2X, the measurements of Δn were carried out by using the Rayleigh Refractometer.

$$dn/dC = (\Delta n/C)_{C \to o} \qquad (7.1)$$

The parameters that can be obtained from the Zimm plot are the weight average molecular weight, M_w, the Z-average radius of gyration ρ_z and the second virial coefficient of interaction B. M_w is obtained from the common intercept (at the ordinate) of the curves of zero concentration and zero angle of the Zimm plot through (c.f. eq. 2.35) the relation

$$\text{Common intercept} = \left(\frac{K'C}{R'_\theta}\right)_{\substack{C \to 0 \\ \theta \to 0}} = \frac{1}{M_w} \qquad (7.2)$$

ρ_z is obtained from the initial slope of the zero concentration Zimm plot through (c.f. eq. 2.34) the relation

$$\frac{\text{initial slope}}{\text{common intercept}} = \frac{16\pi^2}{3\lambda^2}(\rho_z^2) \qquad (7.3)$$

The slope of the zero angle line (i.e. $K'C/R'_{\theta=o}$) is $\frac{2B}{g}$ from which B can be calculated.

In the present work some steps were taken to minimise the calculations involved in obtaining the Zimm plots. The scattered intensity was measured at 15^o intervals over the range 30^o - 135^o, solutions whose concentration were proportional to 1,2,3,4 were used and a constant value for the term g.C was chosen (e.g. a value of 1.5 was chosen for the solution of highest concentration).

It is difficult to give a concise mathematical analysis of the total errors in the evaluation of the parameters which may be obtained from the Zimm plot for a given sample. This is because these errors vary according to several factors such as the number of solutions used in

obtaining the Zimm plot, the lowest available angle of observation and the size and molecular weight of the particles. From experinece, however, it is estimated that for the bentonite samples the total error on any of the previously mentioned parameters was not greater than 10%. The individual errors in estimating M_w being:-

i) the error in measuring R'_θ which was within 1%,

ii) the error in estimating the calibration factor which was within 2%,

iii) an error of 2% arising from the term $(dn/dC)^2$ as (dn/dC) was measured to an accuracy of ± 1%,

iv) another ± 2% error was estimated to arise from the variation in the concentration of the individual solutions. Thus the overall error in M_w is about 7%.

The error in the value of ρ_z^2 as determined from the deviation of the initial slope of the zero concentration Zimm plot was estimated to be within 8%. A further error of 7% is introduced into ρ_z^2 because of the uncertainty in the molecular weight. Thus the overall error in ρ_z is 7.5% (half the error in ρ_z^2). The error introduced in the determined value of B was also estimated to be about 10%.

For both the collagen and the DNA samples the error in M_w was greater than 7%. This is firstly because for these samples the intercept from which M_w was calculated was rather small and also because of the levels of concentration used, higher errors were involved in the measurements of dn/dC and R'_θ . It was estimated that the error in M_w for both of these samples was about 15%. For the hectorite sample these factors were not quite as significant and the error in determining M_w was estimated to be about 12%.

After concluding the conventional light scattering measurements, attempts were made to measure the changes in the scattered intensity

resulting from the application of sine wave electric fields. Under the experimental conditions used in this work this type of measurement was only possible for the bentonite samples and led to the determination of the electrical properties and the average relaxation time for these samples. As the relative changes in the scattered intensity were rather small (up to 15%) it is to be expected that there would be a relatively large error in the values of the parameters determined using this technique. It is estimated that the overall error could be as large as 20%.

As it was difficult to measure the changes in the scattered intensity for several of the samples, the electric birefringence technique was used to obtain the relaxation time (or range of relaxation times if the sample was polydisperse) from the birefringence decay. In certain cases such as with hectorite this was sufficient to give some qualitative information about the electrical properties of the sample. As previously mentioned (chapter 5, part B sec. 5.7) the Kerr effect apparatus used for this type of measurements provides pulses of short duration (2.5 μsec.) and therefore fields of high intensity were used to orientate the particles. The apparatus is capable of producing pulses having voltages in the range 1-10 KV which is equivalent to electric fields of 3-30 KV/cm on the solution.

The method of determining the relaxation time, τ, from the birefringence decay and the accuracy which can be achieved with a monodisperse sample (4%) were discussed previoysly (sec. 5.8).

Only one sample, collagen (sec. 7.6.3), resulted in a linear log plot and thus only one relaxation time was determined for this sample. For the other samples, the two extreme values of τ were determined from the initial and end tangents of the log plot. The errors involved were as large as 30% in certain cases for the values of τ obtained from the initial slope (i.e. for the smallest value of τ). Much lower errors were involved when τ was obtained from the end tangent. It is estimated

that the values of τ in the latter case are accurate to within 12%. Since collagen was found to be monodisperse, a smaller error might be expected but the poor quality of the traces and the small values of τ resulted in an error of comparable magnitude (12%) to the errors in the values of τ obtained from the end tangent. The error introduced in each of the linear dimensions of the particles would be only a third of the error in τ for both disc and rod shaped particles. One disadvantage of the method is that it is difficult to determine the whole distribution of particle sizes.

Finally all the different types of measurements were carried out at a constant temperature of $20^{o}C$.

7.2 Bovine Albumin* (B.A.) cryst. puriss.

7.2.1 Preparation of the mother solution

Two grams of B.A. were dissolved in 100 ml. of freshly double distilled water. The resultant solution which froths easily was handled with great care and was first centrifuged for an hour in an M.S.E. temperature controlled centrifuge at 34,000 g and at a temperature of about $8^{o}C$. The solution was centrifuged at this low temperature because in general proteins tend to aggregate at room temperature. The supernatant was then carefully removed and filtered through an 0.1 μ filter under pressure using nitrogen gas. Five solutions of different concentrations were made from the mother solution by volumetric dilution. The concentration of the mother solution was found to be 1.2×10^{-2} g/ml. A value of 1.95×10^{-1} was also obtained for dn/dC at the wave length 4358 $\mathring{A}$.

7.2.2 Conventional light scattering measurements

The angular distribution of the scattered light intensity for the mother solution was measured over the angular range 30^{o} - 145^{o}. It was found, as fig. (7.2.1) shows, that for the present sample R'_{θ} is independent of θ. Hence the particles must be small compared to the wave length and thus for the determination of the molecular weight it is sufficient to measure the scattered intensity at one angle for every concentration. These measurements and those of the depolarisation ratio were carried out at the angle $\theta = 90^{o}$. As fig. (7.2.2) shows the depolarisation ratio ρ_u was found to be independent of concentration and to have an average value of 0.026 which results in a Cabanne's correction factor of 0.945. It was also found, as fig. (7.2.3) shows, that $K'C/R'_{\theta}$ is independent of concentration and has an average value of

* The sample of Bovine Albumin was obtained from Koch Light Laboratories (Batch No. 58769).

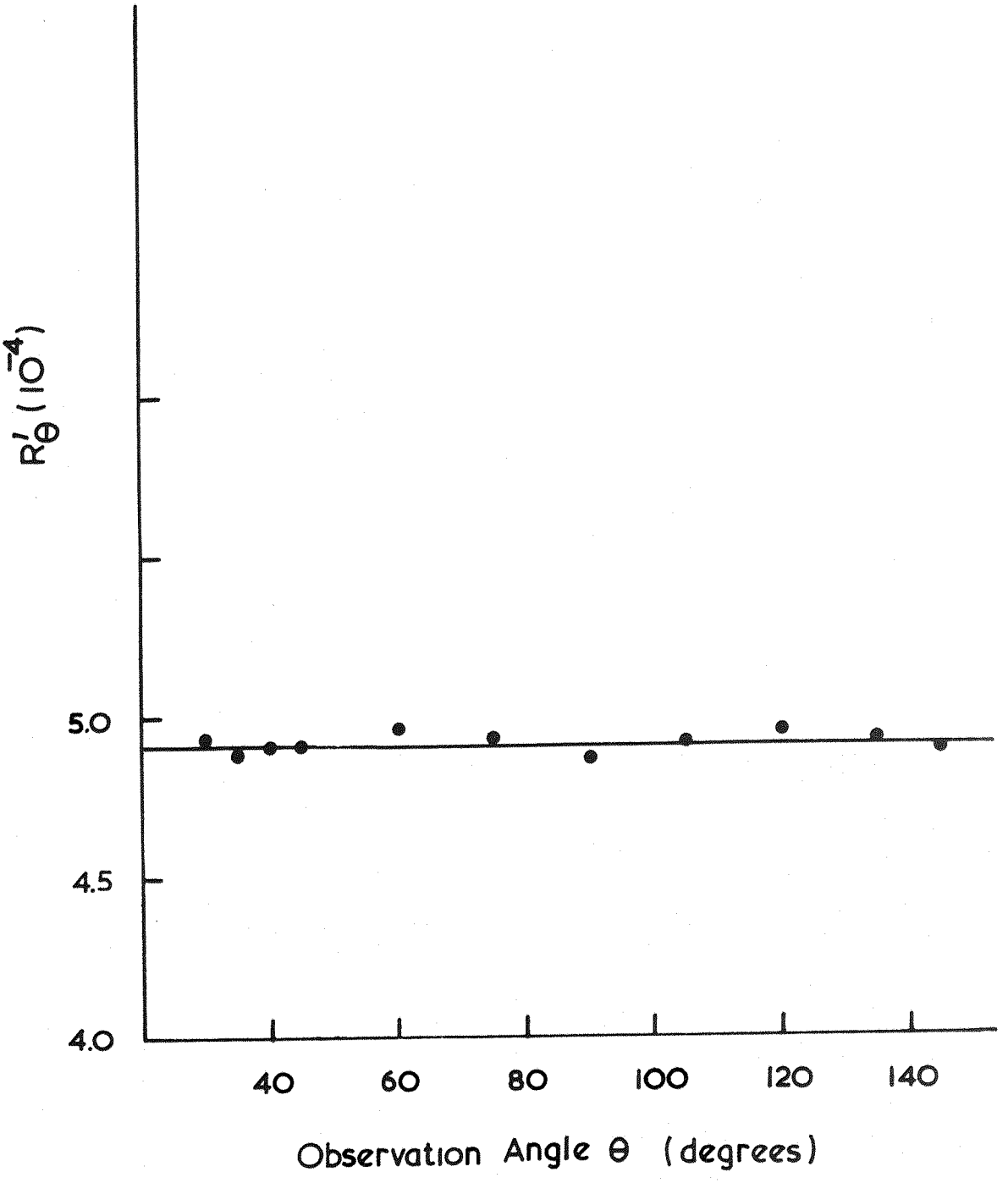

Fig. 7.2.1 Angular distribution of scattered intensity for Bovine Albumin at a concentration of 1.2×10^{-2} g.ml^{-1} and $\lambda_o = 4358$ A°

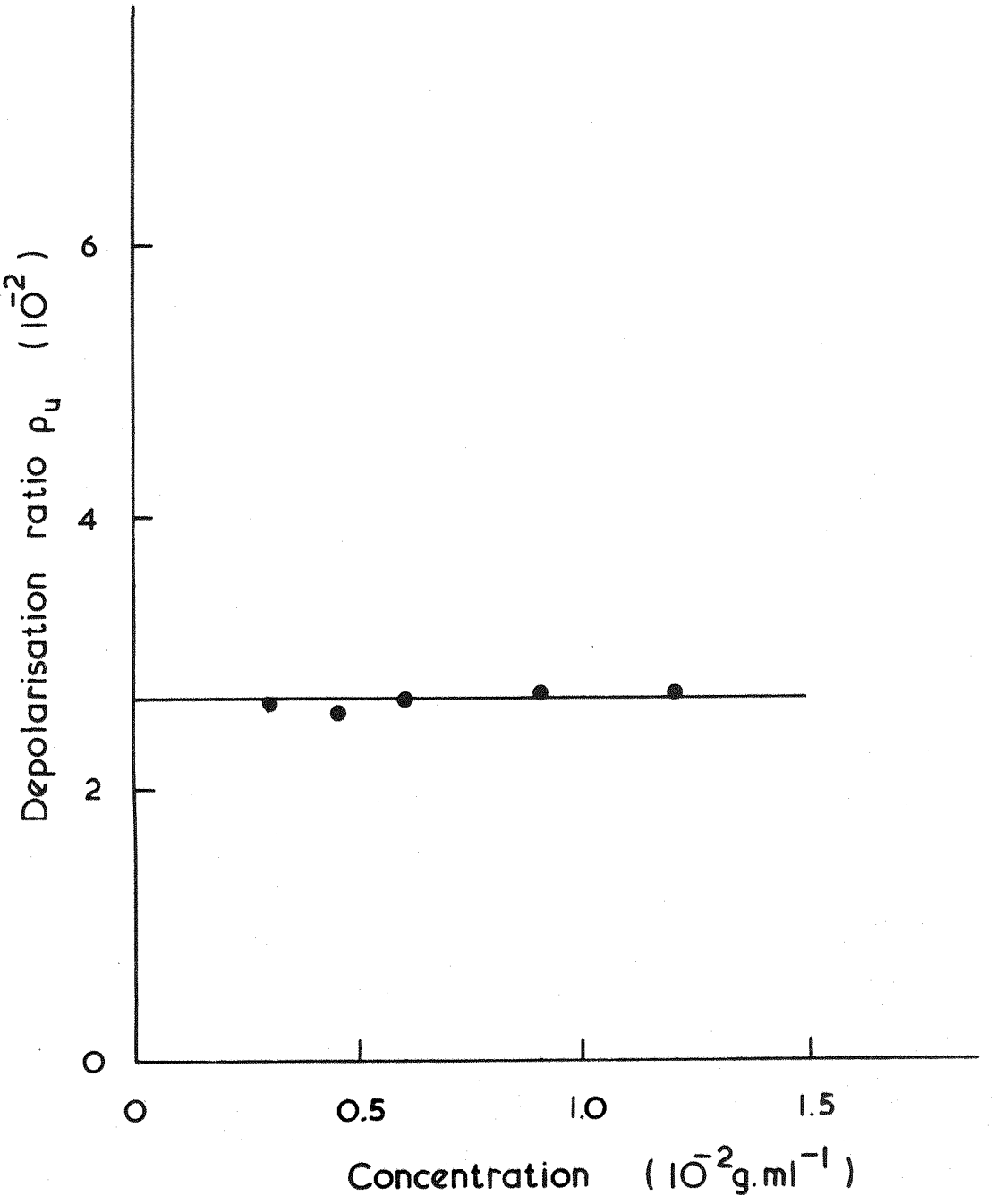

Fig. 7.2.2 Depolarisation of Bovine Albumin

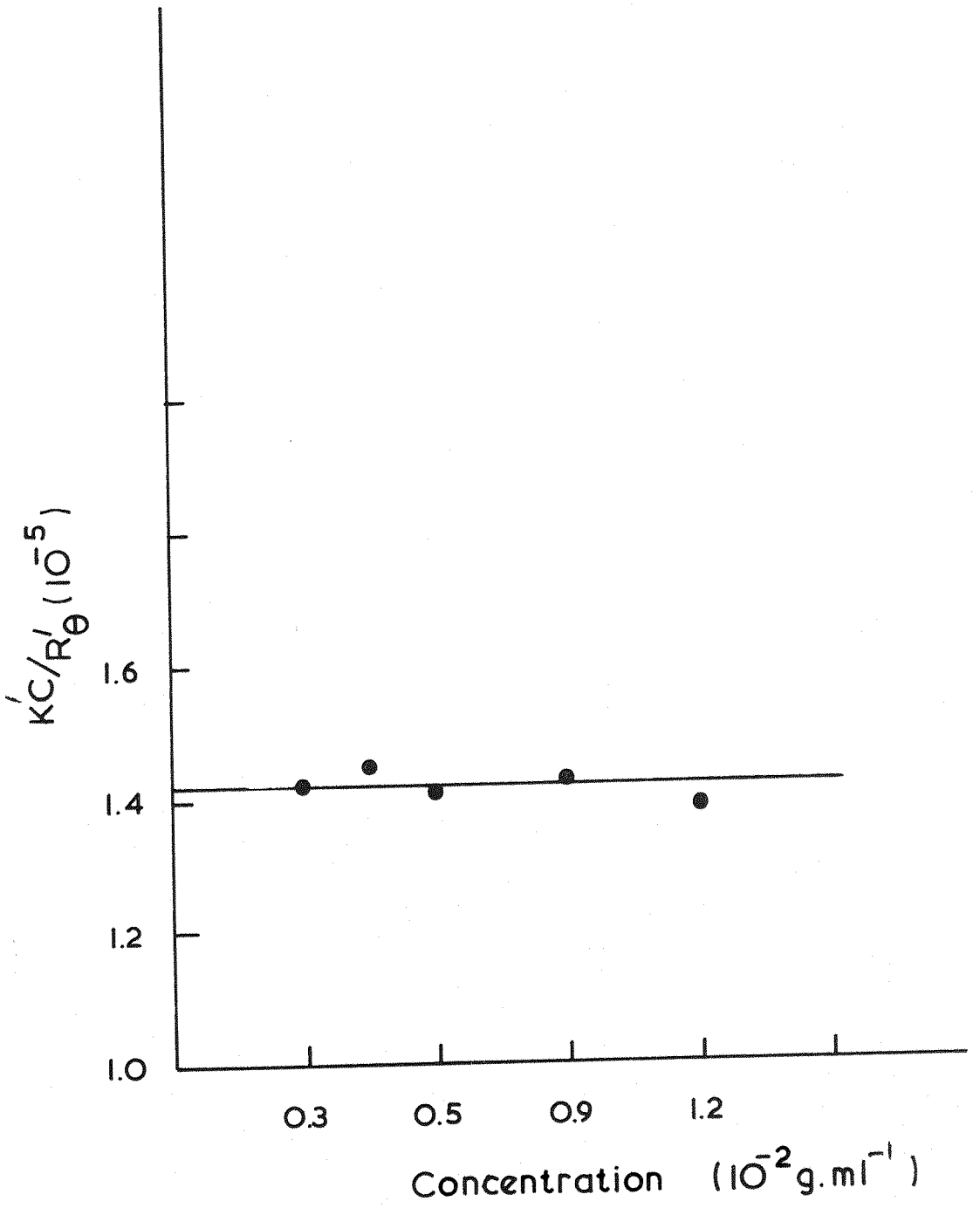

Fig. 7.2.3 Molecular weight determination of Bovine Albumin

$1.42 \ (\pm 0.03) \times 10^{-5}$. Thus the second virial coefficient B is zero. This average value of $K'C/R'_{\theta}$ resulted in a molecular weight of 70,400 which when corrected by the Cabanne's correction factor reduced to 67,000 (± 2,000).

7.2.3 Discussion

It is generally accepted that the molecular weight of B.A. is close to 70,000. Both the osmotic pressure (Scatchard et al - 1946) and the sedimentation and diffusion techniques (Oncley et al - 1947) give 69,000. However when the light scattering technique is used the value obtained for the molecular weight is, in most cases, higher than the previously mentioned value. Most of the values obtained are in the range 67,000 - 78,000 (e.g. see Doyt and Steiner - 1952, Dandliker - 1954 and Sellen - 1962). The higher values are a result of the strong tendency of the solution of (B.A) to aggregate. The light scattering technique leads to a weight average molecular weight which is more effected by aggregation than is the case for techniques such as osmotic pressure and diffusion which give a number average value. The values of the depolarisation ratio determined by many authors are in the range 0.018 - 0.027. Sellen's (1962) measurements show that it is concentration dependent increasing with concentration, while those of Edsall et al (1950) indicate that it is concentration independent except that there is a slight increase at lower concentrations (much smaller than 1%). According to Geidusheck (1954) the depolarisation of B.A. arises from secondary scattering. His conclusion was based on the fact that Ludox and bovine serum albumin gave the same depolarisation when their turbidities were the same and also that since Ludox is made up of spherical optically isotropic particles it has no genuine depolarisation. However it is found from the results of other workers and

those here, that the zero concentration depolarisation of Ludox and albumin is not the same, a conclusion which is contrary to Geiduscheck's. The second virial coefficient takes very different values (c.f. Edsall et al - 1950, Dandliker - 1954 and Timasheff - 1954). It is usually negative in pure water indicating the long range repulsive forces between the electrically charged particles. However when electrolytes are added these forces are suppressed and B becomes positive. For isoionic B.A., even in the absence of salts, B is almost exactly zero.

The previous discussion indicates that the present values of M_w and ρ_u are in satisfactory agreement with those reported in the literature. However, with regard to B the zero value determined was unexpected since no steps were taken to ensure that the mother solution was isoionic. However on measuring its pH it was found to be 5.1 which is very close to the isoionic pH of 5.17 in salt free water (Scatchard et al - 1946).

The purpose of these measurements on B.A. was to check the calibration factor of the light scattering apparatus (c.f. chapter 6, sec. 6.). Although B.A. is not the ideal material to be used for this purpose because of its tendency to aggregate it is still suitable for detecting large errors in the calibration factor. Previously in this laboratory, this check was performed by measuring the Rayleigh ratio for organic solvents (Jerrard and Jennings - 1964). This procedure was not adopted in the present work because the araldite used for cementing the cell together seemed to be susceptible to organic solvents. In fact on one occasion using dichloroethylene as the solvent, it started to leak through the cell to such an extent that a reconstruction of the initially provided cell became necessary.

7.3 Wyoming Sodium Bentonite, W.Na.B.

7.3.1 Preparation of the mother solution.

Eight grams of W.Na.B. powder were added to 300 ml. of freshly double distilled water. The powder was added in small quantities, the container shaken until suspension occurred and the solution was then left standing for six days until all the non-colloidal matter settled out. After this the solution was poured carefully into the centrifuge plastic tubes so that the sedimented matter was left behind. Plastic tube covers were also used because it was found that the highly concentrated W.Na.B solutions attacked stainless steel covers. The solution was centrifuged for 20 minutes at 6,000 g and the relatively highly concentrated strawcoloured supernatant was carefully removed. 200 ml. of this solution, after filtering through 5μ, 3μ and 1.2μ filters, were used for dn/dC measurement. The remainder of the solution was diluted to about twice its original volume and further centrifuged at 9,000 g for 20 minutes so that only the very finest particles were left in suspension and thus a clear stable solution was obtained. The concentration of this stock solution was found to be $\sim 1.5 \times 10^{-3}$ g/ml.

7.3.2 Measurement of dn/dC

The value obtained for dn/dC at the wave length 4358 Å was 0.096 mlg^{-1}. Some previously reported values for this parameter are 0.084 (Wippler - 1956), 0.095 (M'Ewen and Pratt - 1957) and 0.091 (Jennings and Jerrard - 1965). The sample used in this experiment was the same as that used by the last two authors cited above. They accounted for the difference between their value and those previously determined by a difference in the sample composition. The difference between the

present determination of dn/dC (0.096) and that of Jennings and Jerrard (0.091) may be due to the different method of sample preparation. This probably led, because of impurities in the original powder sample, to a sample solution of slightly different composition. The value determined in the present work was obtained by drying a relatively large amount of highly concentrated solution, and was reproducible with an estimated error of less than two percent. This value was therefore used in the determination of the molecular weight and in finding the concentration of other W.Na.B solutions used in this experiment.

7.3.3 Conventional light scattering measurements

The scattered intensity was measured for four solutions of different concentration in the angular range 30^{o} - 135^{o} . The results are shown in the Zimm plot (fig. 7.3.1). The variation of ρ_u with the concentration C is shown in fig. (7.3.2). By extrapolation to zero concentration a value of 3.3×10^{-2} for ρ_u is obtained, which gives a Cabanne's correction factor of 0.93. The pH of the solution of highest concentration used in these measurements was 7.4. The corrected Zimm plot data gave the following parameters:

$8.2\ (\pm 0.7) \times 10^{7}$ for the weight average molecular weight M_w,

$1{,}070\ (\pm 90)$ Å for the Z average radius of gyration ρ_z and

$-1.9\ (\pm 0.2) \times 10^{-6}$ for the second virial coefficient B.

Thus the particles at this pH, as the negative value of B indicates, prefer their own company. However no sign of aggregation was found during the present investigation because only solutions of low concentration were used. Assuming the particles to exist in solution as circular discs* (Shah et al - 1963) of radius r, a value for r of $1510\ (\pm 120)$ Å was obtained from the radius of gyration. A value of

---

* Actually the particles have the shape of flakes. However, for simplicity, it is very usual to treat them as discs.

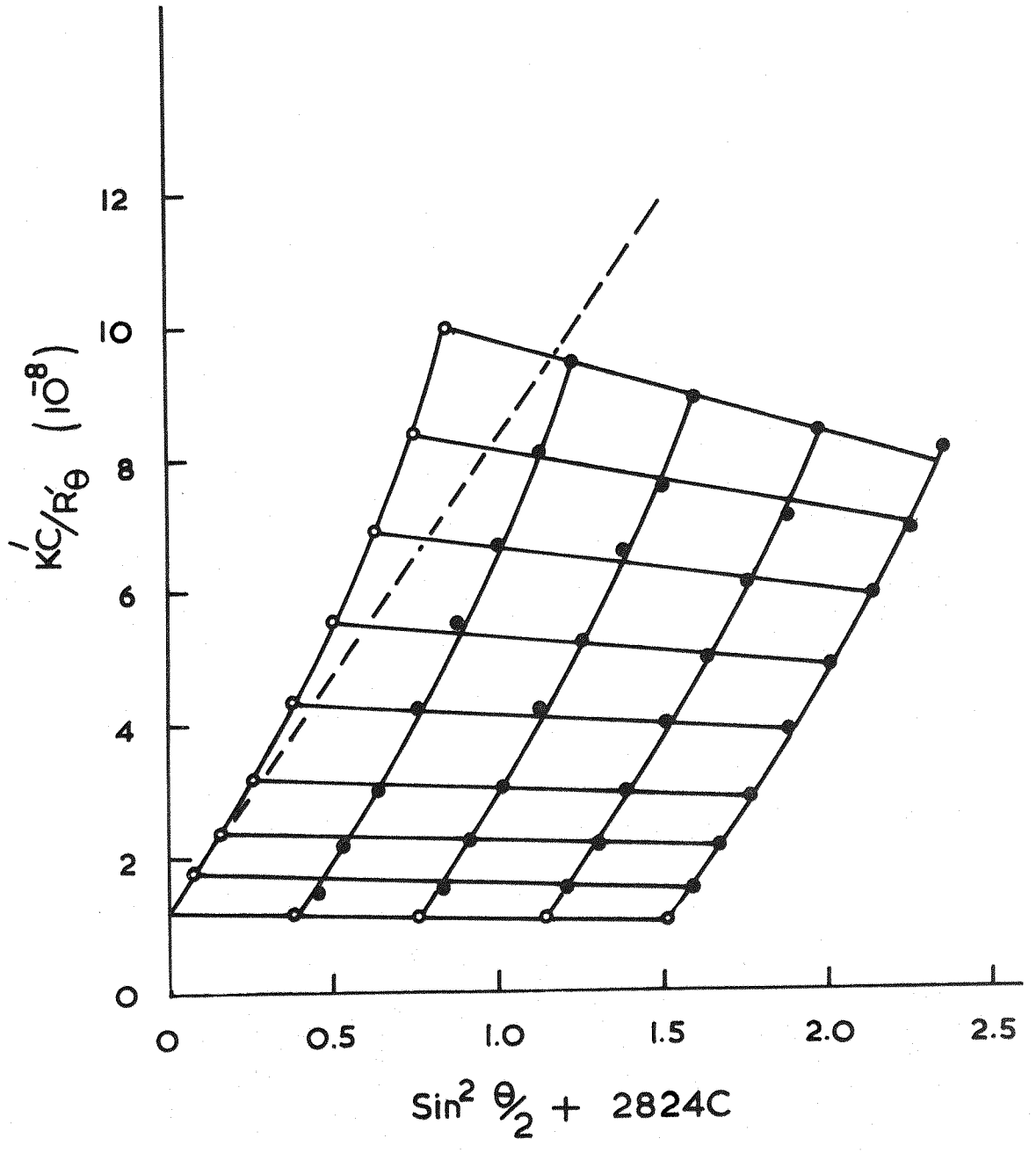

Fig. 7.3.1 Wyoming Sodium Bentonite
(Zimm plot)
at pH 7.4 & wavelength 4358 Å

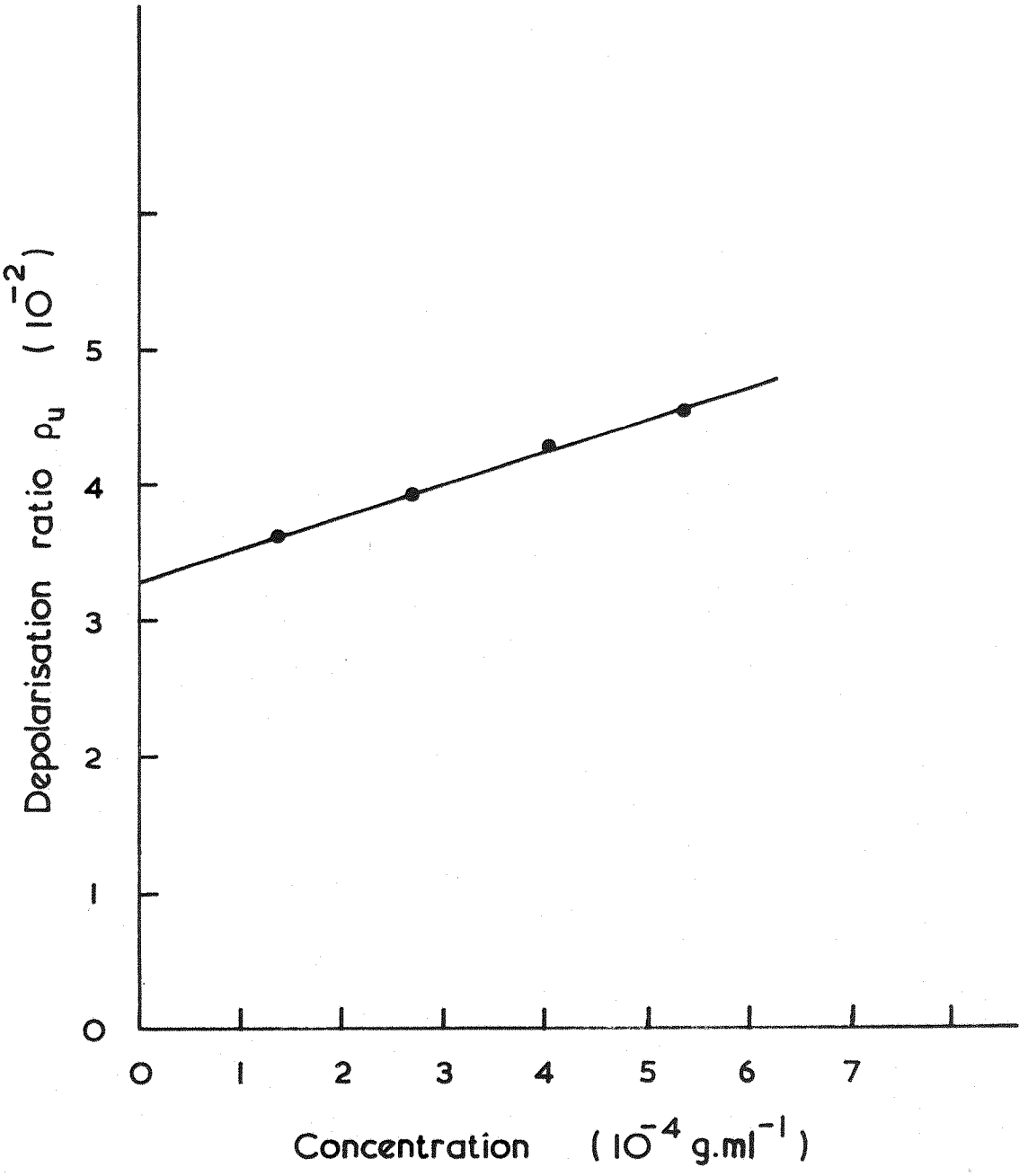

Fig. 7.3.2 Depolarisation of Wyoming Sodium Bentonite

9 Å was also found for the thickness of the disc from the following relationship between the molecular weight M_w, the volume of the particles and their density ρ:

$$M_w = \rho \pi r^2 t N_A \qquad (7.4)$$

where N_A is the Avogadro number.

It is apparent that the thickness of the disc is the parameter that should be used when the present data are to be compared with those obtained by other researchers. This is because the initial solution of W.Na.B is very polydisperse and different methods of preparation result in different distribution of particle sizes left in the solution studied. The present value of t is in good agreement with that reported by Jennings and Jerrard (1965) and also with the expected thickness of the layers of montmorillonite (the major constituent of bentonite) determined by the X-ray techniques. However, Wippler's result (Wippler - 1956) is larger by a factor of 2. It is thought that this discrepancy is partly due to the fact that in each case different fractions of the original polydisperse sample were analysed. The effect of polydispersity* (as can be seen from eq. 7. 4) is to under-estimate the value of t because M_w is a weight average molecular weight while that of r is a Z-average. Thus without knowing the size distribution of the particles, it is difficult to determine their exact thickness.

The present value of t, the regular shape of the Zimm plot and the stability** of the solutions used in obtaining this plot,

---

* The polydispersity of the sample used in this work was verified by the Kerr effect measurements (sec. 7.3.4).

** The stability was verified by measuring, regularly over the period of investigation, the scattering from the most concentrated solution.

support the view shared by other workers (Shah - 1963 , Jennings and Jerrard - 1965 and Stoylov et al - 1968) that the particles exist in solution as individual unaggregated discs. There is no evidence to support the view of M'Ewen and Pratt (1957) that the particles exist in solution as side by side aggregates of five individual discs which these authors have suggested because of kinks in their Zimm plot resembling those that can be associated with ribbons (Stokes - 1957).

7.3.4 Measurement of the relaxation time by the Kerr effect.

Square electric field pulses of about 15 Kv/cm were applied to four solutions of different concentration. The highest concentration used in these measurements was 2.4×10^{-4} g/ml. A typical birefringence trace obtained at this concentration is shown in fig. (7.3.3). Fig. (7.3.4) shows a semi-log graph (see chap. 5 sec. 5.8) of the birefringence decay of this trace. The departure of the log plot from linearity indicates that possibly more than one relaxation time is present suggesting that the sample is polydisperse as the other causes flexibility or asymmetry of shapes can be ruled out (Shah et al. - 1963). The extreme values and thus the range of the relaxation time, τ, as obtained from the slopes of the end tangent and the initial tangent (not shown in the figure) of the log curve were found to be 1.63×10^{-3} sec. and 0.4×10^{-3} sec. respectively. Values of 102 and 417 sec.^{-1} were also obtained for D, the diffusion constant, using the relation $D = {}^{1}/_{6\tau}$ (eq. 4.7). It was also found from analysis of the traces for the other solutions that over the range of concentration used, the determined values of τ were independent of the concentration. This is in agreement with the findings of Khan and Lewis (1954) and

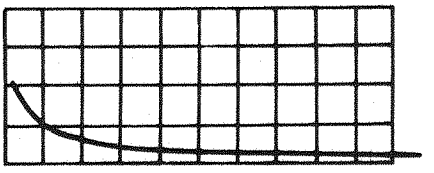

Wyoming Sodium Bentonite

Fig. 7.3.3 Typical experimental birefringence trace obtained at T = 20^{o}c, C = 2.4 x 10^{-4} g.ml^{-1} E = 15 kV cm^{-1} and pulse width of 2.5 x 10^{-6} sec, Time scale 500 x 10^{-6} sec.cm^{-1}

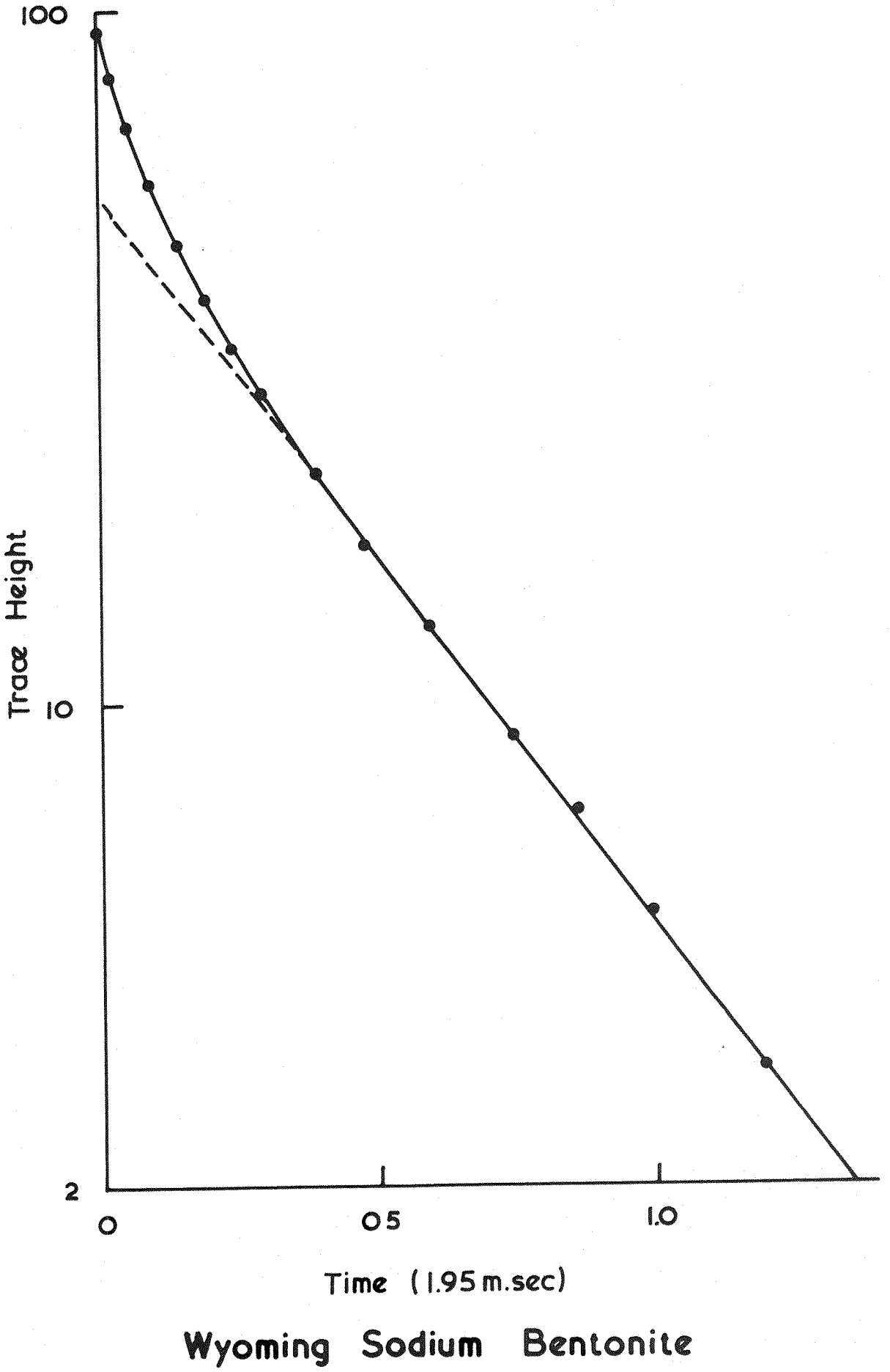

Fig. 7.3.4 Semi-log plot of the birefringence decay of the trace shown in fig. 7.3.3

Shah et al. (1963). The range of τ was however dependent on the field intensity applied, the range increasing with increasing the field intensity as the lower limit of the range decreases. This is because the contribution of the smaller fractions of particles to the birefringence increases and thus their contribution becomes measurable as the field intensity becomes larger.

Applying the relationship of Perrin (1934), viz

$$r^3 = \frac{3kT}{32\eta D} \qquad (7.5)$$

which gives the radius of the disc r in terms of its diffusion constant D, values of r of 980 Å and 1560 Å were obtained. The latter value of r can be associated with the largest particles in the solution that can be detected at such a field strength and is in good agreement with the average value obtained from the light scattering data. This indicates that either the sample was mostly composed of particles having a radius $r \sim 1560$ Å or that there was a fraction of larger particles that cannot be detected probably because these larger particles are few in number. It should be mentioned that the complete distribution in size could be obtained only by using pulses of varied duration and field strength (O'Konski et al. - 1959).

7.3.5 Light scattering in the presence of electric fields

The mother solution was dialysed by using a synthetic resin (Zerolit-DM-F, B.D.H. Chemicals Ltd., Poole, England). On dialysis the pH fell to 5.6 and the resistance rose to greater than 100 KΩ/cm. Measurements of the relative changes in the scattered intensity, $\Delta I_s/I_s$ were made at the observation angle $\theta = 90^o$.

First to be determined was the rigidity parameter R defined by eq. 3.3. This was carried out using the method of measurement described

in Chapter 5, sec. 5.4.1 (see under cell C) as it permits cooling of the cell. The parameter R was determined with an electric field strength of 225 V/cm at two different frequencies (300 and 1000 Hz) on a solution of a concentration of 3.6×10^{-4} g/ml. The two resultant values of R agreed within the experimental error. The average value was 1.95 (± 0.3), indicating that the particles were rigid. Then the dispersion of $\Delta I_s/I_s$ was investigated for four solutions of low concentration ($\leq 3.6 \times 10^{-4}$ g/ml). These investigations were carried out using cell B (Chap. 5, sec. 5.4.1) which permitted vertical electrical fields to be applied to the solution (i.e. $\Omega = 90^{\circ}$).

Fig. 7.3.5 (a and b) shows two typical dispersion curves of the steady component of these changes at an electric field intensity of 225 V/cm in the frequency range 30 - 1000 Hz. These curves indicate that $\Delta I_s/I_s$ increases with frequency until at a relatively high frequency it reaches an asymptotic value. Similar behaviour was reported by Jennings et al(1965,71) and by Stoylov and Stoylov et al(1967,8). As would be expected these dispersion curves are similar to those obtained by Sakmann (1945) and Shah et al. (1963) when investigating the dispersion of the steady component of the electric birefringence.

In accordance with the theory (outlined in Chapter 3, sec.3.3.) the asymptotic value of $\Delta I_s/I_s$ is only due to the induced dipole moment because at sufficiently high frequencies the permanent dipole contribution to $\Delta I_s/I_s$ is zero. Furthermore since the steady component at high frequencies is positive, the induced dipole is along the major axis of the disc. At low frequencies the permanent dipole moment has a contributory effect and results in a decrease of the magnitude of the steady component. This implies that the permanent dipole moment is along the axis of symmetry of the disc particles and that the two

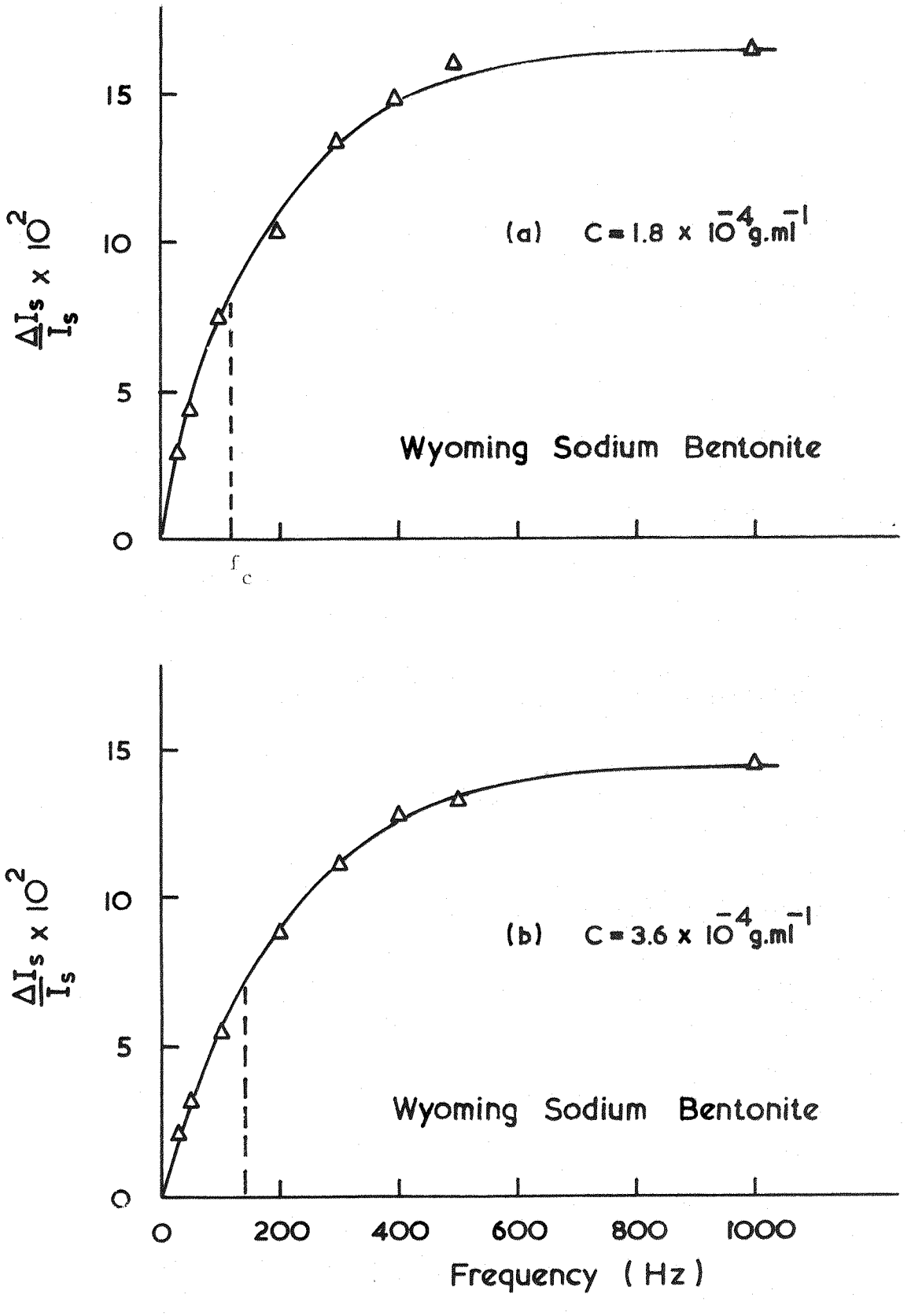

Fig.7.3.5 Frequency Dispersion of the Relative Intensity Change at $\Theta = 90^\circ$ & $E = 225\ V.cm^{-1}$

dipoles are perpendicular to each other.

It is seen from the dispersion data presented in fig. (7.3.5) that at low frequencies $\Delta I_s/I_s$ is rather small and thus would be difficult to measure at these frequencies for electric fields of intensities much smaller than those used in obtaining these measurements (225 V/cm). Therefore the dependence of $\Delta I_s/I_s$ on field intensity was investigated only at the high frequency of 2000 Hz. Fig. (7.3.6) shows $\Delta I_s/I_s$ plotted against the square of the field strength for two of the solutions. From this figure it is seen that $\Delta I_s/I_s$ can be considered to be proportional to the square of the electric field when the intensity is less than or equal to 225 V/cm. These findings are in agreement with the Kerr effect measurements of Shah et al. (1963) who also found that the larger particles saturate at smaller electric field strength. This may perhaps explain the saturation with much smaller fields reported by Jennings and Jerrard (1965). Figs. (7.3.5 and 6) also suggest that, within the experimental error the concentration at the levels used in the experiment has no effect on the values of $\Delta I_s/I_s$.

Since $\Delta I_s/I_s$ is independent of concentration and its value at high frequencies is proportional to E^2, thus it is possible to determine the polarisability of the particles $(\alpha_2 - \alpha_1)$ using eq. (3.10). Furthermore, by extrapolating the dispersion curves to zero frequency and assuming that $\Delta I_s/I_s$ is proportional to E^2 in the low frequency range, it is possible to calculate the value of the permanent dipole moment. It is found that

$$\alpha_2 - \alpha_1 = 2.65 \times 10^{-14} \text{ cm}^3$$

and

$$\mu_1 = 3.3 \times 10^{-14} \text{ e.s.u.}$$

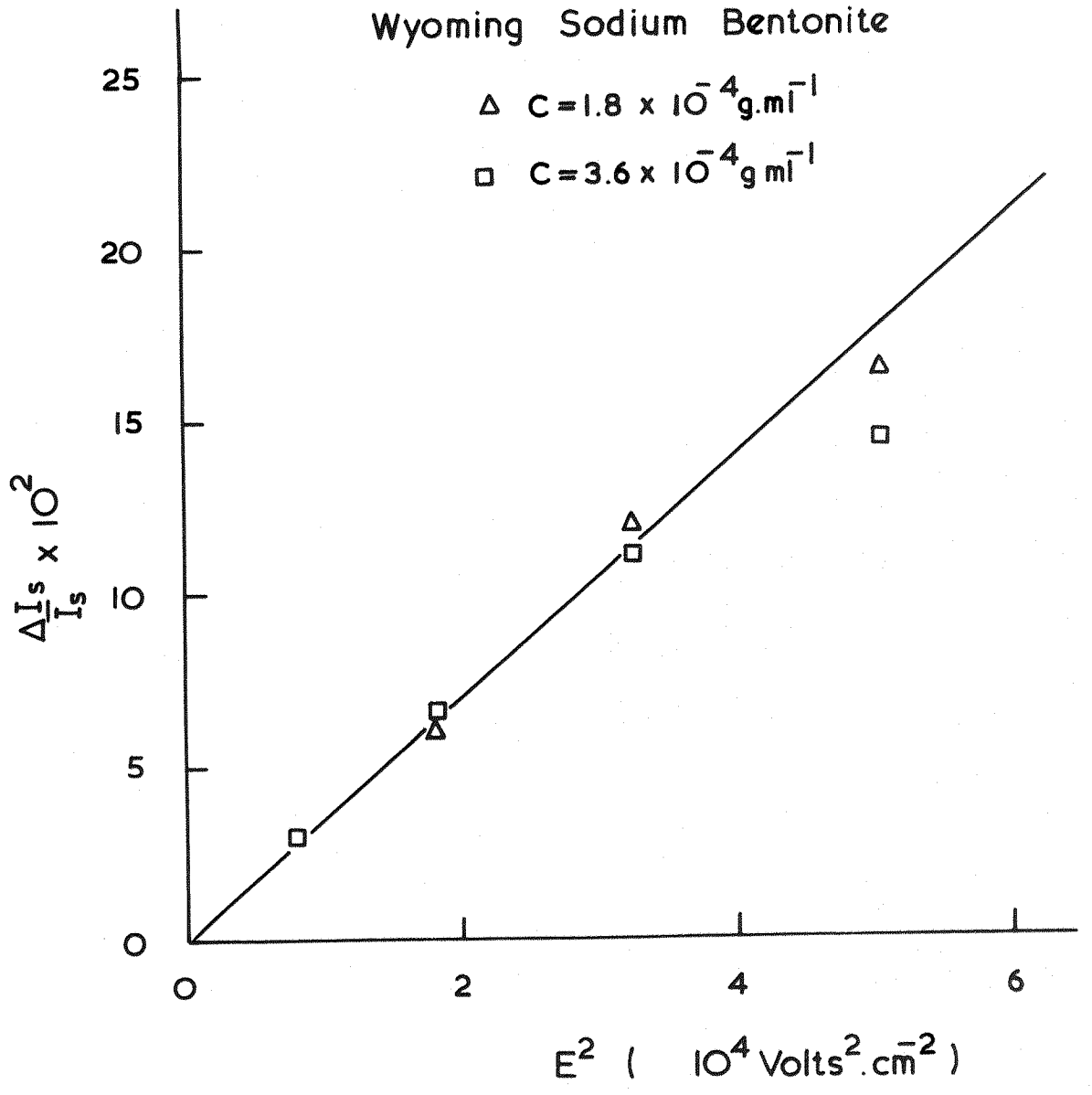

Fig.7.3.6 Variation of the Relative Intensity Change with the Square of the Field Strength at $\Theta = 90^{\circ}$

Stoylov (1971) lists the experimental values for these two parameters obtained by several workers using different techniques for both Wyoming and Chirpan Bentonites. The list shows considerable variation in the values of these parameters even when the size and type of sample are taken into consideration. By comparing the present results with those in the list it is found that they are closest to those obtained by Shah (1963) who gave $\alpha = 6.06 \times 10^{-14}$ cm^3 and $\mu = 2.65 \times 10^{-14}$ e.s.u. for particles of Wyoming Bentonite with a mean diameter of 3000 $\overset{o}{A}$. A closer agreement is found with the values of Schweitzer and Jennings (1971), who for a Redhill montmorillonite gave 4.5×10^{-14} cm^3 and 3.6×10^{-14} e.s.u for α and μ respectively.

Further information about the particles from the present studies can be obtained by finding the rotary diffusion constant D. This can be determined from the dispersion curves by finding the critical frequency f_c, at which $\Delta I_s/I_s$ is half the total contribution due to the permanent dipole moment, and using the relationship between these two parameters, viz.

$$f_c = \frac{d}{\pi} \qquad (3.8)$$

It was found that D is independent of concentration and has an average value of 377 ($\pm$ 75) sec^{-1}.

As it has been suggested (Rabinovitch - 1946) that bentonite is composed of two types* of particles therefore it was also interesting to study the dispersion of the alternating component because (see Chap. 3, sec. 3.2.2) this allows the determination of the rotary diffusion constant which for a sample composed of one type of particles should be the same as that determined from the dispersion of the steady component whereas for a sample composed of two types of particles different diffusion constants are obtained. However, it was difficult to measure the

* Type here refers to electrical properties where there is a distinction between those particles with electrical anisotropy predominantly along the major axis and those with a permanent dipole moment perpendicular to this axis.

alternating component to any reasonable accuracy even with as large a field as 370 V/cm and with the use of the frequency doubler (see Chap. 5, sec. 5.5). The fact that Jennings and Jerrard (1965) were able to carry out such measurements without the use of a frequency doubler is due to the nature of their sample (the particles were of 6800 Å dia.) which produces much larger changes in the scattered intensity (under a similar field intensity) than the present sample. The results of Jennings and Jerrard suggest that bentonite is composed of two types of particles.

7.3.6 Discussion and conclusion

The suggestion by Rabinovitch (1946) that bentonite is a mixture of two types* of particles was put forward to explain the change in sign of the steady component of the birefringence of bentonite solutions which has been reported by many workers (e.g. Norton - 1939, Mueller - 1939, Sakmann - 1945 and Rabinovitch - 1946). The steady component which can be positive or negative can reverse its sign with a change in concentration, field strength, frequency or particle size. However, Shah (1963) has shown that for disc-shaped particles, with a permanent dipole moment along the symmetry axis of the particle and an induced dipole moment along the semi-major axis, the birefringence of the suspension undergoes a minimum and furthermore exhibits a reversal in sign with increasing the field strength at certain values of the ratio of these two dipoles. Therefore the reversal in sign can also be explained by assuming that bentonite is composed of one type of particles only. Jennings et al. (1970) who investigated a

---

* Type has the same meaning as earlier.

synthetic mineral clay, which safely can be assumed to be composed of one type of particles, reported a reversal in sign of both the electrical birefringence and the scattering changes. Also Shah et al. (1963) and Stoylov et al. (1968) analysed their data on bentonite solutions in terms of one type of particles.

The results that have been reported in this work do not enable direct confirmation to be made of wehther bentonite consists of one type of particles or whether it is a mixture of particles. Jennings and Jerrard (1965) obtained values of $\sim 150\ sec^{-1}$ and $34\ sec^{-1}$ for the diffusion constant D from the dispersion of the steady and the alternating components respectively. Thus they concluded that their sample was a mixture as only for a mixture would the dispersion method result in such very different values for D. As would be expected the value of $150\ sec^{-1}$ was then associated with the diffusion constant of polar particles D_{μ} and the value of $34\ sec^{-1}$ with that of the nonpolar particles D_{β}. Thus it was concluded that the average molecular weight of the polar particles is smaller than that of the nonpolar particles (almost by a factor of 2). Furthermore since their value of $D_{\beta}(34)$ is much closer than the value of $D_{\mu}(150)$ to that of D(10) calculated from the parameters resulting from the conventional light scattering measurements, therefore it was also concluded that the nonpolar particles are present in the solution in much greater abundance. Thus one would expect little or no dispersion of the steady component to be observed for a resuspended solution of only the very largest particles obtained by fractionisation of their samples since these particles would be mainly nonpolar. To the knowledge of the author all fractions of bentonite irrespective of their size, origin or whether they are polydisperse or monodisperse show a pronounced dispersion of the steady component. This dispersion has the same form for all samples of bentonites.

Thus if bentonite is a mixture then monodisperse solutions of this material which can be obtained by fractionisation must also be a mixture of two different types both existing in sufficient abundance to show their own effect. This would be difficult to reconcile with the results of Jennings and Jerrard.

The author agrees with the view of Stoylov (1971) that the hypothesis that bentonite is a mixture of two different types of particles can not be excluded for the moment. However, it should be emphasized that the previously described method (i.e. the determination of the diffusion constant from the dispersion of both the steady and the alternating components) cannot be used with disc shaped particles such as bentonite. For these particles D_μ and D_β should have similar values except when the two types of particles have very different average sizes. Since it is preferable to make measurements on mono-disperse solutions as the subsequent data analysis is easier, an entirely different method must be used with these solutions.

It is the view of the author that the method of rapidly reversing the polarity of the applied electric field which was introduced by O'Konski and Haltner (1956) may result in resolving the composition of bentonite. This method was first used by these authors to determine whether T.M.V. is composed of polar or nonpolar particles. The reversing of the polarity of the field was achieved by applying two square pulses of opposite sign one directly after the other. For polar particles it is expected that the level of the observed electro-optic effect* reached at the end of the first pulse, would change significantly when the polarity is rapidly reversed as the particles have to reorientate themselves to the new direction of the field. For nonpolar particles no change in the level is expected as the induced dipole of the particles

---

* Usually the electric birefringence method is employed because it is more sensitive (c.f. sec. 7.4.5.b).

will reverse its direction immediately. As a result the already orientated particles will stay in the same position as before the reversal of the polarity of the field. The method has been also used with DNA (c.f. Colson et al - 1974) and with collagen (c.f. Bernengo et al - 1973).

It can be seen that, with solutions composed of one type of particles the method can be used without any restriction on the intensity of the applied field. It is suggested however, that with a mixture of two types of particles the strength of the applied field must be sufficiently large to produce complete orientation of the particles. Then if there is no change in the level of the observed electro-optic effect it would be an indication that only one type of particles is involved. This is because the level of the electro-optic effect produced by a solution composed of one type of completely orientated particles is expected to be mainly due to the electrical anisotropy of the particles, whereas for a mixture a significant contribution to this level would be expected from the polar electrically isotropic particles. The use of the reversed pulse method with bentonite has been reported by (Schepers and Miller - 1974). However only fields of very low intensities were used. The usefulness of this method could only be discerned by experiment.

Further discussion about bentonite is given in the next section (sec. 7.4) where the data of another bentonite sample of different origin are discussed.

7.4 North African Calcium Bentonite, N.A.Ca.B.

7.4.1 Preparation of the mother solution

Eight grams of N.A.Ca.B. powder were added to 300 ml. of freshly double distilled water. With a little shaking it was possible to suspend this large quantity; the difficulties experienced in suspending sodium bentonite not being met wirh. Experience with this material shows that if the initial solution is left standing for several hours, a lot of the material sediments out and the solution starts aggregating. However, if the initial solution is centrifuged until only the finest fraction of particles is left in suspension then a clear stable* solution can be obtained. Accordingly the initial solution was centrifuged for 20 minutes at 9,000 g, the supernatant removed and then filtered through 1.2 μ and 0.45 μ filters. It was easier to filter the solutions of N.A.Ca.B than those of sodium bentonite of similar concentration. The N.A.Ca.B solutions were colourless when dilute and milky when concentrated.

7.4.2 Measurement of dn/dC

Within the experimental error it was found that dn/dC has the same value for N.A.Ca.B as for sodium bentonite (0.096 ml g^{-1}).

7.4.3 Conventional light scattering measurements

Measurements of the angular scattered intensity are shown in the Zimm plot (fig. 7.4.1), and those of the depolarisation ratio are shown in fig. 7.4.2. By extrapolation to zero concentration a value of 2×10^{-2} for $(\rho_u)_{C=0}$ is obtained which is smaller than that for sodium bentonite. The corrected values of the Zimm plot parameters are:

---

* The stability of the solution is concluded by the daily measurement of its angular scattered intensity for several days.

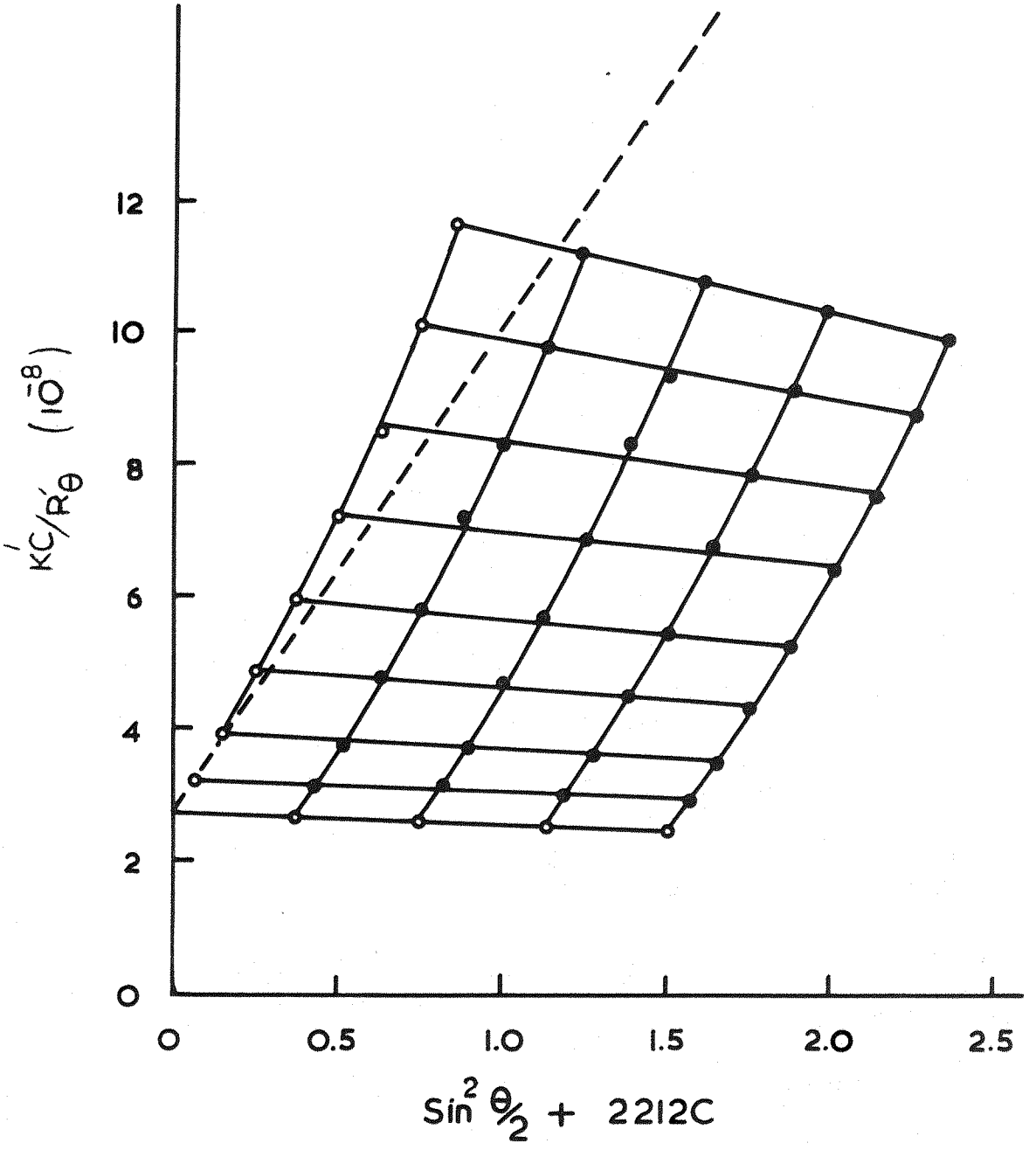

Fig. 7.4.1 North African Calcium Bentonite
(Zimm plot)
at pH 7.9 & wavelength 4358 Å

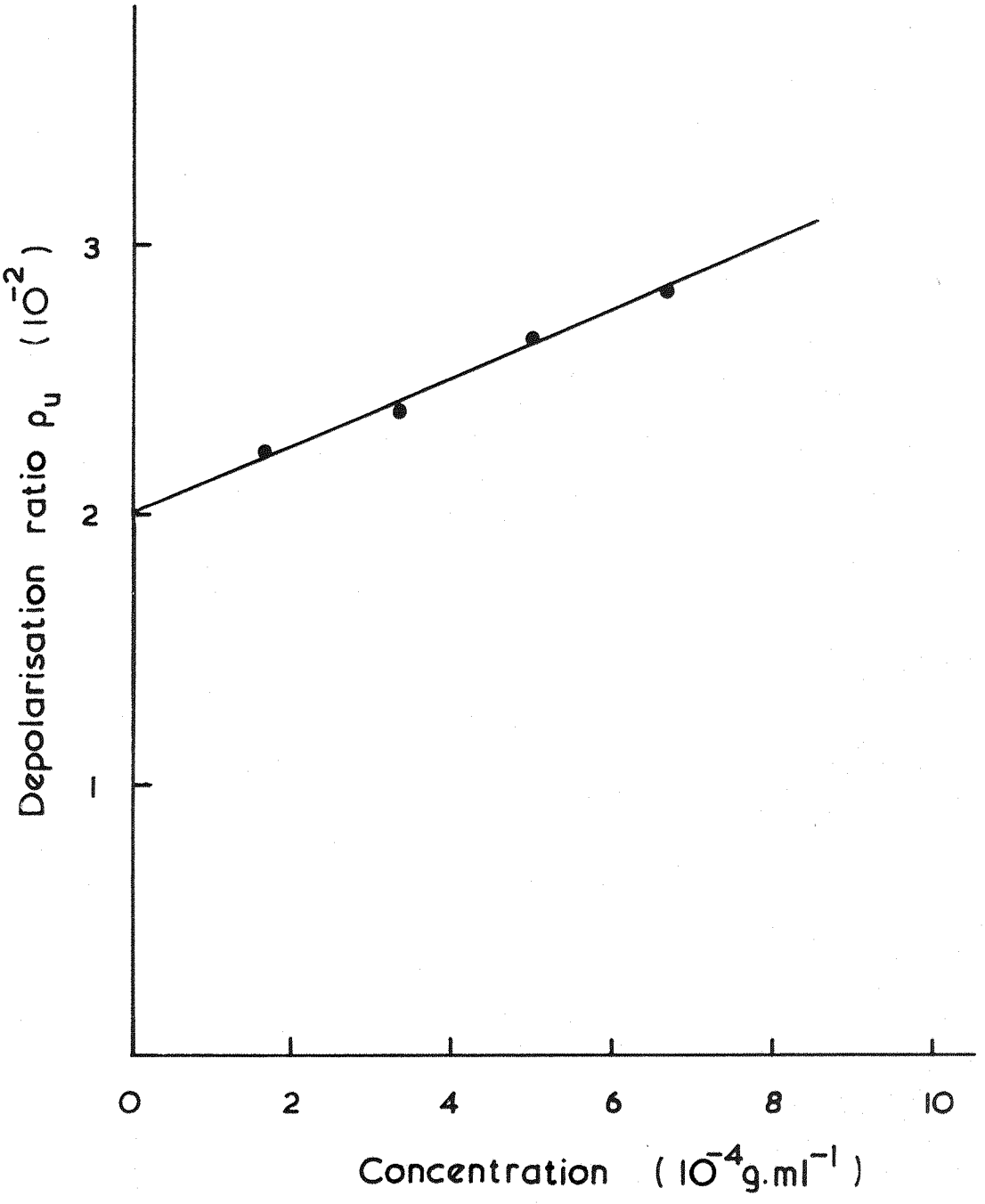

Fig. 7.4.2 Depolarisation of North African Bentonite

$3.7\ (\pm\ 0.3) \times 10^{7}$ for the weight average molecular weight M_w

750 ($\pm$ 60) Å for the Z average radius of gyration ρ_z and

$-(1.8)\ (\pm\ 0.2) \times 10^{-6}$ for the second virial coefficient B.

Here again B is negative showing that the particles prefer their own company.

Assuming the particles to be disc-like in shape of radius r and thickness t, a value for r of 1,060 ($\pm$ 85) Å is found from the radius of gyration. From the relation between the molecular weight, the volume of the particles and their density a value for t of 9 Å is obtained.

7.4.4 Kerr effect, measurement of the relaxation time

These measurements were carried out on four solutions of relatively low concentration, the highest concentration being only 4.6×10^{-4} g/ml. The field intensity was about 15 KV/cm. A typical birefringence trace obtained on the solution of lowest concentration (1.2×10^{-4} g/ml.) is shown in fig. (7.4.3). Fig. (7.4.4) shows a semi-log plot of the birefringence decay of this trace. Here again the log plot is not linear, showing that there is more than one relaxation time, i.e., the sample is polydisperse. As in the case of W.Na.B. analysis of the other traces shows that the concentration over the above mentioned range has no effect on the birefringence decay.

The extreme values of the relaxation time, as determined from the initial and the end tangents of the log plot of fig. (7.4.4), were found to be 80×10^{-6} sec. and 370×10^{-6} sec. respectively. Using Perrin's formula (Perrin - 1934) which relates the relaxation time to the radius of the disc, the determined values of τ result in values of 570 Å and 950 Å for the radius of the smallest and largest particles respectively. It can be seen that, within the experimental error, the value of r of 950 Å is almost the same as that obtained from the light scattering technique.

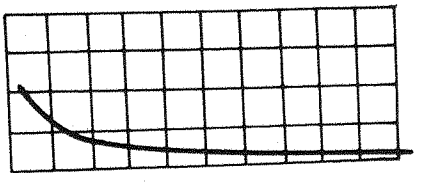

North African Calcium Bentonite

Fig. 7.4.3 Typical experimental birefringence trace obtained at T = 20^{o}c, C = 1.2×10^{-4} $g.ml^{-1}$, E = 15 kV cm^{-1} and pulse width of 2.5×10^{-6} sec, Time scale 100×10^{-6} $sec.cm^{-1}$

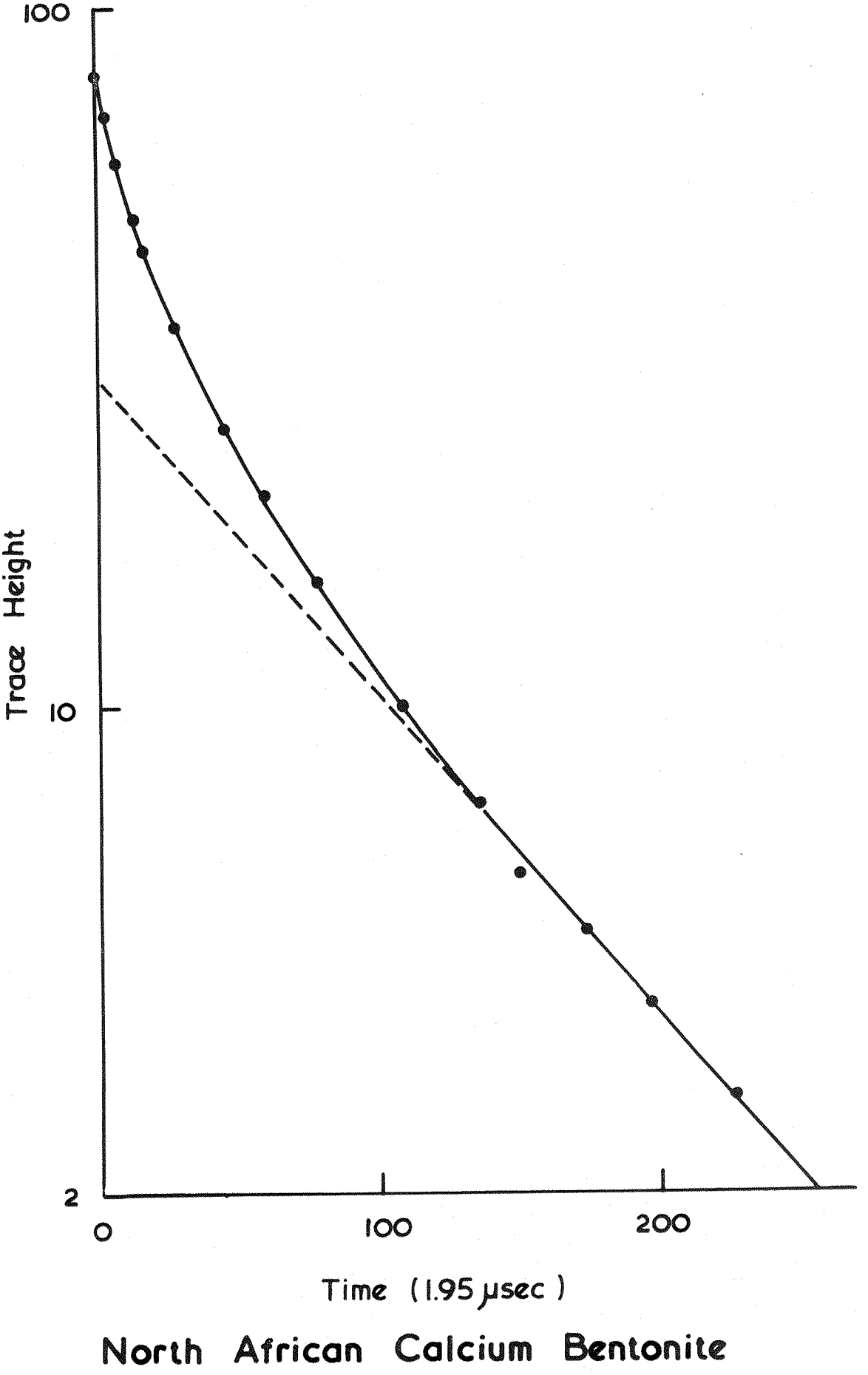

Fig. 7.4.4 Semi-log plot of the birefringence decay of the trace shown in fig. 7.4.3

7.4.5 Light scattering in the presence of electric fields

a) The use of a.c. fields

The changes in the scattered light intensity from N.A.Ca.B. solutions resulting from the application of sine wave electric fields were investigated. The procedure followed was the same as with the sodium bentonite solutions (see sec. 7.3.5). The mother solution was first dialysed until its resistance became greater than 100 KΩ/in. Then after measuring the rigidity parameter, R, of the steady component of the relative changes in scattered intensity ($\Delta I_s/I_s$) and its dependence on the electric field intensity were studied on three solutions of different concentrations. Attempt was also made to measure the dispersion of the alternating component. The measurements were carried out at the observation angle $\theta = 90^o$, with the applied electric fields being perpendicular to the plane of observation except when measuring R.

As would be expected, the particles were found to be rigid as R was found to have a value of 1.92 ± 0.4 This value of R was obtained from measurements on a solution of concentration of 5.3×10^{-4} g/ml applying fields of 300 V/cm and 225 V/cm at the frequency of 2KHz.

Two dispersion curves of the steady component obtained on two solutions of concentration 5.3×10^{-4} and 2.6×10^{-4} g/ml are shown in figs. 7.4.5a and b, respectively. These measurements were carried out at an electric field intensity of 270 V/cm in the frequency range (50 - 2000) Hz. Another dispersion curve obtained at a higher electric field intensity of 360 V/cm on a solution of lower concentration (1.3×10^{-4} g/ml) is shown in fig. 7.4.6. The field intensity was increased to achieve a measurable magnitude of $\Delta I_s/I_s$ at this lower concentration. It can be seen that these dispersion curves are very similar to those obtained for the sodium bentonite solutions, i.e. $\Delta I_s/I_s$ is always positive and increases with increasing frequency until it reaches a

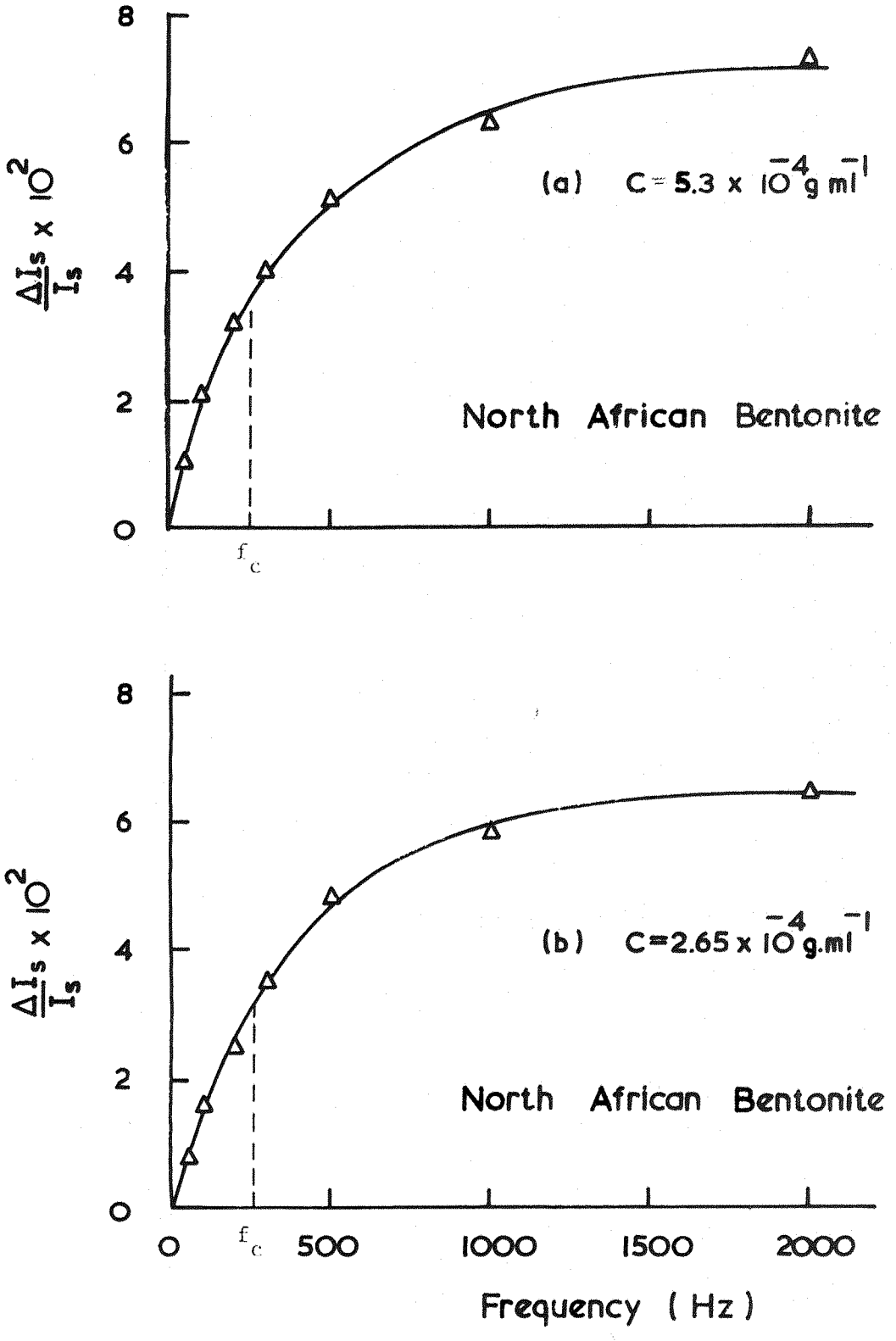

Fig.7.4.5 Frequency Dispersion of the Relative Intensity Change at $\theta = 90^\circ$ & $E = 270\ V.cm^{-1}$

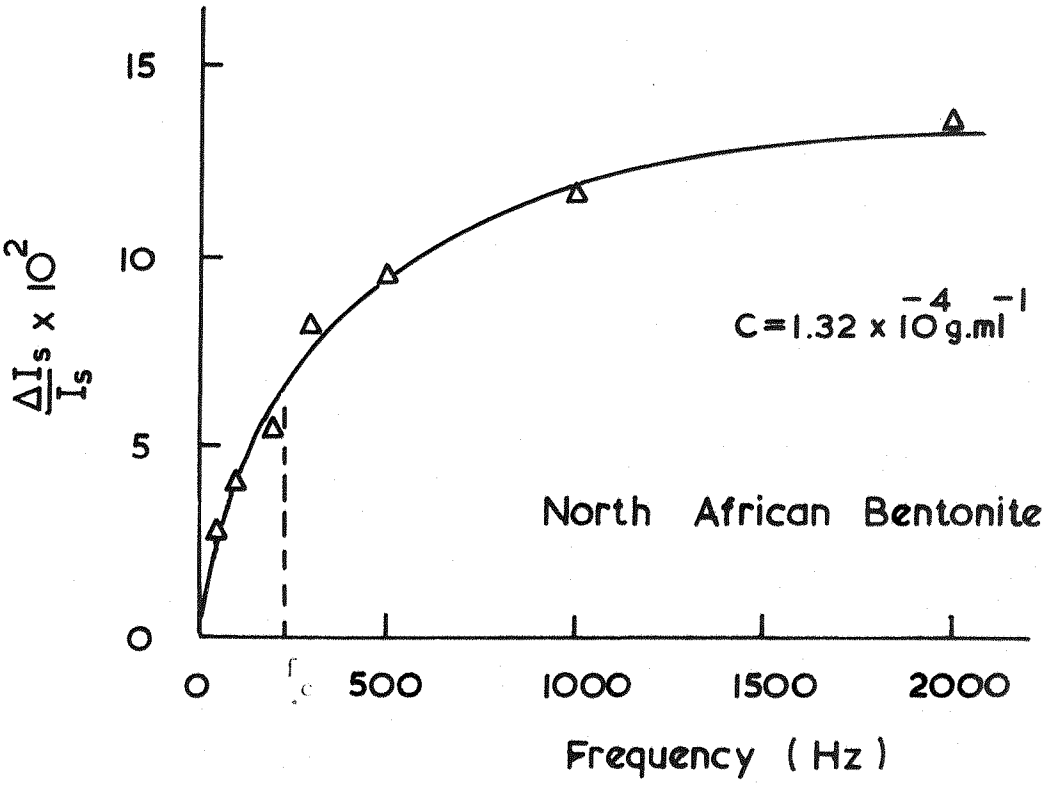

Fig.7.4.6 Frequency Dispersion of the Relative Intensity Change at $\Theta = 90^\circ$ & $E = 360\ V.cm^{-1}$

steady value. Therefore a similar conclusion about the electrical properties of the particles can be made. Thus, as is the case for sodium bentonite, the particles which are disc-shaped have an induced dipole moment along the semi-major axis of the disc and a permanent dipole moment along the axis of symmetry.

For the determination of $(\alpha_2 - \alpha_1)$ and μ, the dependence of $\Delta I_s/I_s$ on the intensity of the electric field was investigated for the above mentioned solutions. This was done only at the high frequency of 2 KHz because it was difficult to measure $\Delta I_s/I_s$ at much lower freuqencies when the intensity of the electric field was small. Fig. (7.4.7) shows $\Delta I_s/I_s$ plotted against E^2 (up to 360 V/cm) for two of the solutions. It is seen that, for the range of electric field strength used, $\Delta I_s/I_s$ is proportional to E^2. The previous measurements (both the dispersion of $\Delta I_s/I_s$ and its dependence on E^2) also indicated that at these levels of dilution $\Delta I_s/I_s$ was independent of concentration. Thus it was possible to use eq. (3.10) to calculate the excess polarisability $(\alpha_2 - \alpha_1)$. The permanent dipole moment was also calculated on the assumption that $\Delta I_s/I_s$ was proportional to the square of the electric field strength in the low frequency range. These calculations resulted in the following values:

$$\alpha_2 - \alpha_1 = 2.83 \times 10^{-14} \text{ cm}^3$$

$$\mu_1 = 3.4 \times 10^{-14} \text{ e.s.u.}$$

The dispersion curves were also used in the evaluation of the diffusion constant D. This was found to be independent of concentration and to have an average value of 785 (± 160) sec^{-1}. This value of D corresponds to a value of τ of 0.212×10^{-3} sec. and gives an average value for r (the radius of the particles) of 790 Å.

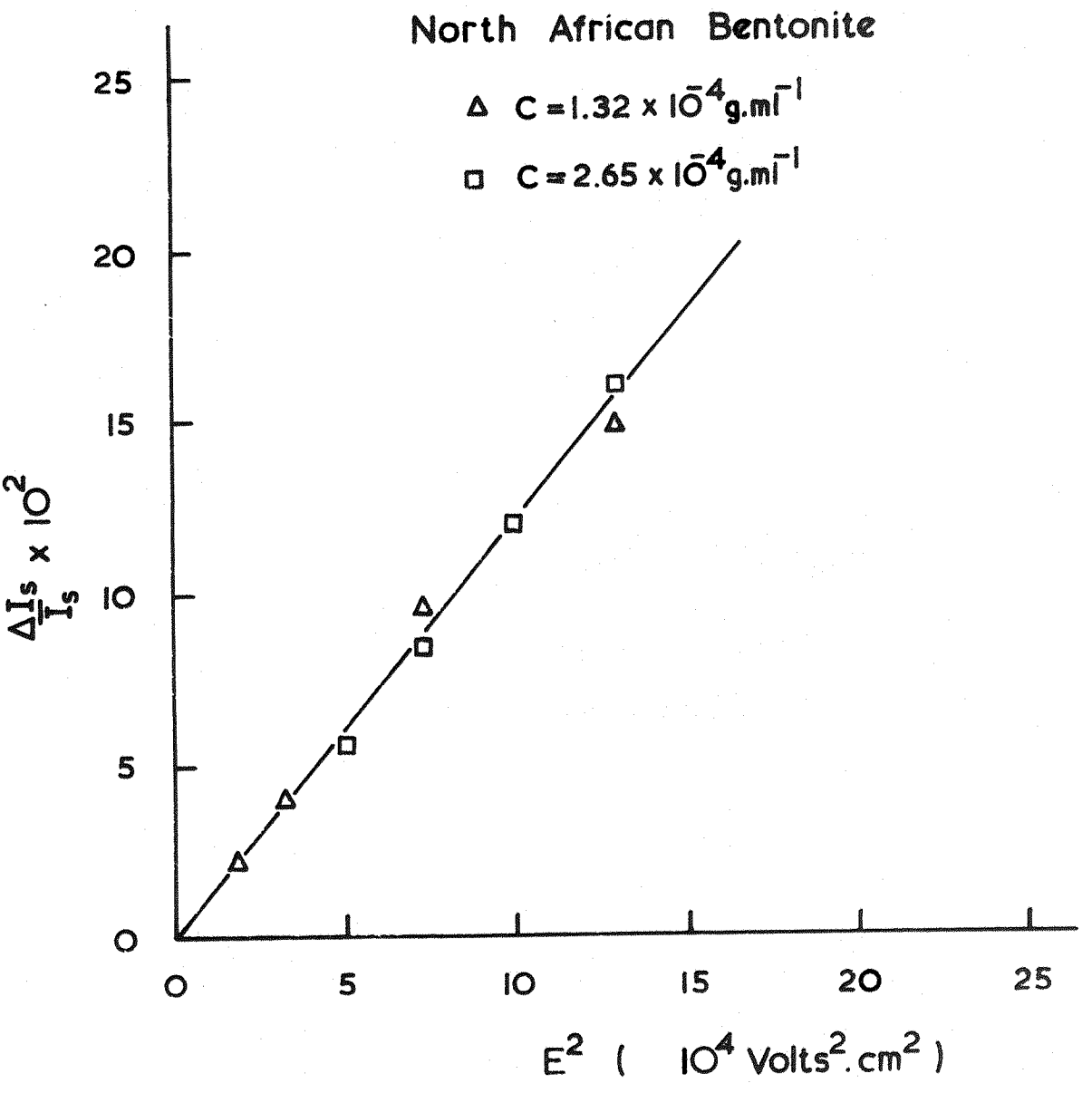

Fig.7.4.7 Variation of the Relative Intensity Change with the Square of the Field Strength at $\theta = 90^{\circ}$

Although it was possible to detect the alternating component of the changes in the scattered intensity in the low frequency range, it was difficult to measure these changes with an accuracy sufficient to permit the determination of the diffusion constant. Thus it was not possible to compare the two values of D that can be obtained from the dispersion of both the steady and alternating components of the changes in the scattered intensity.

b) The use of square pulsed fields

The changes in the scattered intensity and also the birefringence arising from the application of square pulsed fields were obtained for both of the bentonite samples under study. This was carried out using a single instrument designed by the present worker. It will be sufficient here to mention that the width of the electric pulse can be varied between 0.1 and 20 m.sec. Also the intensity of the applied field can be as large as 600 V/cm. Field intensities of this magnitude (or even smaller) can be sufficient to orientate particles as large as those of bentonite when applied for a long duration.

The traces from the electric light scattering method in general showed a lot of noise and thus were not expected to result in data as accurate as those previously reported (see sec. 7.3.5 and 7.4.5.a). Fig. (7.4.8.a) shows a typical transient trace obtained by applying an electric field of 400 V/cm for a duration of 2 m.sec. on a solution of North African calcium bentonite, the particles of which had an average diameter of 3,000 $\mathring{A}$. The traces obtained from the electric birefringence method showed much less noise. This can be seen by comparing the trace shown in fig. 7.4.8.a with that shown in fig. 7.4.8.b which was obtained under the same experimental conditions as with the light scattering method. Similar observations were made by Jennings and coworkers (c.f. Jennings et al - 1070). Thus although both of these two methods result in similar molecular information, the electric bire-

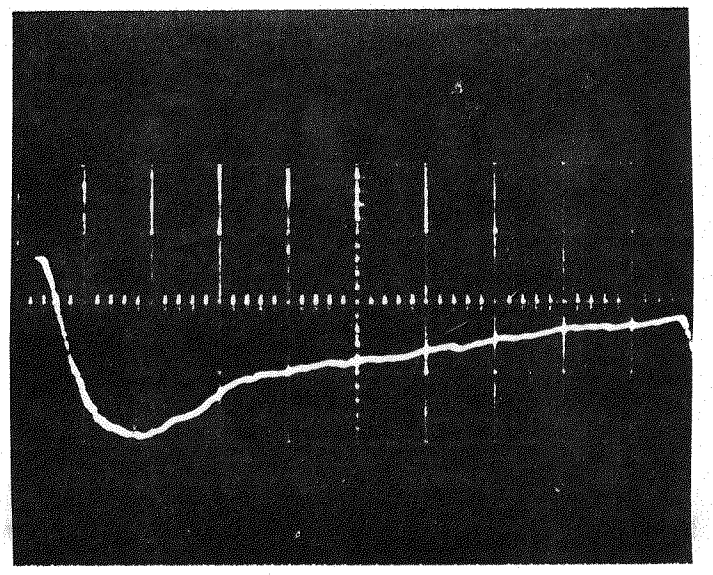

(a)

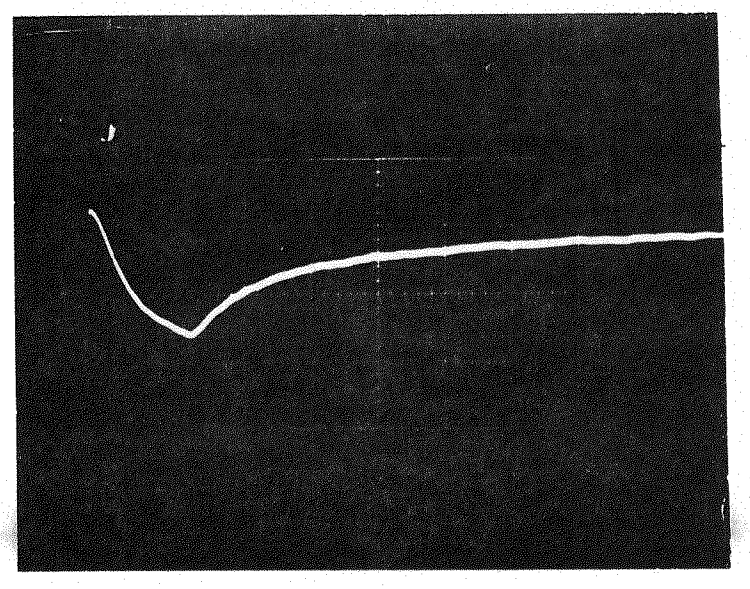

(b)

North African Bentonite

Fig. 7.4.8 a) Electric light scattering
b) Electric birefringence

pulse width 2 m.sec.
electric field 400 v/cm

fringence method is to be preferred. This is not only because it is a more sensitive method but also because it can be used with particles of any size (small or large). This is not the case with the light scattering method as the particles must be large ($\sim \lambda$) if significant changes are to be observed.

The lower degree of sensitivity of the electric light scattering method is due to the fact that the changes in the scattered intensity are observed superimposed on a much larger steady level of scattered light (i.e. the scattered intensity in absence of the electric field, see fig. 3.1). Whereas with the Kerr effect method, the birefringence is observed about an ambient of zero light intensity.

Because of the small power of the pulse generator and also because the instrument of Jerrard et al (1969) is more sensitive when small relaxation times are to be observed, the dual purpose instrument referred to in this section was no longer used.

7.4.6 Discussion and conclusion

In solution, there is a great similarity between both of the bentonite samples under study. The second virial coefficient of interaction is negative, the particles existed as individual unaggregated discs and the form of the changes in the scattered intensity is similar. However, the degree of stability of the solutions of these two substances is very different. For calcium bentonite, only dilute solutions of relatively small sized particles are stable for a long enough time to permit their investigation.

For both substances, the alternating component was not measurable and therefore it is not possible to decide whether the particles are composed of one type or of a mixture of two types of particles having

different electrical properties. However, the similarity in the form of the steady changes in the scattered intensity for the two substances makes the discussion outlined in connection with sodium bentonite applicable to calcium bentonite and adds weight to the view that the particles may be of one type.

In table 7.4.1 are presented the values of the electrical polarisability α and the permanent dipole moment μ obtained in this work together with those of Schweitzer and Jennings (1971), and those obtained by other workers (using electric light scattering, electric dichroism and electric birefringence methods) as given by Stoylov (1971). Only with electric dichroism is a permanent dipole moment obtained directed along the particle's major axis of value in accordance with the theory suggested by Tolstoi and coworkers (see table). The list of Stoylov has no information on North African calcium bentonite. To the knowledge of the author, the present values are the only ones to be reported for this material.

As previously mentioned the list of Stoylov shows that the values of α and μ vary considerably even when the size and origin of the samples are taken into account. However, the other results and those in the list of comparable size (the underlined in the table) seems to be in reasonable agreement, except for those of Stoylov (1967) and Stoylov and Petkanchin (1966/7). The observed differences between these values can be attributed to polydispersity of the samples, the different methods used for obtaining the average size of the particles and the fact that the particles are not actually discs (c.f. Schweitzer and Jennings - 1971). In addition, the effect of the age of the solutions should not be neglected: Schweitzer and Jennings (1971) found that after 4 weeks the molecular weight of their montmorillonite sample

increased about ten times forming aggregates of a rather complicated configuration. Filtration of solution before use may result in a significant reduction of this ageing effect but can not totally eliminate it .

It should be mentioned that the values of α given in the table are larger than those predicted from the theory of Peterlin and Stuart (1943) for nonconducting solutions. This is the case for many other substances such as T.M.V. and DNA and is due to the ionic polarization.

7.4.7 Summary

Although in general calcium bentonite solutions have a great tendency to aggregate, it was found that the dilute solutions of North African calcium bentonite of low molecular weight are stable for a sufficiently long time to permit their investigation.

The conventional light scattering measurements and those in the presence of electric fields indicated that the behaviour of North African calcium bentonite in solution is in all respects similar to that of Wyoming sodium bentonite. For both of these samples, the particles were found to exist in solution as unaggregated discs of ~ 9 Å thick. The tendency for aggregation and sedimentation is reflected in the negative value of the second virial coefficient of interaction B . It was also found that the particles have a predominant permanent dipole moment acting along the symmetry axis and an excess polarisability α along the semi major axis. The values of α and μ when compared with those in the literature tended to suggest that a fair reproducibility of these values might be possible.

Finally table 7.4.2 shows the values of the parameters under study for these two samples.

Table 7.4.1

Electric polarisability and permanent dipole moment of bentonite

Electric polarisability $\alpha \times 10^{13}$ cm^3	Permanent dipole moment and direction in respect to the major axis $\mu \times 10^{13}$ esu	Mean diameter (μ)	References	Method of measurement	Remarks
1.3	2	1.1	Wippler (1956)	Light scattering in an electric field	Wyoming bentonite
0.6-5.8	0.1-1.7	0.6-1.2	Shah & Hart (1963)	Electric birefringence	idem
0.61	0.27	0.3	Shah (1963)	idem	idem
30	2	0.68	Jennings & Jerrard (1965)	Light scattering in an electric field	idem
0.8	3	0.25	Stoylov (1967)	idem	Chirpan bentonite
3	1	0.15-0.45	Stoylov et al (1968)	idem	idem
5.6	-	0.25	Stoylov & Petkanchin (1966/67)	idem	idem
-	9	0.7	Tolstoi et al (1967)	Electric dichroism	
-	7.8	0.67	Trusov (1968)	idem	
0.2	-	0.2	Isemura & Mukohata (19)	Electric birefringence	
13	3.3	0.6	Thurston & Bowling (1969)	idem	Wyoming bentonite

Table 7.4.1 (Contd)

0.45	0.36	0.3	Schweitzer & Jennings (1971)	Light scattering in an electric field	Redhill (Eng) Montmorillonite
0.27	0.33	0.3	This work	idem	Wyoming bentonite
0.28	0.34	0.2	This work	idem	North African calcium bentonite

Table 7.4.2

Bentonite Results
(for the values of α and μ see table 7.4.1)

	$M_w \times 10^7$	ρ_z (Å)	r_z (Å)	$B \times 10^6$	$\rho_u \times 10^2$	$\bar{D}$ (sec^{-1})	$\bar{r}$ (Å)	D (sec^{-1})	r (Å)	t (Å)	dn/dC
Wyoming bentonite	8.2	1070	1510	-1.9	3.3	377	∿1000	102-417	980-1560	9	0.096
North African	3.7	750	1060	-1.8	2	785	∿750	405-2080	570-950	9	0.096

r_z : radius of disc as obtained from radius of gyration (i.e. z-average)

$\bar{D}$: average of diffusion constant from dispersion measurement

$\bar{r}$: average radius equivalent to $\bar{D}$

D : range of diffusion constant obtained from Kerr effect

r : range of radius equivalent to D

t : thickness of disc

7.5 Hectorite

7.5.1 Preparation of the mother solution

Hectorite is naturally a magnesium rich mineral clay. However, the sample used in this work was provided in a sodium form which was achieved by an ion exchange process.* Preliminary light scattering investigations indicated that the sample was very polydisperse. For example, several values for the dissymmetry ratio (c.f. Chap. 2 sec. 2.3.2) ranging from 1.3 - 3.3 were obtained from solutions that had been prepared by centrifugation at different speeds for the same length of time. Therefore the preparation procedure was directed not only at clarifying the solution but also at obtaining a narrow particle size distribution.

A relatively large quantity of the hectorite powder, 6 grams, was suspended in 400 ml. of freshly double distilled water. The solution was left standing for six days so that the non-colloidal matter settled out and was then centrifuged for 20 minutes at 2,000 g. The supernatant was removed carefully and recentrifuged for 30 minutes at 4,000 g. The sedimented fraction resulting from the last centrifugation was resuspended and the solution so obtained was used in the present investigation after filtering it through 1.2μ millipore cellulose filters. The concentration of the mother solution was found to be 8.3×10^{-4} g/ml. This was determined by the use of a predetermined value of 0.085 ($\bar{+}$0.002) ml gm^{-1} for the refractive index increment at the wave length 4358 $\overset{o}{A}$.

7.5.2 Conventional light scattering measurements

The Zimm plot obtained is shown in fig. (7.5.1). The depolarisation ratio was found to be independent of concentration, see fig. (7.5.2), and had an average value of 7×10^{-2} which introduced a Cabanne's correction factor of 0.86. The corrected Zimm plot data gave the following parameters:

* The conversion of a sample of calcium montmorillonite to a sodium form has been described by Schweitzer and Jennings (1971).

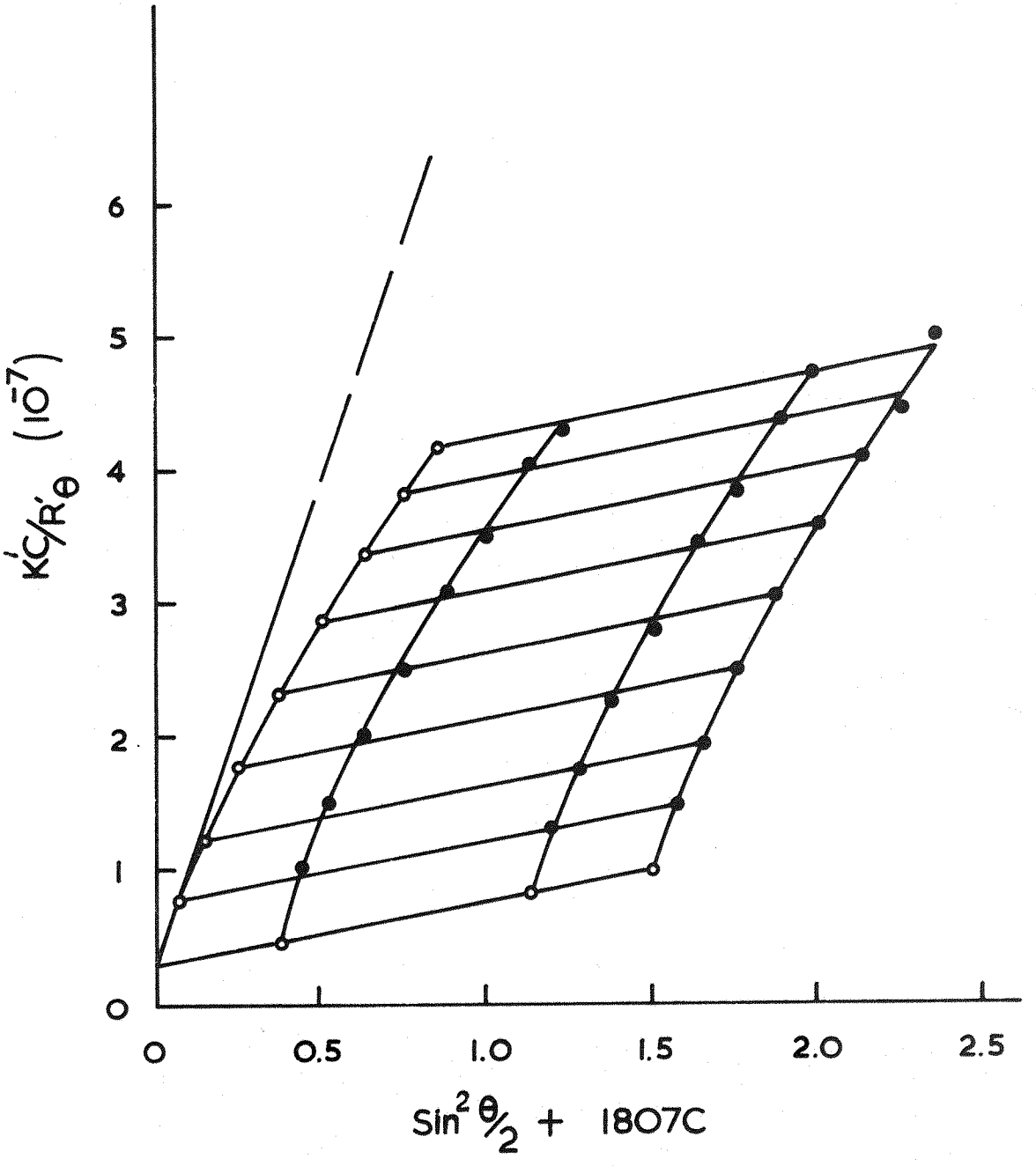

Fig. 7.5.1 Zimm plot for Hectorite at pH 8.2 & wavelength 4358 Å

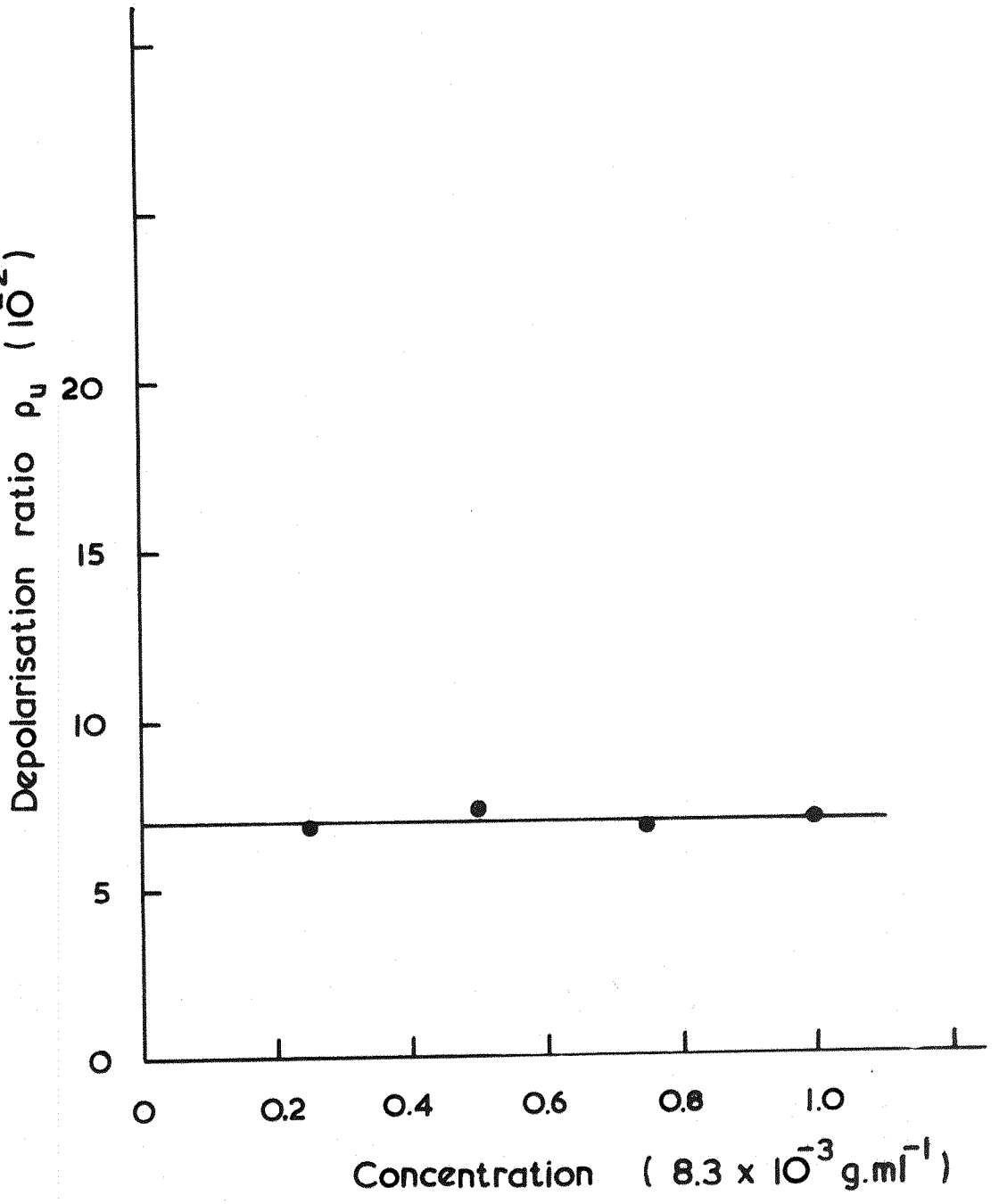

Fig. 7.5.2 Depolarisation of Hectorite

2,230 (± 230) Å for the Z-average radius of gyration ρ_z,

3.03 (± 0.40) x 10^7 for the weight average molecular weight M_w,

4.2 (± 0.6) x 10^{-5} for the second virial coefficient of interaction B.

The positive value of B indicates stability of the solution. The rather low ratio of molecular weight to radius of gyration (see table - 7.5.1) excludes the possibility that the particles are disc shaped, as was found by Wippler (1956), since then the thickness of the disc would be too small to be reasonable. The electron microscope (Grim - 1953) shows that hectorite particles are laths of length about 1 μ, width up to 0.1 μ and minimum thickness of ∿ 18 Å. If the particles are assumed to be rodlike in shape as suggested by Jennings and Plummer (1968), the determined radius of gyration gives a value of 7,715 (± 800) Å for the Z-average length of the rod L_Z. Moreover taking the density of the particles to be 2.5 (Grim - 1953) and using the relation giving the molecular weight in terms of the dimensions of the particles and their density, a value of 58 Å is obtained for the diameter of the rod. It can be seen that the value of the diameter will always be underestimated, except for a monodisperse system, as the molecular weight is a weight average and the radius of gyration a Z-average. For an unfractionated sample of natural (i.e., magnesium rich) hectorite,Jennings and Plummer (1968) obtained 6300 Å for L_z and 150 Å for the diameter (their diameter value of 150 Å appears to be in error, as a value of 120 Å was calculated by the author from their data). Thus the present results suggest that the particles, which were left in the mother solution, are very thin narrow laths. The results also suggest that the exchange of Mg^{++} by Na^{+} ions altered the interaction factor B as this was found to be zero by both Wippler (1956) and Jennings and Plummer (1968).

7.5.3 Light scattering in the presence of electric fields.

The solution was dialysed* until its resistance became greater than 100 KΩ/cm. On dialysis the pH changed from 8.9 to 5.6. Fields up to 350 V/cm and of different frequencies, in the range 60 to 2000 Hz, were applied. No changes in the scattered intensity were noticed. Similar studies were carried out by Wippler (1956) and Jennings and Plummer (1968). Both sets of workers observed substantial changes in the scattered intensity even at much lower electric field intensities. The results of Jennings and Plummer (1968), which are for the greater part in qualitative agreement with the earlier results of Wippler (1956), indicate (from the dispersion of the steady component of the changes in the scattered intensity, (c.f. chapter 3, sec. 3.2.2) that the particles have a permanent dipole momnet along the short axis (i.e. across the particle) and an induced dipole along the major (longitudinal) axis. Their results also indicate (from the dispersion of the alternating component of these changes) that the particles are all alike (i.e. their electrical properties are the same) and that they are not a mixture of two types of particles (i.e. a mixture of particles with different electrical properties) as was postulated by Wippler. The average molecular relaxation time for the particles, as determined from these dispersion measurements, was about 3.3 m.sec.

7.5.4 Kerr effect, measurements of the relaxation time

Pulses of 15 KV/cm were applied to four undialysed solutions of different concentrations. The concentrations of these solutions were in the range $(2 - 8) \times 10^{-4}$ g/ml. A typical transient trace of the birefringence is shown in fig. (7.5.3). Fig. (7.5.4) shows the birefringence decay curve of this transient on a semi-log scale. As in the case of

---

* As with bentonite solutions the dialysis was carried out by using the synthetic resin Zerolit, DM-F.

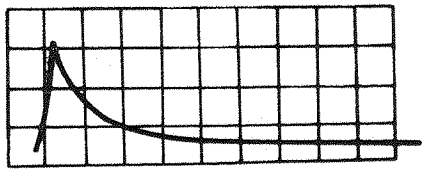

Hectorite

Fig. 7.5.3 Typical experimental birefringence trace obtained at T = 20^{o}c, C = 8.3×10^{-4} g.ml^{-1}, E = 15 kV.cm^{-1} and pulse width of 2.5×10^{-6} sec, Time scale 5.0×10^{-6} sec.cm^{-1}

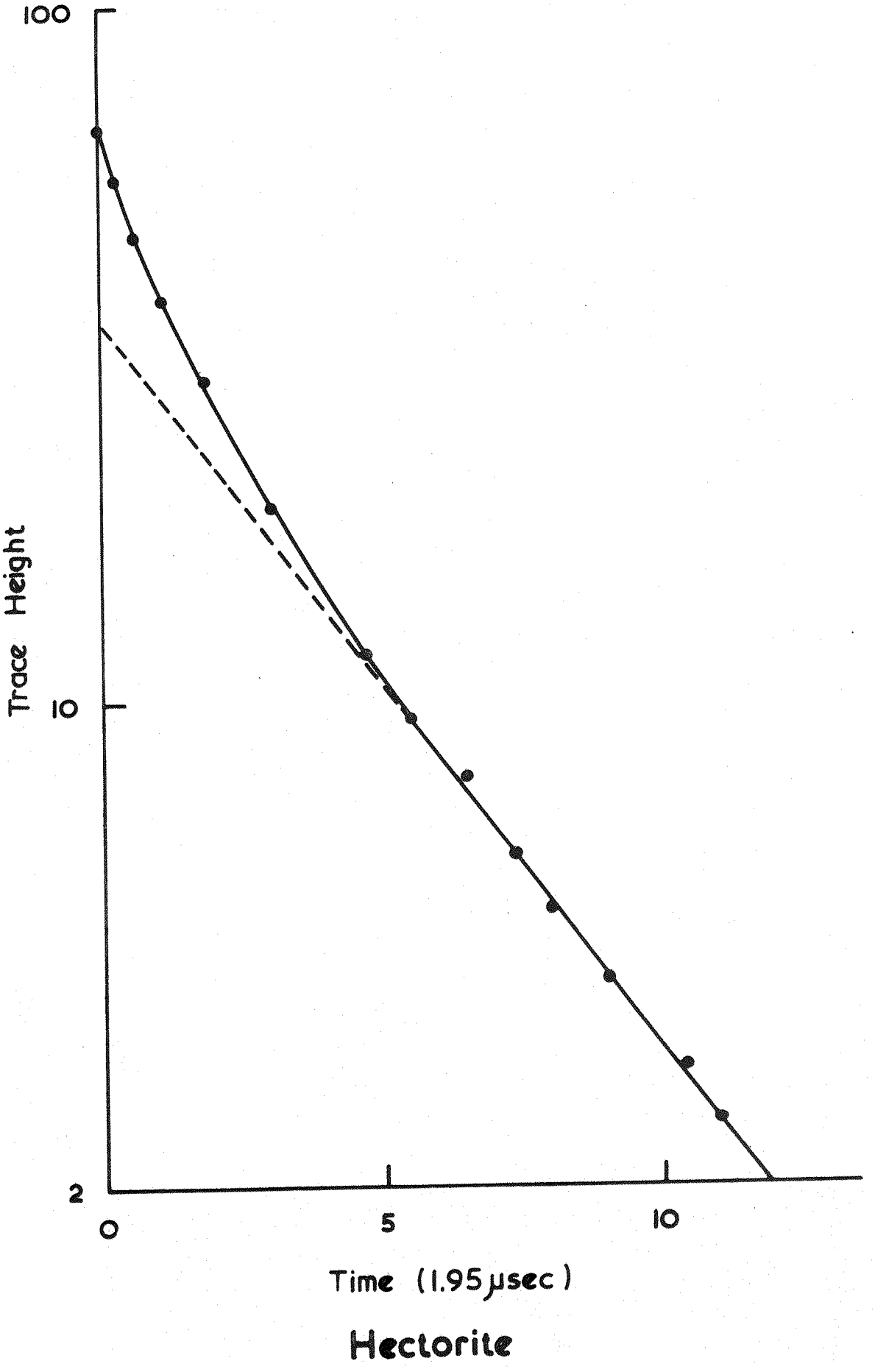

Fig. 7.5.4 Semi-log plot of the birefringence decay of the trace shown in fig. 7.5.3

the bentonite samples (see figs. 7.3.4 and 7.4.4) the log plot is not a straight line. This indicates the presence of more than one relaxation time and is therefore an indication of the sample polydispersity as it can be assumed that the particles are rigid. The initial and end tangents of the decay curve give relaxation times of 4.5×10^{-6} sec. and 16.3×10^{-6} sec., respectively.

Analysis of the traces obtained on the other solutions by applying fields of the same intensity gave (within the experimental error) the same range for τ, indicating that τ was independent of the concentration. However, the range of τ increased steadily from its lower end when the field intensity was increased from (6-12) KV/cm.

7.5.5 Discussion and conclusion

The small values of τ obtained from these measurements indicate that the particles are not rotating about the minor axis as rotation about this axis would result in a much larger relaxation time. Values of the length and diameter of the particles which were obtained from the present light scattering measurements were substituted into Perrin's formula (Perrin - 1934). This formula gives the relaxation time τ for a rod rotating about its major axis and is given by

$$\tau = \frac{16\pi \eta ab^2}{9kT} \qquad (7.\ )$$

where η is the viscosity of the solvent at temperature T and 'a' and 'b' are the values of the semi major axis (half the length of the rod) and the semi minor axis (the radius of the rod), respectively. A value for τ of 4.5 μ sec. was then obtained. This value of τ is of the same order as the two values obtained from the log plot and suggests that the particles do in fact rotate around the major axis. Thus it can be

concluded that the particles of the present hectorite sample have no appreciable dipole moment (induced or permanent) along the major axis of the rod. If they did have such a dipole moment this would cause a rotation about the minor axis and a much larger relaxation time would be expected. As the values of the relaxation time for this sample are of the order of the pulse duration it is possible to evaluate the area over the build up and that under the decay and thus determine the ratio of the permanent to the induced dipole (c.f. chapter 4 sec. 4.4). However, this method applies only when the electric birefringence obeys the Kerr law. As the mineral clays in general saturate at rather small electric field intensities, therefore this method does not apply to the present results since the lowest intensity available from the Kerr effect apparatus was $\sim$ 3 KV/cm.

It is seen that the value of τ as calculated from the parameters obtained from the light scattering data is identical to the smallest value of τ determined from the Kerr effect method, whereas a larger value of τ would have been expected. This may be due to the fact that the particles are not exactly rod shaped but are in fact laths. It is to be expected that rod like particles should have a smaller relaxation time than laths when both have the same length and molecular weight. The thinner the laths the more the relaxation time will be different from that of a rod of similar length and molecular weight.

It should be noted that in this case of rotation about the major axis the relaxation time is proportional to ab^2 i.e. to the weight average molecular weight, whereas for rotation about the minor axis with $b/a << 1$, the relaxation time is proportional to a^3 and is independent of b. As the light scattering gives a Z-average value for 'a' therefore the relaxation time for this latter case as calculated from the parameters obtained by the light scattering would be proportional to a^3 and would not correspond with the minimum value of τ obtained from the Kerr effect.

It is seen that for the present sample the electrical properties are not in agreement with those found by earlier workers (Wippler - 1956 and Jennings and Plummer - 1968). This difference in the electrical properties may be due to difference in the microscopic structure of the samples which is probably due to their different place of origin.

7.5.6 Summary

A sample of hectorite, in which the magnesium ions (Mg^{++}) had been synthetically exchanged with sodium ions (Na^{+}), has been investigated by both the light scattering and the Kerr effect techniques. The results from the light scattering measurements indicate that the particles exist in solution as very narrow thin laths with a relatively high depolarisation ratio and that the exchange of Mg^{++} by Na^{+} ions has resulted in a more stable solution. Furthermore, the results from the Kerr effect suggest that these particles, in disagreement with the results of other workers, have no dipole moment along their major axis. However, there is a dipole moment acting across the particle but it can not be determined from the present experimental results whether it is induced or permanent. This difference, in the electrical properties of the present sample and those investigated by other workers, may be due to differences in the microscopic structure of the samples investigated which is probably due to their different places of origin.

Finally the present values and those given by other workers for the parameters under study are listed below in table (7.5.1).

Table (7.5.1)

Parameter	This work	Jennings & Plummer (1968)	Wippler (1956)
Molecular weight M_w	3.03×10^7	1.02×10^8	9×10^8
Radius of gyration ρ_z	2230 Å	1800 Å	2720 Å
M_w/ρ_z	0.1410^5	0.5510^5	3.3×10^5
Interaction factor B	4.2×10^5	0	0
Depolarisation ratio ρ_u	7×10^{-2}	3.4×10^{-2}	-
Relaxation time τ	4.5-16.3 μsec	3 m. sec average value	-
Diameter of rod	58 Å	150 Å 120*	-
pH undialysed dialysed	8.9 5.6	9 6.2	

* The corrected value

7.6 Acid Soluble Calf Skin Collagen,* A.S.C.S.C.

7.6.1 Preparation of the mother solution

100 m.grams of A.S.C.S.C. were dissolved in 70 ml. of dilute acetic acid of 2N x 10^{-3} ionic strength. Thus the initial concentration of the solution was about 1.4 x 10^{-3} g/ml. which satisfied the experimental condition of Boedtker and Doty (1956) who found that optical clarification will not take place unless the initial concentration is smaller than 2 x 10^{-3} g/ml. The collagen did not didsolve easily and was therefore left to soak for not less than 36 hrs. before trying to dissolve it by stirring with a glass rod. The solution was then dialysed for 24 hrs. in a visking tube against a large quantity of the solvent. The resultant solution had a pH of 3.4 and was rather turbid indicating the presence of particles of very high molecular weight. This was not surprising as previous workers (e.g. M'Ewen and Pratt - 1953, Gallop-1955 and Boedtker and Doty - 1956) using the light scattering method had obtained molecular weights of several millions. However, it was also found by Boedtker and Doty (1956) that the apparently high molecular weight drops sharply to about 3 x 10^{5} when optical clarification takes place. These workers achieved this centrifugation for several hours under high centrifugal forces, 40,000 g over 10 hrs and 70,000 g over 2 hrs being used. It was also found that in some cases optical clarification was not achieved unless the solution was centrifuged more than once. But even when optical clarification was not fully achieved the molecular weights were not much higher than those obtained when clarification was complete. Taking these findings into consideration the solution was centrifuged for 12 hrs at 40,000 g, filtered through 1.2 μ filters and again recentrifuged for a total of 12 hrs (in two stages) at 90,000 g. To avoid denaturation the temperature of the solution was

* The sample was obtained from Sigma Chemical Company.

never allowed to become higher than 20°C and for most of the time was well below this temperature. The concentration of the mother solution was found to be 1.16×10^{-3} g/ml by drying the solution to constant weight. A value of 0.187 (± 0.06) at the wave length of 4360 Å was also determined for dn/dC.

7.6.2 Conventional light scattering measurements

To ensure that the clarification of the solution had been carried out to its limit, the solution was centrifuged several times until the dissymmetry ratio Z (see chap. 2, sec. 2.3.2) approached a steady value of 4.1 as the following table shows:

No. of times centrifuged	Z	Gravitational field	Period of centrifugation
1	8.00	40,000 g	12 hrs
2	4.10	90,000 g	5 hrs
3	4.10	90,000 g	7 hrs

Only then were measurements of the angular distribution of the scattered intensity carried out. These measurements are shown in the Zimm plot, fig. (7.6.1), which gives the following values:

$1.65 \ (\pm 0.25) \times 10^6$ for the weight average molecular weight M_w,

2,120 (± 270) Å for the Z-average radius of gyration ρ_z and

zero for the second virial coefficient of interaction B.

According to Boedtker and Doty (1956), Yoshioka and O'Konski (1966) and Ananthanarayanan and Veis (1972) individual unaggregated collagen particles are rodlike in shape, of a length of about 3,000 Å, diameter of 14 Å and have a molecular weight of $\sim 3 \times 10^5$. Assuming the particles to be rodlike in shape the determined radius of gyration results in a value of 7,300 (± 900) Å for the length of the rod, which is at least twice the length of the individual collagen particles (monomers), whereas the determined molecular weight is, within the experimental error, 4 or

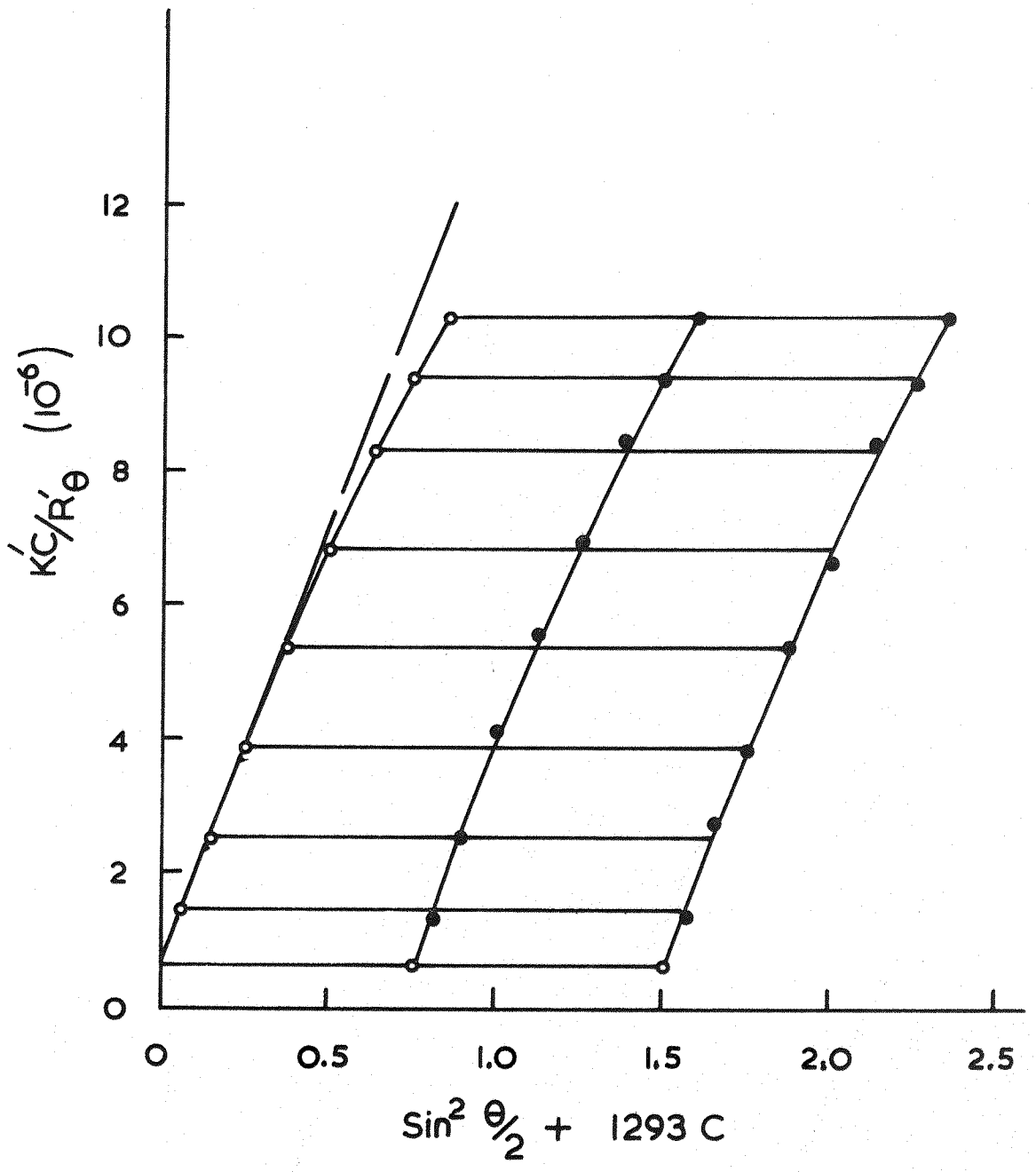

Fig. 7.6.1 Zimm plot for Calfskin Collagen. at pH 3.4 & wavelength 4358 Å

5 times the molecular weight of the individual particles. Thus the present results are not descriptive of individual collagen particles but of an aggregated sample. This is not surprising: Ananthanarayanan and Veis (1972), investigating calf skin collagen using the Kerr effect technique, found that the unaggregated collagen particles (monomers) account for only 28% of the weight of their sample, the other 72% of the weight consisting of dimers. These dimers are of the end to end type (i.e. linked end to end) and thus have a length which is twice that of the monomer unit. They also found that the tendency of collagen to aggregate is less when it is extracted from younger animals. The present determined molecular weight indicates a higher degree of aggregation (at least 4 monomer units). This aggregation of at least 4 monomer units can not be completely of the end to end type because this would result in a much higher value for the radius of gyration. Since the value of the radius of gyration suggests dimers of the end to end type it is thought that the aggregated particles in the present sample result from the association of two dimers joined side to side as shown in fig. (7.6.2.a). This model also seems to be the most suitable for the explanation of the present Kerr effect results to be discussed in the next section.

7.6.3 Measurements of the relaxation time by the Kerr effect

These measurements were carried out on three solutions of concentrations in the range $(1.3 - 4.0) \times 10^{-4}$ g/ml. Electric fields of equal intensity (15 KV/cm) were applied to each of these solutions and fields of different intensities ($\sim$ 6 to 15 KV/cm) were applied to the solution of highest concentration. A typical transient trace of the birefringence, obtained at 15 KV/cm, is shown in fig. (7.6.3). Fig. (7.6.4) shows the decay of this transient on a semi-log scale. It appears that, apart from

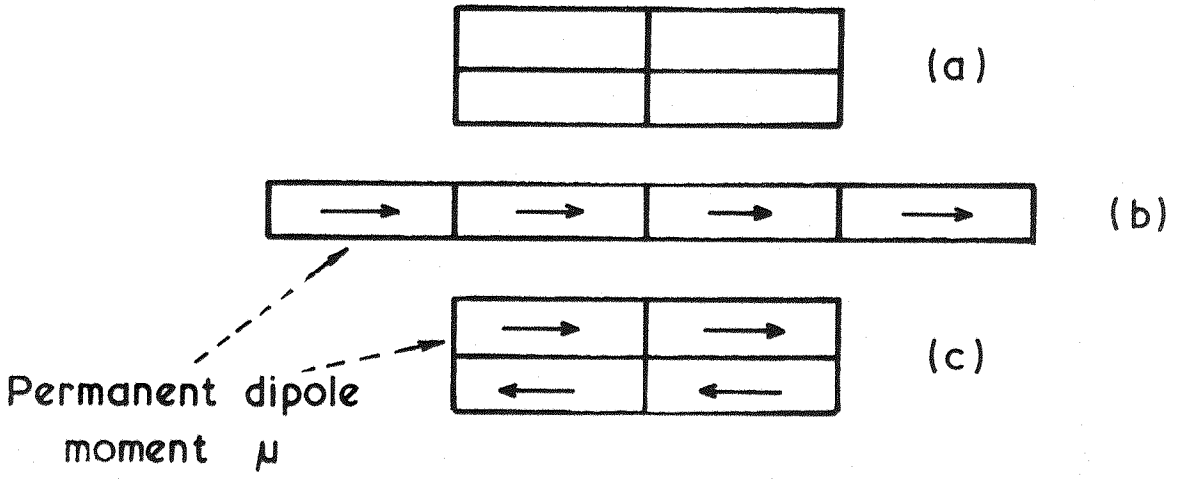

Fig. 7.6.2

a - Type of aggregation for two dimers of collagen as suggested from the light scattering data.

b - End to end aggregation of four monomers of collagen each having a dipole moment μ along the major axis. This type of aggregation also results in a dipole moment along the major axis of the aggregated particle. The applied field forces the particles to rotate about the minor axis in which case large relaxation times would be expected.

c - Two dimers, of the end to end type, joined side-to-side. The dipole moment of each dimer cancels with that of the other joined side to it. Assuming that this type of aggregation results in a dipole moment acting only across the resultant particle then the applied field forces the particle to rotate about the major axis resulting in a small relaxation time.

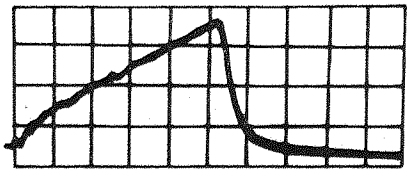

Calf skin Callogen

Fig. 7.6.3 Typical experimental birefringence trace obtained at T = 20^{o}c, C = 4.0×10^{-4} g.ml^{-1}, E = 15 kV.cm^{-1} and pulse width of 2.5×10^{-6} sec. Time scale 0.5×10^{-6} sec.cm^{-1}

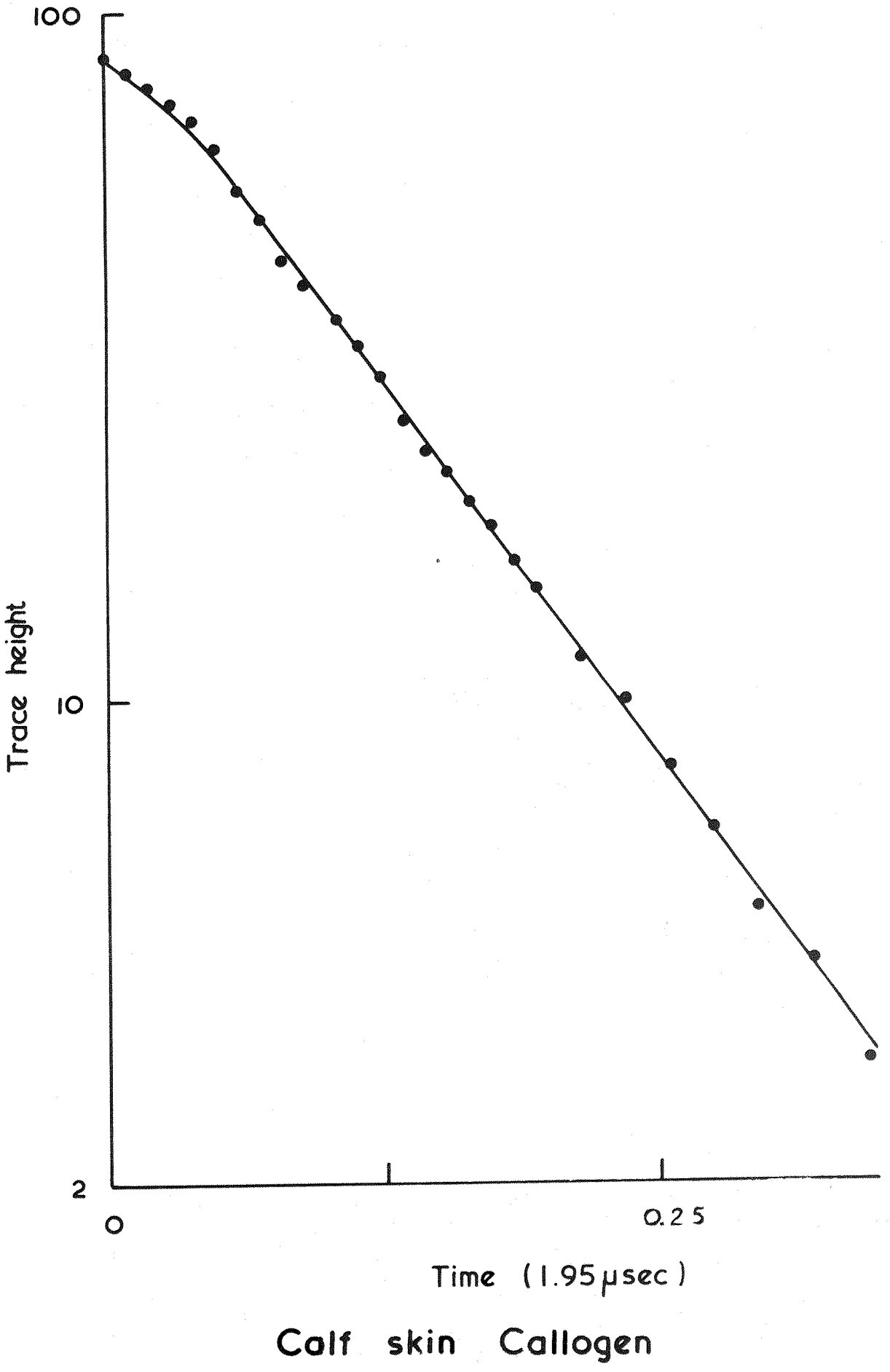

Fig. 7.6.4 Semi-log plot of the birefringence decay of the trace shown in fig. 7.6.3.

the downward curvature near t = 0 which is the start of the decay, the log plot is linear and its slope leads to a relaxation time of 0.39 x 10^{-6} sec.

Analysis of the other traces indicated that the relaxation time is insensitive to the strength of the applied field in the range* (6-15)KV/cm or to the concentration of the solution in the above mentioned range. The downward curvature near to t = 0 can be explained by the fact that the applied pulse, see fig. 5.12.a, was not well-defined and that there was a relatively large error in defining the time t = 0 due to noise.

The present results indicate that the sample was composed of particles of similar size; other particles of different size if they existed could not be detected because they were too few in number. Applying Perrin's theory (Perrin - 1934) it was found that the present value of τ is much smaller than that which would result from a monomer unit rotating about its minor axis but it is of the same order and in fact exactly four times the relaxation time of a monomer unit rotating around its major axis. Thus the determined relaxation time can be associated with the relaxation time of two dimers joined end to end since for rotation around the major axis the relaxation time is proportional to the total length of the aggregated particles. Findings from the light scattering experiment do not support this form of aggregation because this would result in too high a value for the radius of gyration. Also as the monomer units have their permanent and induced dipole moments along the major axis (Yoshioka and O'Konski - 1966) thus, as fig. (7.6.2.b) shows, all end to end aggregates should have their total dipole moment also along the major axis which would result in a large relaxation time. In fact the experimental values for the

* Transient traces obtained by applying electric fields < 6 KV/cm were rather noisy and difficult to analyse.

relaxation time of monomers and dimers as determined by Ananthanarayanan and Veis (1972) were found to be 0.2 and 1.6 x 10^{-3} sec. respectively. Thus it can be concluded that the particles in the present sample are neither monomers nor aggregates of the end to end type. However, they may be (as suggested by the light scattering measurements) two dimers of the end to end type aggregated side to side. As then the most likely form of aggregation is that shown in fig. (7.6.2.c) in which the permanent dipole moment of one monomer unit should cancel with that of another one when the two particles are joined side to side. Assuming that, somehow, this type of aggregation results in a dipole moment (whether permanent or induced) acting only along the minor axis then a small relaxation time is to be expected. Thus this assumption is a precondition for this form of aggregation to be suitable for explaining the data from both the light scattering and the Kerr effect techniques.

7.6.4 Further discussion about collagen aggregation

It is seen that the side to side form of aggregation results in a small relaxation time (as obtained in the present measurements) only if the aggregated particles have no dipole moment acting along their major axis. This may be evident (for an even number of monomers) for the resultant permanent dipole moment but not so easy to visualise for the resultant induced dipole moment as all the induced dipoles of the monomers should be in the same direction of the applied electric field. However, one can not exclude the possibility that the overall electrical anisotropy is somehow quite different from that of the individual components (the monomers).

Very recently Kahn and Witnawer (1975) found that "the presence of an electric field promotes aggregation of collagen particles suspended in an aqueous buffered medium" and that the range of aggregates stays within definite limits. The smallest value of diffusion constant obtained by

these authors corresponds to dimers rotating about their minor axis. However these authors also stated that: "this does not necessarily mean that the largest particle present is an end to end dimer because a staggered side-to-side structure of several particles having an overall length equal to that of dimer is possible". There are no reported measurements showing a relaxation time as small as the one reported in the present measurements. This may be because the other samples used have a lesser degree of aggregation than the present sample, with the monomers and individual dimers being dominant in the other samples.

A new difficulty arises when adopting such a model: the exact relaxation time can not be calculated because the diameter of the aggregated particles can not be exactly known. If the length of the aggregated particles is assumed to be 5,600 $\mathring{A}$, that is twice the length of a monomer, then the measured relaxation time results in a value of 20 $\mathring{A}$ for the effective diameter of the aggregated particles which is not unreasonable as it leads to the reasonable conclusion that their effective cross section is exactly twice that of the monomer units. Thus it does not seem unreasonable to state that both the light scattering and the Kerr effect measurements suggest that the majority of the particles in the sample used were aggregates composed of two dimers joined side to side with each dimer being of the end to end type. However,it can also be mentioned that small relaxation times can be associated with the rotation of small segments of the same particle which can occur if the particles are flexible. Particularly, it is known that the denaturation of collagen results in the separation of individual rigid collagen particles. However, in such a case more than one relaxation time would be expected whereas only one relaxation time was obtained for the collagen sample used in the present work. In addition, smaller values of the molecular weight and the radius of gyration would be expected for denatured collagen.

It is known (Ananthanarayanan and Veis - 1972) that the solutions of collagen which are not pronase treated are prone to aggregation even when great care is taken in handling these solutions. Thus it is not of importance to speculate about when the aggregation has taken place. However, if the present results were correctly analysed then it is seen that the aggregation has been complete even for the dimers. This is rather surprising, as Kahn and Witnauer (1975) have shown that the aggregation in their sample, which was caused by the applied electric field pulse, stays within definite limits with the decay curves still showing a relaxation time corresponding to the monomers.

7.6.5 Summary

A sample of calf skin acid soluble collagen, which was obtained from Sigma Chemical Company, has been investigated. The conventional light scattering method indicated that the sample was composed mainly of aggregates having a length of about twice that of the monomer unit and of a molecular weight (4-5) times that of this unit. An even number form of aggregation of the side to side type is more likely as it may result in a small relaxation time as found from the present Kerr effect measurements.

7.7 Sodium Salt of Deoxyribonucleic Acid (DNA)

7.7.1 Preparation of the mother solution

One gram of ex-calf thumus DNA (obtained from Koch-light-Laboratories, Batch No. 53092) was dissolved in 500 ml. of freshly double distilled water. To avoid denaturation, the pH of the solution was kept close to 7 and its temperature was for most of the time kept well below 20^{o}c (c.f. Krasna - 1972). The buffer was a mixture of PO_4Na_2H and PO_4NaH_2 added in equal ionic strength which was $2N \times 10^{-3}$. It was found that the DNA did not dissolve easily. The procedure followed in this experiment was to cut the fibrous DNA into small pieces and to leave it to soak for not less than 24 hours at a temperature around 5^{o}c. The solution was then stirred gently with a glass rod, shaking being avoided as it might cause denaturation. Moreover to prevent bacterial growth all glass-ware was cleaned with a suitable detergent and after thorough washing with distilled water was dried in an oven at a temperature of 130^{o}c. When most of the sample was dissolved a very turbid solution was obtained indicating the presence of large particles. The solution was then centrifuged at about 25,000 g. for two hours at a temperature of 8^{o}c in an M.S.E. centrifuge. The supernatant was then carefully removed using a sterilised syringe. The plastic centrifuge tubes were washed thoroughly and the supernatant recentrifuged under similar condition to the first centrifugation except that the g value was increased to 35,000. Again the supernatant was carefully removed and a mother solution of 1.2×10^{-3} g/ml. was obtained which proved difficult to filter even through 5 μ filters. Sellen (1962) experienced the same difficulty with a calf thumus DNA sample obtained from the same previously mentioned commercial firm, although Jennings & Plummer (1970) were able to filter a similar sample

through 1.2 μ filters. The measured value of dn/dC at the wave length 4358 Å was found to be 0.187 ± 0.004. This value was used in calculating the optical constant K' and in determining the concentration of the solutions used in the measurements.

7.7.2 Conventional light scattering measurements

The angular scattered intensity measurements for three solutions are displayed in the Zimm plot, fig. (7.7.1). The measured depolarisation for these solutions is shown in fig. (7.7.2) and was found to be independent of concentration and has an average value of 3.7×10^{-2} which yields a Cabanne's correction factor of 0.92. The corrected values of the parameters as obtained from the Zimm plot are:

$4.5\ (\pm 0.7\ ) \times 10^6$ for the weight average molecular weight M_w,

3,000 (± 420) Å for the Z average radius of gyration ρ_z and

zero for the second virial coefficient of interaction B.

The light scattering technique has been used by a large number of workers to investigate DNA obtained from different sources and extracted by different methods. Sadron et al (1957) listed 28 results, 50% of these had a molecular weight in the range $(3\text{-}6) \times 10^6$. However, it is now accepted (c.f. Krasna - 1972) that the upper limit of the size of DNA particles is difficult to specify because it is difficult to obtain an unfragmented sample as the particles are very long and rather thin.

The present high value of the radius of gyration suggests that the particles are very elongated. Assuming the particles to be rod shaped, the Z-average length L_z, was found to be 10,500(±1500)Å. If the values of the density and diameter given by Reichmann et al (1954) are used (viz. 1.63 and 20 Å respectively), then the weight average molecular weight results in a value of ∿15,000 Å for the weight average length L_w. A much higher value for L_z would be expected as it is known that in gen-

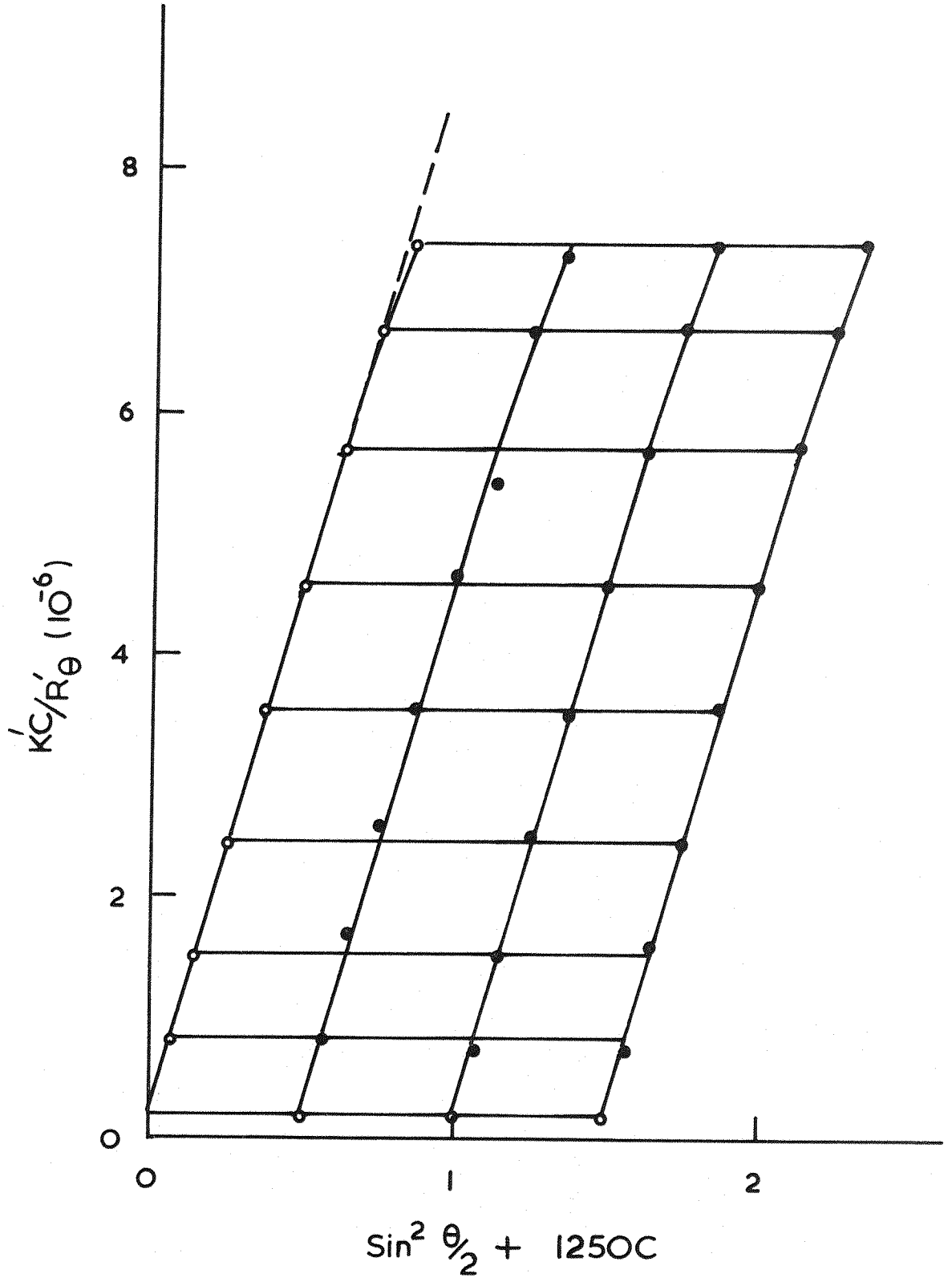

Fig. 7.7.1 Zimm plot for DNA (ex Calf thymus) at pH 7 & wavelength 4358 Å

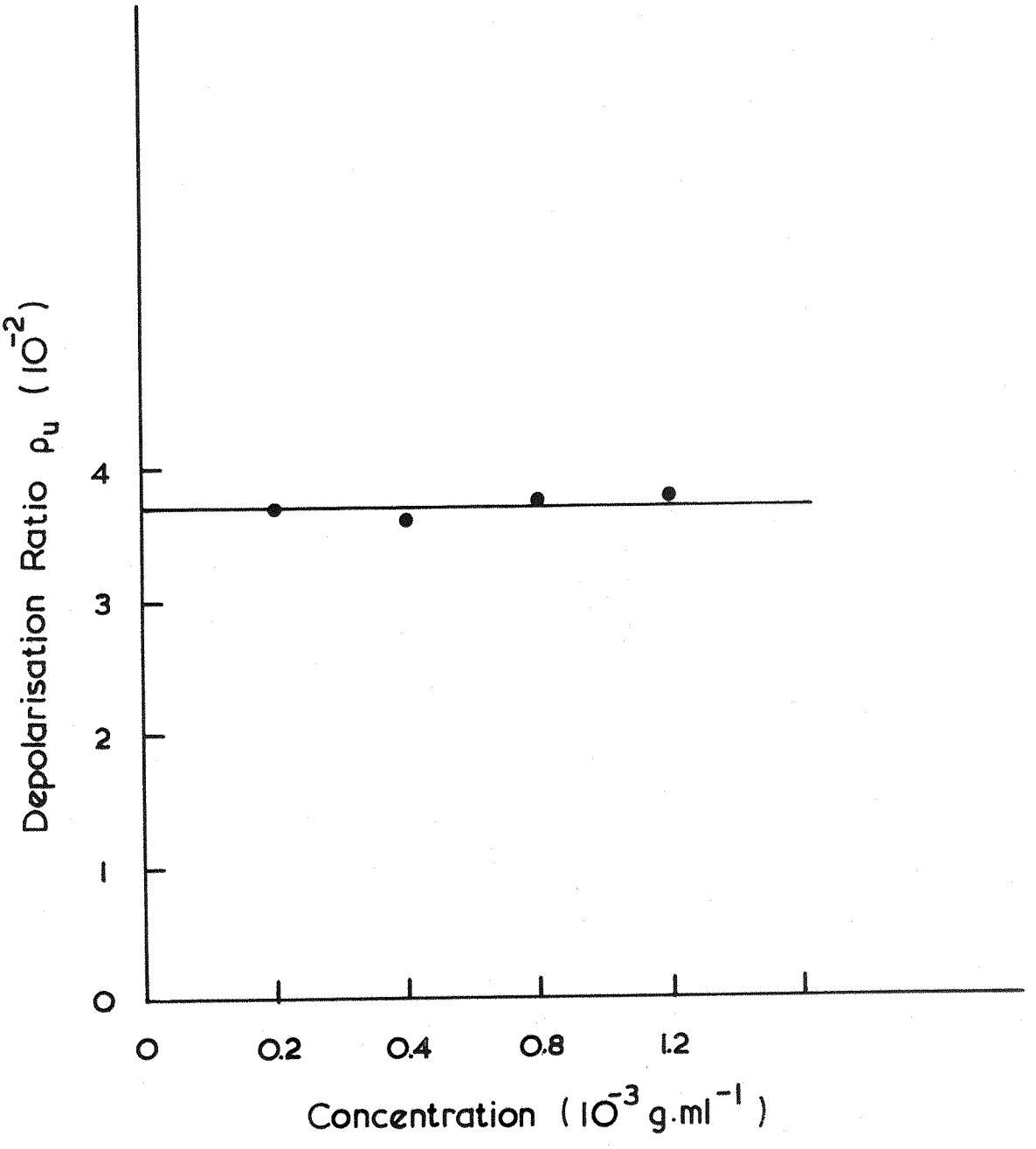

Fig. 7.7.2 Depolarisation of DNA (ex Calf thymus)

eral DNA samples are polydisperse (c.f. Takashima - 1967 and Jennings & Plummer - 1970). Thus, although very elongated one can not assume that the particles are perfectly rod shaped.

The actual model to choose for DNA is not exactly known. However, on the basis of experimental evidence, the wormlike (or continuously curved) coil model of Kratky and Porod (1949) has been considered a promising model to represent the solution behaviour of high molecular weight DNA (c.f. Peterlin - 1953 a and b and Sharp and Bloomfield - 1968). This is because the model incorporates the properties of a perfect rod and a random chain. A major feature of this model is the representation of the chain stiffness by a statistical length "a" (usually called the persistance length), a parameter which increases with increasing chain stiffness. The $\overline{P(\theta)}$ factor for this model has been derived in terms of the statistical length 'a'. Thus it is possible to obtain 'a' from the zero concentration Zimm plot. However, the determination of 'a' was not considered to be particularly significant in view of the wide range of values that have been quoted in the literature for this parameter. This wide difference in the reported values of 'a' is considered to arise from differences in ionic strength,polydispersity and poorly characterized molecular weights (Schmid et al - 1971). Thus this study was aimed towards determining the molecular weight of the sample used so that the measurements from the other methods used in this work can be related to a specified molecular weight.

It should be mentioned that linear extrapolation of the data was assumed in finding the molecular weight of the present sample although the lowest angle of observation was 30°. Doubts can be raised about the validity of the linear extrapolation from an observation angle as

high as 30^{o} because firstly the model to choose for DNA is not exactly known, it is therefore impossible to draw the corresponding theoretical curve of the scattering envelope and secondly even if a correct model was available an estimate of the sample polydispersity is impossible at this time. However, by comparing the molecular weights for several samples of DNA obtained with an instrument enabling measurements in the range 30^{o} - 150^{o} with those obtained for the same samples using an instrument that enables measurements at angles as low as 16^{o}, Froelich et al (1963) found that the usual range (30^{o} - 150^{o}) is sufficient if the molecular weight is $\leq 6 \times 10^{6}$. For higher molecular weight the data obtained in the usual range do not give even a suggestion as to how large will be the error (c.f. Froelich et al - 1963 and Krasna - 1972).

7.7.3 Light scattering in the presence of electric fields

Electric fields of up to 200 v/cm and of frequencies in the range (60 - 2000) Hz were used. Almost immediately the scattered intensity started to oscillate. This was due to the increase in the temperature of the solution caused by the failure of the cooling system to remove the relatively large amount of heat produced by the applied field in the relatively highly conductive solution. The failure of the cooling system is mainly due to the low thermal conductivity of the glass material used in constructing the light scattering cell. It should be mentioned that all the solutions of the materials, other than DNA, previously studied in this laboratory were dialysed prior to their investigation by this method. However, dialysis was ruled out because of the well known profound effects which the pH has on the properties of DNA (Krasna - 1972). Therefore to reduce the amount of heat produced in the solution another DNA sample was prepared without the addition

of the buffer. When this sample solution of pH 6.6 was used the thermal effect was still strong enough to permit any meaningful measurements. It seems that only a radical change in the design of the cell which permits a quick removal of the heat generated in the solution can alter this situation. Some of the results obtained using this method by other workers will be considered in the following section where the present Kerr effect measurements are reported.

7.7.4 Determination of the relaxation time, using the Kerr effect method

Electric field pulses of up to 10 KV/cm were used on four solutions of concentration in the range $(1.25 - 5) \times 10^{-4}$ g/ml. Fig. (7.7.3) shows a typical transient trace of the birefringence and fig. (7.7.4) shows the birefringence decay of this transient on a semi-log scale. It is seen from the log plot that the decay is not linear. Thus there is more than one relaxation time. The initial and end tangents of the log plot gave relaxation times of 3.4×10^{-6} sec.and 43×10^{-6} sec. respectively. Analysis of the other traces obtained for the other solutions under equal field intensity suggested that the determined range of the relaxation time was independent of concentration. Applying fields of different intensities in the range (3 - 10)KV/cm, to the most concentrated solution it was also found that the measured range does not vary considerably with the intensity of the field in the above mentioned range.

The presence of more than one relaxation time can be attributed to several factors such as assymmetry of shape, polydispersity of sample or flexibility of the particles (c.f. sec. 4.4). It has already been mentioned that DNA samples are usually polydisperse. As regards the flexibility, there is strong evidence to suggest that the particles are rigid in the presence of low intensity electric fields. The measured

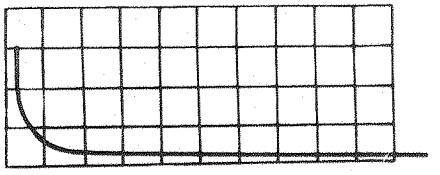

D.N.A. (ex calf thymus)

Fig. 7.7.3 Typical experimental birefringence trace obtained at T = 20^{o}c, C = 2.5×10^{-4} g.ml^{-1}, E = 9 kV.cm^{-1} and pulse width of 2.5×10^{-6} sec, pH = 7, Time scale = 20×10^{-6} sec.cm^{-1}

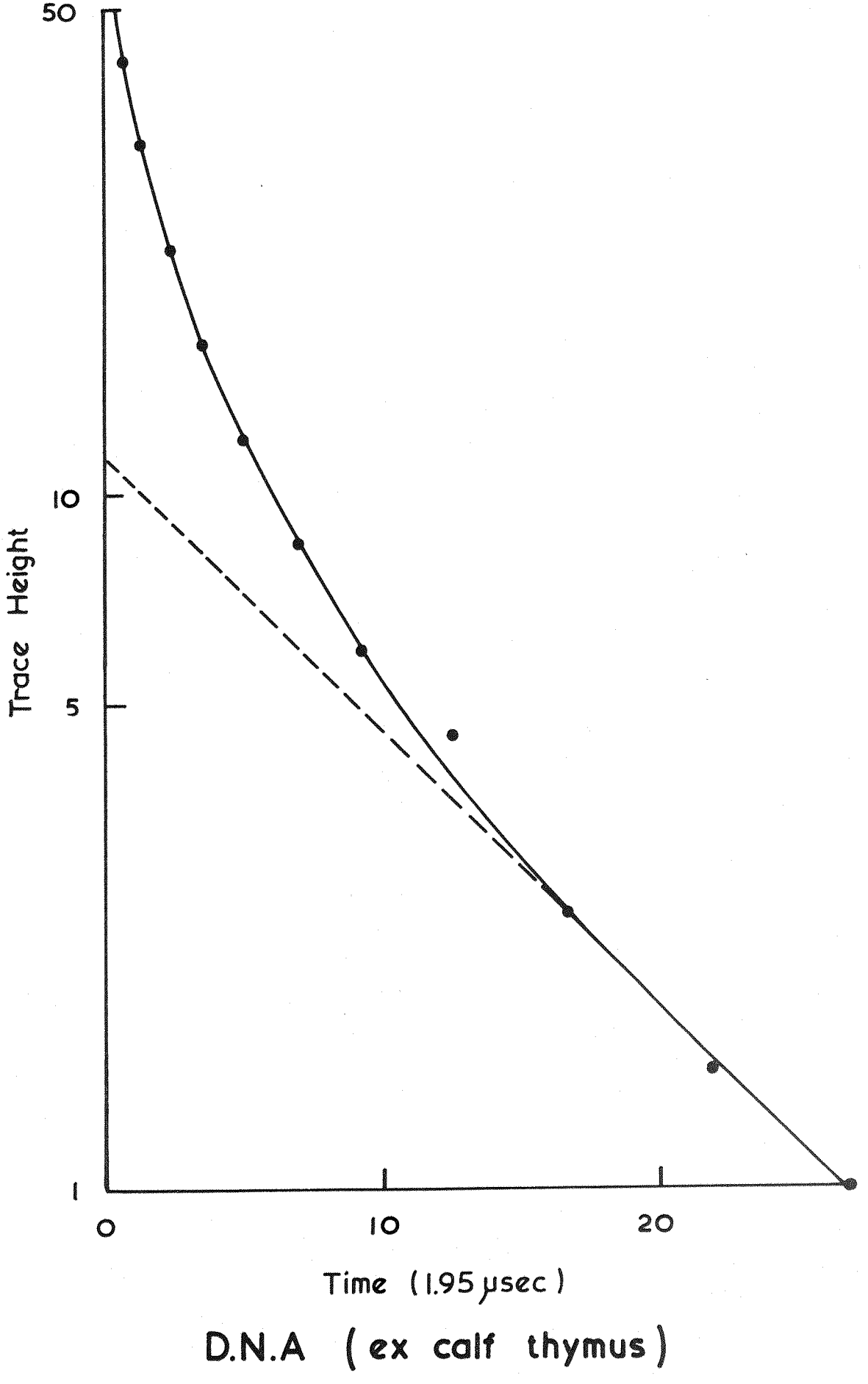

Fig. 7.7.4 Semi-log plot of the birefringence decay of the trace shown in fig. 7.7.3

values of the rigidity parameter R (Jennings and Plummer - 1970 and Hornick and Weill - 1971) are indicative of rigid particles. However, Golub (1964) using high intensity electric field pulses (3 KV/cm and 700 μsec. duration) found that the particles were flexible and rotate in segments of ∿4000 Å length, although O'Konski (1965) using 10 KV/cm obtained relaxation times large enough to suggest the rigidity of the particles.

Widely different conclusions have also been drawn about the electrical properties even with equivalent solvent conditions and using similar experiments. For example Benoit (1951), Hornick and Weill (1971) and Grave and Heij (1975) found that the orientation of the DNA particles was due only to the electrical polarisability anisotropy in the longitudinal and transverse directions $(\alpha_1 - \alpha_2)$ with $\alpha_1 >> \alpha_2$. The observed values of $(\alpha_1 - \alpha_2)$ are much larger than those predicted from the theory of Peterlin and Stuart (1943) for nonconducting solution. Hornick and Weill who studied the variation of α with the nature and concentration of counter ions found that, of the available theories of the ionic type polarisation (see ch. 4 sec. 4.5) the theory of Oosawa (1970) represents the best approach.

The data of Wippler (1956), those of Jennings and Plummer (1970) and Colson et al (1974) are consistent with the presence of a permanent dipole moment μ acting along the major axis. Data consistent with μ being across the particles have also been reported (Jungner et al - 1949, Allgen - 1950, Jerrard and Simmons - 1959 and Scheludko and Stoylov - 1967). The very small relaxation times observed by Allgen, Jungner et al and Jerrard and Simmons were considered to arise from the rotation of the particles about their axis of symmetry. This in turn led them to the conclusion that the dipole moment was acting across the particles.

For simplicity, it is a very common practice to treat the particles as if they were perfect rods. On this basis, the largest measured relaxation time (43 μsec) is found to be much smaller than that resulting from the rotation of a rigid rod of a length of 10,500 Å about its minor axis. Thus if the particles of the present sample have any dipole moment along the symmetry axis then the observed relaxation times would indicate that the particles were not rotating as rigid entities but in segments (i.e. being flexible) as was found by Golub (1964). However, the value of τ of 43 μsec is only $\sim 1/10$ of the largest τ observed by Golub.

If the particles were assumed to have a dipole moment acting only along the minor axis, the calculated relaxation time would be < 1 μsec. This calculated value of τ is even smaller than the smallest observed value and $\sim 1/50$ of the largest. To a certain extent the large difference between the measured and the calculated values of τ may be attributed to such factors as polydispersity and the inadequacy of the rod model to represent DNA particles of high molecular weight. However the fraction of the sample of the least molecular weight should result in a small relaxation time which was not observed in these measurements. Thus it may be concluded that under the present experimental condition the particles are flexible with at least one orientating mechanism acting along their axis of symmetry.

7.7.5 Summary

The conventional light scattering measurements indicated that the present sample of ex calf thymus DNA had a molecular weight of 4.5×10^6 and a radius of gyration of 3,000 Å. These values show that at neutral pH the particles are not sufficiently stretched to be considered as rod shaped. The large conductivity of the solutions did not permit measurements of the changes in the scattered intensity and thus it was not

possible to obtain any information about the electrical properties of the particles.

Analysis of the birefringence decay under rather high field intensities (3 - 10 KV/cm) shows that the particles are flexible.

Chapter 8

SUMMARY AND GENERAL CONCLUSIONS

1) The conventional light scattering and both the electric light scattering and the electric birefringence methods have been used to investigate the macromolecular properties of bentonite, hectorite, collagen and DNA.

The measurements were carried out with instruments designed by Jerrard and Co-workers (1962 and 1969). The angular light scattering measurements were obtained using semicylindrical cells which were constructed by the present worker. These semicylindrical cells were of similar design to those used by Jerrard and Co-workers except that the electrode assembly was modified to make construction easier. The electrode assembly of the square cell used for measuring the rigidity parameter, R, was also modified. This modification not only resulted in easier construction but also permitted the use of a different method of measuring R. This different method permits the temperature of the solution inside the cell to be easily controlled. A further modification to the light scattering apparatus was the incorporation of a frequency doubler in to the detecting system which provided a clear reference signal when measuring the alternating component of the changes in the scattered intensity. The Kerr effect apparatus was used for measuring the relaxation time(s) without any modification.

2) Before making the conventional light scattering measurements the geometry of the light scattering apparatus was checked and it was then calibrated using solutions of syton 2X. A check on the accuracy of this calibration was made using bovine albumin as it has an established molecular weight. Although bovine albumin has a tendency to aggregate, it

was considered to be suitable for indicating whether there were large errors involved in the determination of the calibration factor.

3) Although in general bentonite in its calcium form has a great tendency to aggregate, it was found that the dilute solutions of the finest fractions of North African calcium bentonite are stable for sufficient time to permit their investigation. The measurements which were carried out on the solutions of two samples of bentonite of different origins showed that the two samples have similar molecular properties which are now summarised:-

i) In dilute solutions the particles exist as individual unaggregated discs of thickness of about 9 Å. The exact thickness can not easily be determined without estimating the effect of polydispersity. This is because the method of light scattering results in different averages for the molecular weight and the radius of gyration.

ii) The tendency of the particles to aggregate and sediment is reflected in the negative value obtained for the coefficient of interaction.

iii) The magnitude of the alternating component of the changes was too small to be measured. Thus it was not possible to determine whether bentonite is composed of one type or is a mixture of two types of particles both having different electrical properties. Assuming that the particles are all of one type, the dispersion of the steady changes in the scattered intensity indicates that the particles have a predominant permanent dipole moment μ acting along the axis of symmetry of the disc and an excess polarisability α along its semi major axis. For a mixture of two types of disc like particles then one type must be polar but electrically isotropic ($\alpha = 0$) and the other nonpolar but electrically anisotropic.

iv) It can be seen that the method of comparing the two values of the diffusion constant as determined from the dispersion of the two components of the changes in the scattered intensity is not suitable for resolving this ambiguity except when the two types in the sample under study have different average sizes. This is because for a disc like particle D_μ and D_β will be the same for particles having the same size. Thus in general an entirely different method should be used with disc like particles.

It was suggested that the method of reversing the polarity of the applied electric field may result in the determination of the composition of bentonite, provided it is used with fields of sufficiently high intensities to produce complete orientation of the particles.

v) Although bentonite is one of the most studied of mineral clays there are few measurements on particles having a similar size and most of these have been carried out on Wyoming sodium bentonite and none at all on North African calcium bentonite. However, the present values of α and μ, when compared with those in the literature, tend to suggest that they might be reproducible if the measurements were carried out on fresh solutions and the effect of polydispersity, configutation and size were taken into account.

4) It has been shown that the rather small relaxation times observed for the hectorite sample can be considered to arise from the rotation of the rod shaped particles of hectorite around their major axis. Thus the particles have no dipole moment along this axis as otherwise much larger relaxation times would have been observed. An induced dipole moment along the major axis has been observed by other workers using the same techniques as in the present work.

Tolstoi (see table 7.4.1) who investigated bentonite also

observed that the induced and the permanent dipoles were parallel to each other rather than perpendicular as found by most workers. Stoylov (1971) questioned whether the substance used by Tolstoi was actually bentonite. The possibility that any of the samples were not actually hectorite can not be ruled out. This is because the methods that have been used in the reported investigations are not suitable for determining the nature of the sample under study. It should also be pointed out that differences in the microscopic structure could be the cause of the apparent differences in the electrical properties.

The reproducibility of data (at least for samples of same origin) is very advantageous as it permits the comparison between the experimental values and the values that can be predicted from present and future theories on polarisation of conducting solutions.

5) The parameters observed for the collagen sample are descriptive of aggregated collagen particles of the type shown in fig. 7.6.2.a (i.e two dimers of the end to end type joined side to side). One difficulty is met when explaining the Kerr effect data on the basis of this configuration. There should be no dipole moment (induced or permanent) along the major axis of the aggregated particles. This can be seen to be true for the overall permanent dipole but is difficult to ascertain for the resultant induced dipole moment. However the redistribution of the charges of the particles which is associated with the aggregation process could result in these particles having no induced dipole moment along their major axis. Complete denaturation is unlikely to be reached under the conditions under which the experiment was performed (c.f. Yoshioka and O'Konski - 1966). This is supported by the fact that only one relaxation time was observed.

6) The molecular weight and the radius of gyration were determined for a sample of ex calf thymus DNA. These parameters were obtained from light scattering measurements over the range 30^{o} - 135^{o} (only the lowest observation angle being significant). Fortunately this range was sufficient for the present sample as the molecular weight was found to be $< 6 \times 10^{6}$. If this were not the case it would have been difficult to determine the molecular weight with any known accuracy (see Krasna - 1972). Thus the apparatus must be modified to enable measurements at an observation angle much lower than that available at present if high molecular weight samples of DNA ($> 6 \times 10^{6}$) are to be investigated.

The radius of gyration indicated that at neutral pH the particles were very stretched but not sufficiently to be considered rod shaped.

The high conductivity of the solutions of the DNA sample prevented the determination of the electrical properties from light scattering measurements in the presence of a.c. fields. The heat generated in the solution inside the cell by the action of the applied field could not be removed at a rate sufficient to keep the temperature of the solution constant and thus these measurements were not possible. A modification of the apparatus is necessary if highly conductive solutions in their undialysed form are to be investigated.

The use of pulsed electric fields with the present light scattering apparatus would not be very productive even if a pulse generator of sufficient power was available. This is because this apparatus was not designed for this type of measurement. In comparison with many other light scattering instruments, the scattered intensity is significantly attenuated because of the existence of a large number of optical components in the path of the scattered light beam. Thus the changes in the scattered intensity which are usually small are also attenuated.

The results from the Kerr effect method were not very productive Only the high voltage pulse generator could be used and under fields of high intensities the particles were found to be flexible.

It is thought that future investigations of the electrical properties of DNA will show diversity because of the effect of several factors, the contribution of which may differ significantly from one sample to another. For example, although in theory DNA particles should have no permanent dipole moment, a dipole moment could be observed because of the presence of impurities such as residual proteins, single stranded regions or an irregular ionic-charge distribution in some regions of the molecule (c.f. Colson et al - 1974).

7) The causes for the higher sensitivity of the electric birefringence method have been stated and experimentally demonstrated in sec. 7.4.5b. Under similar experimental conditions, it was found that the transients of the electric light scattering were very noisy compared with those observed for the electric birefringence. In general only by applying electric fields of high intensity ($\sim$ KV/cm) on solutions of large particles (with a characteristic dimension $\sim$ 1μ) would it be possible to obtain satisfactory results from the transients of the electric light scattering. Unfortunately when fields of high intensity are used, the method results in little or no information about the electrical properties. Thus the electric birefringence is the obvious choice for investigating the electrical properties of macromolecular solutions whether the particles are large or small. The advantages associated with the electric light scattering method (e.g. no calibration being needed as only the relative changes in the scattered intensity are measured) are generally outweighed by the high level of noise present on the traces.

For reasons that have been mentioned before (c.f. sec. 8.6) the transients of the changes in the scattered intensity were observed with an instrument designed by the present worker instead of using the apparatus of Jerrard and Sellen. It is also possible to use this instrument for recording the transients of the electric birefringence. This instrument in fact is a typical Kerr effect apparatus. However, the detector can be remounted perpendicular to the main optical bench of this instrument to detect the scattered intensity in a direction perpendicular to the incident light beam (i.e. $\theta = 90^{o}$). The main features of this instrument are now briefly described:

a) The light source was a mercury lamp instead of the laser (see sec. 5.7) because the scattered intensity is greater the lower the wave length of the incident light beam. To obtain a parallel incident light beam, an optical system similar to that shown in fig. 5.3 was used.

b) The cell was all of glass and square-shaped so that both the transmitted and the scattered light beams could be observed. The cover of the cell holds two parallel electrodes with an adjustable separation. The electrodes were constructed of stainless steel measured 1 cm by 1 cm and permitted vertical electric fields to be applied to the solutions.

c) The pulse generator was capable of generating electric field pulses of variable duration (0.1 - 20 m sec.) and of intensity up to 600 V/cm. However, because of its limited power it can be used only with solutions having a rather high resistance of several kΩ/cm. A brief description and the circuits for this pulse generator are given in appendix A.

Finally the reasons for not using this instrument have been stated before (see sec. 7.4.5b).

REFERENCES

Allgen, L.G.: Acad.Physiol (Suppl) 22, 76 (1950)

Ananthanarayanan, S. and Veis, A.: Biopolymers 11, 1365, (1972)

Beattie, W.H. and Booth, C.: J.Phys.Chem 64, 696-697 (1960a)

Beattie, W.H. and Booth, C.: J.Polymer Sci. 44, 81-89 (1960b)

Beidl, G., Bischof, M., Clatz, G., Porod, G., Von Sacken, J.Ch. and Wawra, H.: Z.Electrochem. 61, 1311-1318 (1957)

Benoit, H.:

Benoit, H.: Ann.Phys. 6,561, (1951)

Benoit, H.: J.Polymer Sci. 11, 507-510 (1953)

Benoit, H., Holtzer A.M., Doty, P.: J.Phys.Chem. 58, 635 (1954)

Bloch, E.: Compt.Rend. 146, 970 (1908)

Boedtker, H. and Doty, P.: J.Amer.Chem.Soc. 78, 4267 (1956)

Boel, M.: Ph.D. Thesis (1966) Polytechnique Inst. Brooklyn, New York.

Born, M.: Ann.Physik. 55, 177-240 (1918)

Brice, B.A., Halwer, M., Speiser, R.S: J.O.S.A. 40,768 (1950)

Brown, B.L.. Jennings, B.R., and Plummer, H: Applied Optics, 8, 2019 (1969)

Cabannes, J.: "La Diffusion Moleculaire de la Lamiere", Les Presses Universitaires, Paris (1929)

Candler, C.: "Modern Interferometers", Hilger and Watts Ltd., London (1951)

Carpenter, D.K.: J.Polymer Sci. A-2, 4, 923-942 (1966)

Chu, B.: Rev.Sci.Instr. 35, 1201 (1964)

Colson, P., Houssier, C. and Frederieq, E.: Biochim. Biophys. Acta. 340, 244 (1974)

Dandliker, W.B.: J.Amer.Chem.Soc. 76, 6036 (1954)

Debye, P.: Ann.Phys. (Leipzig) 46, 809 (1915)

Debye, P.: J.App.Phys. 15, 338 (1944)

Debye, P.: J.Phys. and Coll. Chem. 51 18 (1947)

Doty, P. and Steiner, R.F.: J.Chem.Phys. 18, 1211 (1950)

Doty, P. and Steiner, R.F.: J.Chem.Phys. 20, 85 (1952)

Edsall, J.T., Edelhoch, H., Lontie, R. and Morrison, P.R.: J.Amer.Chem.Soc. 72, 4641,(1950)

Einstein, A.: Ann.Phys. (Leipzig) 33, 1275 (1910)

Froelich, D., Strazielle, C., Bernardi, G. and Benoit, H.: Biophy. J. 3, 115 (1963).

Gallop: P. M. Arch. Biochem, Biophys. 54 486 (1955).

Gans, R.: Ann. Phys. (Leipzig) 62, 351 (1919)

Gans, R.: Ann.Phys. (Leipzig) 76, 29 (1925)

Geiduschek, E.P.: J.Poly.Sci. 13, 408 (1954)

Golub, E.I.: Biopolymers, 2, 113 (1964)

Greve, J. and De Heij, M.E.: Biopolymers 14, 2441 (1975)

Grim, R.E.: "Clay Mineralogy" McGraw Hill, New York (1953).

Guinier, A.: Ann.Phys. (Paris) 12 161 (1939)

Harpst, J.A., Krasna, A.I. and Zimm, B.H.: Biopolymers 6 585 (1968)

Hermans, J.J., Levinson, S.: J.O.S.A. 41 460 (1951)

Holtzer, A.: J. Polymer Sci. 17 432 (1955)

Horn, P.: Compt.Rend.234 1870 (1955)

Hornick, C. and Weill, G.: Biopolymers 10 2345-2358 (1971)

Huglin, M.B.: "Light scattering from polymer solution" London and New York, Academic Press (1972)

Ingram, P. and Jerrard, H.G.: Brit.J.Appl.Phys. 14 572 (1963)

Isemura T. and Mukohata, Y.: Nippon Kagaku Zasshi 80 657 (1959).

Jennings, B.R.: Ph.D. Thesis, University of Southampton (1964)

Jennings, B.R.: Ch.13 in Light Scattering from Polymer Solutions (Edited by M.B. Huglin) pp.529-579, Academic Press, New York (1972)

Jennings, B.R. and Brown, B.L. and Plummer, H.: J.Coll.Int.Sci.32 606 (1970)

Jennings, B.R. and Jerrard, H.G.: J.Poly.Sci.Part A2 5 2025 (1964)

Jennings, B.R. and Jerrard, H.G.: J.Chem.Phys. 42, 511-516 (1965)

Jennings, B.R. and Jerrard, H.G.: J.Chem.Phys. 44, 1291 (1966)

Jennings, B.R. and Plummer, H.: J.Coll.Int.Sci. 27, 377 (1968)

Jennings, B.R. and Plummer, H.: Biopolymers, 9, 1361 (1970)

Jerrard, H.G., Riddiford, C.L. and Ingram, P.: J.Sci.Instruments Ser.2, V.2, 761.

Jerrard, H.G. and Sellen, D.B.: Applied Optics 1 243 (1962)

Jerrard, H.G. and Simmon, B.A.W.: Nature 184, 1715 (1959)

Jungner, G., Jungner, I. and Allgen, L.G.: Nature, 63 849 (1949)

Kahn, A. and Lewis, D.R.: J.Phys.Chem. 58, 801 (1954)

Kahn, L.D. and Witnauer, L.P.: Biochim.Biophys.Acta 393 247 (1975)

Kerker, M.: "The Scattering of Light" Academic Press (1969)

Kerr, J.: Phil.Mag. 50(4) 337, 446 (1875)

Krasna , A.I.: J.Coll.Int.Sci. 39 632 (1972)

Kratky, O. and Porod, G.: J.Coll.Sci. 4, 35 (1949)

Kratky, O. and Porod, G.: Rec.Trav.Chim. 68 1106 (1949)

Kratohvil, J.P.: Anal.Chem.36 458R (1964)

Kratohvil, J.P.: Anal.Chem.38 517R (1966a)

Kratohvil, J.P.: J.Colloid.Interface Sci. 21 498 (1966b)

Kratohvil, J.P.: (1972) Chapter 7 in the book edited by Huglin (see Huglin M.B.)

Krause, S. and O'Konski, C.T.: J.Am.Chem.Soc. 81 5082 (1959)

Langevin, P.: Le Radium, 7 249 (1910)

Maron, S.H. and Lou, R.L.H.: J.Poly,Sci. 14 29 (1954)

Martin, W.H.: Trans.Roy.Soc.Canada 17 151 (1923)

Matsumoto, M., Watanabe, H. and Yoshioka, K.: J.Phys.Chem. 74 2182 (1970)

Maxwell, J.C.:"Treatise in Electricity and Magnetism" Vol.1, p.451 Oxford (1892)

M'Ewen, M.B. and Pratt, M.I.: "The Nature and Structure of Collagen". Butterworths, London (1953)

M'Ewen, M.B. and Pratt, M.I.: Trans.Faraday Soc. 53, 535 (1957)

Mie, G.: Ann.Physik, 25, 377 (1908)

Mueller, H.: Phys.Rev. 55 792 (1939)

Napper, D.H. and Ottewill, R.H.: Kolloid.Z.u.Z.Polymere, 192, 114-117 (1963)

Napper, D.H.: Kolloid.Z.u.Z. Polymere, 223, 141 (1968)

Neugebauer, T.: Ann.Phys. (Leipzig) 42 509 (1943).

Nishinari, K. and Yoshioka, K.: Kolloid.Z.u.Z.Polym. 235, 1189 (1969)

Norton, F.J.: Phys.Rev.55, 668 (1939)

O'Konski, C.T.:J.Phys.Chem. 64, 605 (1960)

O'Konski, C.T.: Encycl.Pol. Sci.Technol. 9, 551 (1968)

O'Konski, C.T. and Haltner, A.J.: J.Am.Chem.Soc. 78, 3604 (1956)

O'Konski, C.T. and Haltner, A.J.: J.Am.Chem.Soc. 79, 5634 (1957)

O'Konski, C.T. and Stellwagen, N.C.: Biophys. J.5 607 (1965)

O'Konski, C.T., Yoshioka, K. and Orttung, W.H.: J.Phys.Chem. 63, 1558 (1959).

O'Konski, C.T. and Zimm, B.H.: Science, 111 113 (1950)

Oncley, J.L. et al.: J.Phys.Coll.Chem. 51 184 (1947)

Oosawa, F.: Biopolymers 9 677 (1970)

Oster, G.: Anal.Chem. 25, 1165 (1953)

Perrin, F.: J.Phys.Rad. 5 497 (1934)

Peterlin, A.: J.Polymer Sci. 10 425-436 (1953a)

Peterlin, A.: Macromol.Chem. 9, 244-268 (1953b)

Peterlin, A.: Prog. in Biophys. 9 175 (1959)

Peterlin, A.: Proceedings of the Interdisciplinary Conference on Electromagnetic Scattering. (Ed: M. Kerker), Pergamon Press, London (1963) p.357.

Peterlin, A. and Stuart, H.A.: Hand- und Jahrbuch der Chemischen Physik, Vol.8, Section 1B, Becker and Erler, Leipzig (1943)

Picot, C., Weill, G. and Benoit, H.: J.Coll.Int.Sci. 27(3) 360-376 (1968)

Plummer, H. and Jennings, B.R.: British J.Appl.Physics 1 1753 (1968)

Plummer, H. and Jennings, B.R.: J.Chem.Phys. 50 1033 (1969)

Ptitsyn, O.B.: Zh.Fiz.Khim. 31 1091-1102 (1957)

Putzeys, P. and Brosteaux, J.: Trans.Frad.Soc. 31 1314 (1935)

Pytkowicz, R.M. and O'Konski, C.T.: Biochim.Biophys.Acta 36 466 (1959)

Rahinovitch, J.: J.Phys.Radium 7, 228 (1946)

Ravey, J.C.: Eur. Polymer J. 8 937 (1972)

Rayleigh, Lord: Phil.Mag. 41 107, 274, 447 (1871)

Rayleigh, Lord: Phil.Mag. 12 81 (1881)

Rayleigh, Lord: Proc.Roy.Soc.A 84 25 (1911)

Rayleigh, Lord: Phil.Mag. 35 373 (1918)

Reichmann, M.E., Rice, S.A., Thomas, C.A. and Doty, P.: J.Amer.Chem.Soc. 76 3047 (1954)

Riddford, C.L.: Ph.D. Thesis, University of Southampton (1968)

Ridgeway, D.: J.Am.Chem.Soc. 88 1104 (1966)

Ridgeway, D.: J.Am.Chem.Soc. 90, 18 (1968)

Rudd, P.J. and Jennings, B.R.: J.Coll.Int.Sci. 48 302 (1974)

Sadron, C.H., Pouyet, J. and Vendrely, R.: Nature 179, 263 (1957)

Saito, N. and Ikeda, Y.:J.Phys.Soc.Japan 6 305-308 (1951)

Sakmann, B.W.: J.Opt.Soc.Am. 35 66 (1945)

Scatchard, G. et al: J.Am.Chem.Soc. 88 2320 (1946)

Scheludko, A. and Stoylov, S.P.: Kolloid-Z.u.Z. Polymere 199 36 (1964)

Scheludko, A. and Stoylov, S.P.: Biopolymers, 5 723 (1967)

Schepers, J.S. and Miller, R.J.: Miner.clay Miner. 213 22 (1974)

Schmid, C.W., Rinehart, F.P. and Hearst, J.E.: Biopolymers 10 883 (1971)

Schwarz , G.J.: Phys.Chem. 66 2636 (1962)

Schweitzer, J. and Jennings, B.R.: J.Coll.Interface Sci. 31 443 (1971)

Schweitzer, J. and Jennings, B.R.: Biopolymers 11 1077 (1972)

Schweitzer, J.F. and Jennings, B.R.: Eur.Polymer J. 10 459 (1974)

Sellen, : Ph.D. Thesis, Southampton University (1962)

Shah, M.J.: J.Phys.Chem. 67 2215 (1963)

Shah, M.J. and Hart, C.M.: IBMJ.Res.Develop.7 44 (1963)

Shah, M.J., Thompson, D.C. and Hart, C.M.: J.Phys.Chem. 67, 1170 (1963)

Sharp, P. and Bloomfield, V.A.: Biopolymers 6 1201 (1968)

Sheffer, H. and Hyde, J.C.: Canad.J.Chem. 30 817 (1952)

Shultz, A.R. and Stockmayer, W.H.: Macromolecules-2 178 (1969)

Smoluchowski, M.: Ann.Phys. (Leipzig) 25 205 (1908)

Sokerov, S. and Stoimenova, M.: J.Colloid and Interface Sci. 46 94 (1974)

Stacey, K.A.: "Light Scattering in Physical Chemistry", Butterworths, London (1956)

Stokes, A.R.: Proc.Phys.Soc. (London) 70 379 (1957).

Stoylov, S.P.: Collection Czech.Chem.Commun. 31 2866 (1966)

Stoylov, S.P.: Izv.Inst.Fizkhim 6 79 (1967)

Stoylov, S.P.: Advan.Coll.Int.Sci.3 45 (1971)

Stoylov, S.P. and Petkanchin : Godishnik Sofiiskiya Uni. Khim. Fak.61 227 (1966/67)

Stoylov, S.P. and Sokerov, S.: J.Coll.Int.Sci. 24 235 (1967)

Stoylov, S.P. and Sokerov, S.: J.Coll.Int.Sci. 27 542 (1968)

Stoylov, S.P. and Sokerov, S.: Izv.Otd.Khim.Nauki.Bulgar.Akad.Nauk. 2 191 (1969)

Stoylov, S.P., Sokerov, S., Petnakchin, I. and Ibroshev, N.: Doki.Akad.Nauk.SSSR. 180 1165 (1968)

Takashima, S.: Advan.Chem.Ser. 63 232 (1967)

Thurston, G.B. and Howling, D.I.: J.Colloid.Interface Sci. 30 34 (1969)

Timasheff, S.N.: Coleman B.D. Kirkwood J. G. (1954) 125th Meeting A C S.

Timasheff, S.N. and Townend, R.: Principles Tech.Protein Chem. (Pt.B) p.147-212. (Ed.: S.J. Leach). Academic Press, New York (1970)

Tinoco, I.Jr.: J.Am.Chem.Soc. 77 4486 (1955)

Tinoco, I.Jr. and Yamaoka, K.: J.Phys.Chem. 63, 423 (1959)

Tolstoi, N.A., Spartakov, A.A. and Trusov, A.A.: Issled.Obl.Poverkh.Sil.Dokl.Knof, 3rd Moscow (1967) p.56.

Trusov, A.A.: Thesis, Leningrad (1968)

Utiyama, H.: Chapters 3 and 4 in the book edited by Huglin (see Huglin-1972)

Wagner, K.W.: Arch.Elektrotech.3, 83, (1914)

Wallach, M.L. and Benoit, H.: J.Polymer Sci. 57 41 (1962)

Wallach, M.L. and Benoit, H.: J.Polymer Sci. A2 4, 491 (1966)

Wippler, M.C.: J.Phys.Rad. 14 65 (1953)

Wippler, M.C.: J.Chem.Phys. 51 122 (1954)

Wippler, C.: J.Chim.Phys. 53 316, 328 (1956)

Wippler, C.: J.Poly.Sci.23 199 (1957)

Wippler, C., and Scheibling, G.: J.Chim.Phys. 51 201 (1954)

Yoshioka, K. and Watanabe, H.: Nippon Kagaku Zasski 84 326 (1963)

Yoshioka, K. and O'Konski, C.T.: Biopolymers 4 499 (1966)

Yoshioka, K. and Watanabe, H.: in "Physical Principles and Techniques of Protein Chemistry, Part A." S.J. Leach, Ed. Academic Press Inc., New York, N.Y. p.335 (1969)

Zernicke, F.: Dissertation, Amsterdam (1915)

Zimm, B.H.: J.Chem.Phys. 16 1093 (1948a)

Zimm, B.H.: J.Chem.Phys. 16 1099 (1948b)

APPENDIX A

THE PULSE GENERATOR

The following is a brief description of the pulse generator referred to in chapter 8 sec. 7.

This generator consists of two stages. The first stage is a pulse generator (P.G.) that gives a square pulse having an amplitude of 15 V and of variable width (0.1 - 20 msec) and rate (2 - 2000 c/s). The second stage is a pulse amplifier (P.A.). The pulse generator was designed to give a single pulse at a time or to run continuously. Figs 1 and 2 give the circuit diagrams of the P.G. and the P.A. respectively.

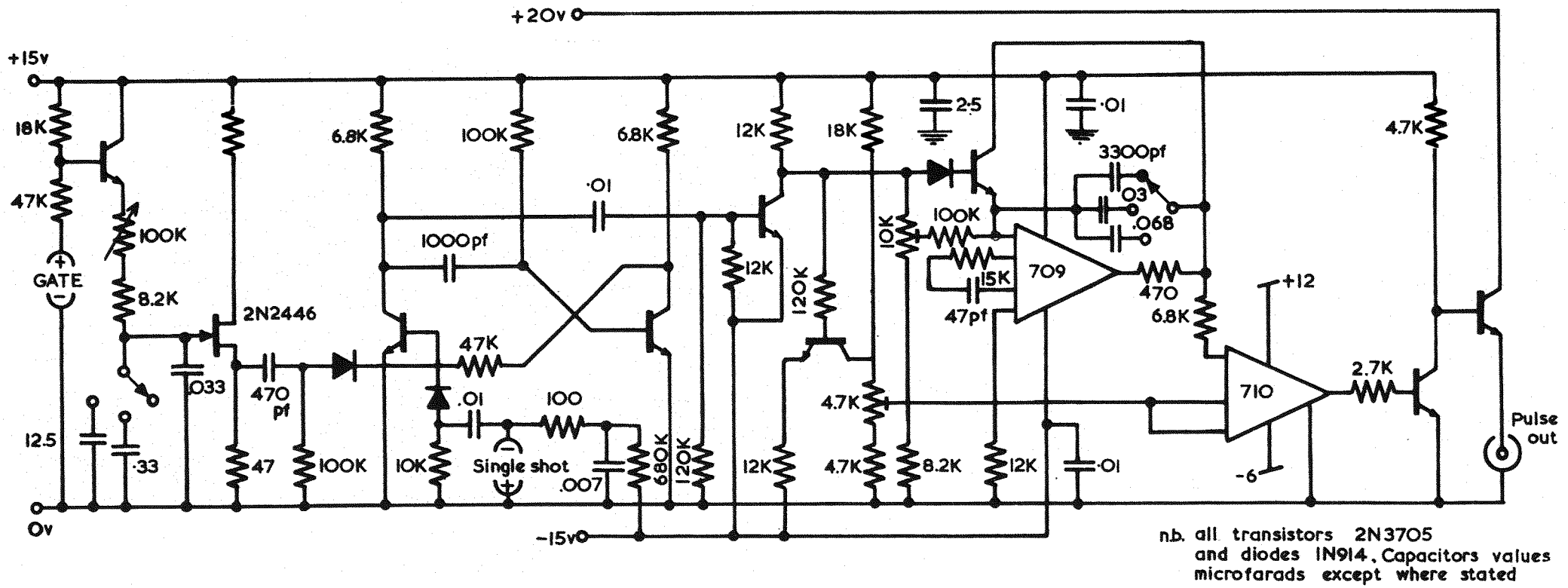

Fig·1 - Pulse Generator

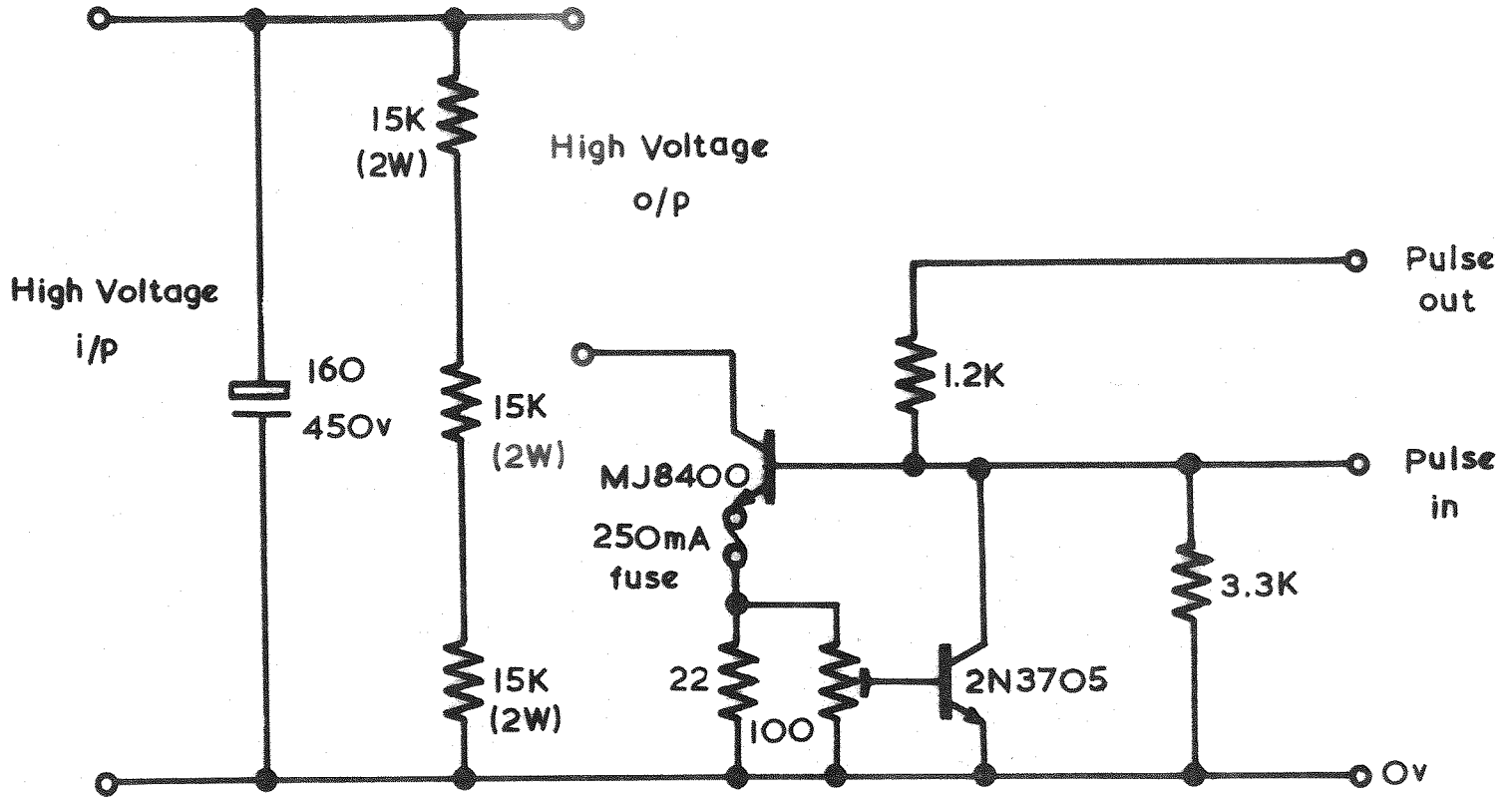

Fig. 2. Pulse Amplifier